

Neuronal regulation of impulsivity and metabolic adaptation

Jessica Ashley Hatter

Waynesboro, Virginia

M.S. Biological and Physical Sciences, University of Virginia, 2020

B.S. Biochemistry, Juniata College, 2016

A Dissertation presented to the Graduate Faculty  
of the University of Virginia in Candidacy for the Degree of  
Doctor of Philosophy

Department of Pharmacology

University of Virginia

May 2023

Michael M. Scott, Ph.D.

Mark Beenhakker, Ph.D.

John N. Campbell, Ph.D.

Ali. D. Guler, Ph.D.

## ABSTRACT

---

Dysfunction and the resulting behavioral aberrations are highly associated with the development of over 200 types of mental disorders. Thus, increased understanding of the cognitive causes of psychopathologies is important for directing pharmacologic interventions. To further explore how disparate systems affect behavior, we conducted studies exploring cortical control of behavior and transcriptomic studies of a subset of neurons in the hindbrain that are highly implicated in the control of feeding and response to metabolic adaptation.

While dysfunction of the PFC is highly correlated with mental disorders and the development of addiction, little is known about how alterations in neuron activity can drive changes in behavior. To query how the cortical microcircuit functions during specific behavioral tasks, I harnessed a method of specific caspase-3-mediated ablation to explore how it modulated behavior. Using this animal model, I revealed a novel circuit-level mechanism in which a subtype of cortical interneuron functions as a gate to modulate behavior during periods of high expectation.

Glucagon-like peptide-1 (GLP-1) is believed to be the most potent effector of gut-hindbrain communication and is implicated in appetite suppression and feeding behavior. GLP-1 agonists have been pharmacologically relevant in the treatment of type 2 diabetes and induce weight loss in obese individuals. Previous research found that activation of GLP-1 neurons in the hindbrain reduced food intake in both lean and obese, but selectively mediated weight loss only in obese animals. To query how obesity may influence neuronal action, we conducted transcriptomic profiling in GLP-1 neurons from the hindbrain in lean and obese animals.

## ACKNOWLEDGEMENTS

---

I started this journey in 2018 and it has been a truly insane 5 years and I feel so lucky to have made it through and be on the other side. I look forward to taking the next steps in my career and moving onto even more new and exciting endeavors. I am forever grateful to Dr. Michael Scott for his continued support and tenacity as we established new and groundbreaking research and to Dr. Mohan Manjgowda who aided us in the establishment of our sequencing pipeline and was always a smiling face during trying times in the lab.

I came to the University of Virginia in 2016 as a fresh college graduate to work as a laboratory technician in Sarah Ewald's lab in the Beirne B. Carter Center for Immunology research, where I studied cachexia during *Toxoplasma gondii* infection. I was blessed to be in the company of great scientists such as Dr. Stephanie Melchor, Xiaoyu Zhao, and Dr. Bocheng Yin, who shaped my enthusiasm for science and helped me blossom into the researcher that I am today. I am especially grateful to Stephanie, who remains one of my dearest friends to this day, who was an invaluable resource to me as I navigated graduate school and was a listening ear when I thought I might never be done with my doctorate.

My husband, William Koenig, who was less than enthused when I started grad school a year into our relationship, has been a continual source of support, love, and encouragement. He has been there during the many emotions of grad school, and I think he may be the most excited out of the lot that I am finally done. He has been on my side since day one, has believed in me and my ability to get literally anything done, and has been my constant companion during every single step of this journey. Truly, without him, I wouldn't be here. I owe him so much and I hope that I can repay even half the support that he has given me through this journey.

Last August, I was fairly convinced that I was going to master out of my program, after a multitude of roadblocks that had cropped up through the last year. My mom sat with me for hours and listened to my concerns and told me to give it another two weeks. Those two weeks turned into a month, turned into a paper, turned into a dissertation, and finally led me to graduating. Without her, I truly would not be here. I cannot thank her enough for her encouragement and the model of hard work, diligence, and love for learning that she has been since I was just a baby.

My dad has been there for me in big ways and small. He has taken care of every single car trouble that either William or I have had in the past 5 years. Any time I have made a small comment about not being able to get something done, guess who shows up the next day? My dad, without complaint. I cannot overstate how much these two people and their support have been integral to me graduating.

Many thanks to my bonus parents - my stepdad, Mark; my stepmom, Monique; and my in-laws Jeff and Teri. My stepparents came into my life during the terrible teens and yet continued to love and support me as I've grown up. My stepdad has helped me move into every apartment, took my wedding pictures, and has modeled what a truly loving husband looks like. Monique has given me many free haircuts, made me laugh more

times than I can count, and is responsible for bringing the love of my life, my baby sister Gigi, into this world, and so I owe her many thanks. My in-laws, especially my father-in-law Jeff, have been such a constant rock throughout this whole process. My fear as a young person was always that I would have horrible in-laws, but I truly feel as if I gained two wonderful parents (and a bonus sister) who love and support me as though I am their own. They have fed us, given us rides and reminded me that I am a person and a daughter with my own intrinsic value.

My baby sister, Giovanna, has consistently been a source of light, laughter, and motivation in my life since she was brought into this world almost 15 years ago. I am constantly in awe of what an intelligent, precocious, and talented young woman she is, and I am so proud to call her my sister. I am always thankful to her for reminding me that life is so much bigger than the walls of the lab and to be grateful that at least I'm no longer in eighth grade algebra.

My grandparents, Jerry and Swecker, Judy Geiser, Jean Geiser, and my grandma Louise Hatter, have been such a wonderful community who have surrounded me with love and comfort for my whole entire life. I feel so blessed to have such wonderful grandparents who have developed rich relationships with me. I owe them everything and am so extremely appreciative of the love, dedication, and warmth that they have all provided me. They have supported me through every stage of life and have been some of my biggest cheerleaders for everything from my ballet recitals to my dissertation defense.

A very big thank you to the two teachers that were truly pivotal in getting me here - Dan Dries and Heather Gildea. Dan was my college research professor, and he has continued to be my biggest advocate and cheerleader through every step of my career. He has gone to bat for me, written me some of the most beautiful recommendation letters, and has been a model of mentorship that I truly strive to reach myself one day. He is literally the person who made me realize that even getting a PhD was possible and so I owe him so many thanks for opening my horizons and telling me that my opportunities were so much bigger than I could ever believe. Heather, my high school biology teacher, imparted on me such a love and wonder for science that has fueled my love for science for almost half my life. Her effusiveness and excitement for science was truly contagious and led to me getting my bachelor's in biochemistry, even though it felt like taking a huge leap without a safety net. She was truly a huge part of my life as a teenager and though she may not realize it, has molded the path of my life in a way that only she could have.

My bestie Nik Iacovelli who simply provided an escape for me whenever I needed it and never expected me to show up as anything other than my true self. We have grown up together, figured out adulthood together, and struggled through big life transitions together. He has been a shoulder to cry on, a smile when I most need one, and a Fortnite buddy when I just didn't want to think about anything. Thanks for being a wonderful friend.

Finally, thank you to everyone who has offered even a small amount of encouragement and support throughout this journey, I would not have made it through this journey without my community.

## TABLE OF CONTENTS

---

Abstract .....	2
Acknowledgements .....	3
Table of Contents .....	5
1.1 General organization of the mPFC .....	7
1.1.1 Neuronal subtypes and circuit organization .....	7
1.1.2 Adaptive disinhibitory gating and gain modulation .....	10
1.2 Executive function .....	10
1.2.1 Impulsivity and novelty-Seeking .....	10
1.3 Molecular control of behavior .....	14
1.3.1 Dopaminergic control of cognitive function .....	14
1.3.2 Cholinergic control of cognitive function .....	16
1.3.3 Serotonergic control of cognitive function .....	18
1.3.3.1 5-HT <sub>1</sub> Receptors .....	18
1.3.3.2 5-HT <sub>2</sub> Receptors .....	19
1.3.4 Noradrenergic control of cognitive function .....	20
2.1 Abstract .....	23
2.2 Introduction .....	23
2.3 Results .....	24
2.3.1 VIP-driven caspase-3 AAV injection into rodent mPFC selectively ablates VIP-expressing neurons .....	24
2.3.2 Ablation of VIP interneurons increases impulsive responding in long-delay trials	27
2.3.3 Ablation of VIP interneurons does not affect interest in novel animals .....	32
2.3.4 VIP Interneuron ablation does not increase spatial anxiety-like behavior .....	32
2.3.5 Ablation of VIP interneurons does not increase palatable food intake .....	32
2.4 Discussion .....	37
2.5 Experimental Methods .....	39
2.5.1 Experimental animals .....	39
2.5.2 Adeno-associated viral vector and stereotaxic viral injections .....	39
2.5.3 Brain tissue preparation .....	40
2.5.4 Quantitative analysis of VIP ablation by caspase .....	40
2.5.5 Three-choice serial reaction time task .....	40
2.5.6 Open Field Test .....	41
2.5.7 Social interaction .....	41
2.5.8 Binge-like eating assay .....	41
2.5.9 Statistical analysis .....	41
3.1 Obesity .....	43
3.1.1 Obesity and Co-Morbid Pathologies .....	43
3.1.2 Economic Impacts .....	43
3.1.3 Metabolic adaptation during obesity .....	43
3.1.3.1 Discrete metabolic profiles of metabolic adaptation through the lens of bariatric surgery .....	44
3.1.3.2 Summary .....	45
3.2 GLP-1 in The Control of Appetite .....	48

3.2.1 Gene expression and posttranslational processing .....	48
Figure 3-1: GLP-1 is produced as a product of posttranslational processing of proglucagon. Differential cleaving of proglucagon is mediated by organ-specific expression of prohormone convertases. Processing occurring in the intestines and brain produces GLP-1, GLP-2, glicentin, and oxyntomodulin, which have been implicated in the regulation of food intake. Processing in the pancreas produces glicentin-related pancreatic polypeptide (GRPP), glucagon, and the Major Proglucagon Fragment (MPGF). .....	49
3.2.2 GLP-1-mediated activation of appetite-regulatory networks.....	50
3.2.3 GLP-1R agonists and emerging combinatorial therapies in the control of obesity and type 2 diabetes .....	52
3.2.3.1 Growth differentiation factor 15 .....	52
3.2.3.2 Amylin .....	52
3.2.3.3 Adipokines: leptin, adiponectin, and interleukin-6.....	53
3.2.3.4 Endocrine-released hormones.....	54
4.1 Abstract.....	57
4.2 Introduction .....	57
4.3 Results .....	61
4.3.1 Established single-cell isolation techniques do not yield sufficient numbers of neurons .....	61
4.3.2 Significant levels of cellular debris during nuclear isolation prevents selective isolation .....	61
4.3.3 Pilot experiment using microfluidics-based cellular sorting and Smart-seq.....	64
4.3.4 Transcriptomic analysis of single-nuclei RNA-seq .....	66
4.4 Discussion.....	72
4.5 Experimental Methods.....	75
4.5.1 Experimental animals.....	75
4.5.2 Nuclei isolation protocol used for pilot experiment.....	75
4.5.3 Sorting of Nuclei Using NanoCollect WOLF Cell Sorter.....	76
4.5.4 Transcriptomic analysis.....	76
5.1 Summary.....	78
5.2 Discussion.....	78
5.2.1 GLP-1, Addiction, and the PFC .....	79
5.2.1.1 Cocaine .....	79
5.2.1.2 Amphetamines .....	80
5.2.1.3 Alcohol.....	80
5.2.2 The microbiome, reward, and addiction.....	80
5.2.2.1 Microbial metabolites and VAN activation .....	80
5.2.2.2 Microbiome and drugs of abuse.....	81
5.3 Future Directions .....	82
5.3.1 mPFC Control of Behavior .....	82
5.3.2 The Role of the Hindbrain in Obesity .....	84
References.....	86

# 1 CHAPTER 1: INTRODUCTION TO THE PREFRONTAL CORTEX

---

The prefrontal cortex (PFC) regulates executive functions (i.e., working memory, planning, decision making) in a goal-dependent manner through the control of diverse brain regions. Because aberrant PFC signaling is linked to mental illness and addiction, it is vital to explore possible mechanisms driving atypical cortical function.

## 1.1 GENERAL ORGANIZATION OF THE MPFC

The human PFC is divided into five distinct regions – dorsolateral (dlPFC), dorsomedial (dmPFC), medial (mPFC), ventromedial (vmPFC), and ventrolateral (vlPFC). Three of these brain regions share homology with the rodent PFC, based on Brodmann Areas (BA). The human vmPFC contains BA 25, which is homologous to the rodent infralimbic (IL) region. Both BA 32 and BA 24 span multiple subdivisions in the human brain and are homologous to the rodent prelimbic (PL) region and anterior cingulate cortex (ACC), respectively<sup>1</sup>. Together, these three regions of the rodent PFC are referred to as the medial PFC (mPFC) to differentiate it from other cortical structures.

Various studies have described the differential and specialized role the mPFC subregions have in the control of behavior<sup>2-6</sup>. These roles result from distinct innervations that each mPFC subarea receives from various other brain areas as well as their specific projections to brain areas to exert cortical control<sup>7-9</sup>. Apart from common projections to the orbitomedial prefrontal cortex, olfactory forebrain, and midline thalamus, the PL and IL innervate discrete brain areas<sup>8,9</sup>. IL neurons preferentially innervate brain areas regulating autonomic function such as the forebrain and the brainstem, while PL neurons preferentially innervate limbic brain areas, consistent with its role in cognitive function<sup>9</sup>. While these brain areas are functionally distinct, mPFC activation of both allows for integration of both autonomic and limbic systems to drive goal-directed behavior.

### 1.1.1 Neuronal subtypes and circuit organization

The rodent mPFC consists of large amounts of pyramidal neurons (PY) that span multiple layers and target extracortical brain regions to exert mPFC control. The output of these pyramidal neurons is strongly regulated by inhibitory  $\gamma$ -Aminobutyric acid (GABA)-expressing interneurons (IN). These interneurons can be divided into three distinct populations defined by the expression of parvalbumin (PV), somatostatin (SST), or serotonin receptor 3a (5-HT<sub>3A</sub>R)<sup>10</sup>. 5-HT<sub>3A</sub>R-expressing neurons can be further stratified by expression of cholecystokinin (CCK), vasoactive intestinal peptide (VIP), reelin, or neuron-derived neurotrophic factor (NDNF)<sup>10</sup>.

Interneuron connectivity is mediated by subtype-specific wiring rules that mediate the location of inhibitory input (i.e., synapsing onto dendrites or soma) and the preferential targeting of a specific subtype of neuron (i.e., inhibition of either PY or IN)<sup>11</sup>. These wiring

rules result in a local mPFC circuit (**Figure 1-1**) that establishes multiple mechanisms of feedback and feedforward inhibition, which stabilizes the activity of pyramidal neurons<sup>12,13</sup>. The cortex is comprised of approximately 70-80% pyramidal neurons, with the remaining 20-30% representing the entire population of GABAergic interneurons. This 20-30% of GABAergic neurons can be subdivided into the following three non-overlapping subclasses<sup>14</sup>:

- (1) PV-expressing neurons, which represent 30-50% of the GABAergic neurons (6-15% of total cortical neurons) and preferentially target the peri-somatic region of PY neurons to quickly control spike output.
- (2) SST-expressing neurons, which represent approximately 30% of cortical GABAergic neurons (~6-9% of total cortical neurons) and preferentially target PY dendrites to control distal inputs.
- (3) VIP-expressing neurons, which represent ~12% of cortical GABAergic neurons (~3-4% of total cortical neurons) and synapse onto PY neurons, PV neurons, and preferentially target SST neurons.

VIP neurons are of particular interest in the study of cortical control and dysregulation in cases of disease, particularly as extra-cortical inputs preferentially converge onto VIP interneurons, as indicated by greater density of innervation onto VIP interneurons than in any other interneuron subclass<sup>15-18</sup>.

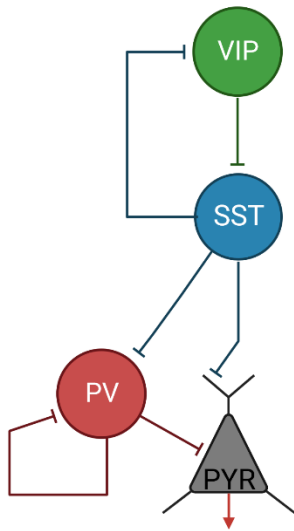


**Figure 1-1: mPFC wiring diagram.** The mPFC cortical circuit is comprised of three distinct subtypes of inhibitory interneurons that direct pyramidal neuron output through direct inhibition, as well as feedforward and feedback inhibition that increases stability of pyramidal neuron output. Created with BioRender.com. VIP = vasoactive intestinal peptide; SST= somatostatin; PV = parvalbumin; PYR = pyramidal neuron

### 1.1.2 Adaptive disinhibitory gating and gain modulation

VIP interneurons mediate pyramidal output via disinhibition, or relief of inhibition from SST and PV neurons onto PY neurons (**Figure 1-1**). This disinhibition has been implicated in an adaptive gating mechanism that can affect behavioral adaptation. VIP neurons have been associated with behavioral modification and increased cortical response to stimuli, indicating that VIP interneurons may affect cortical response to novel or unexpected stimuli<sup>19-21</sup>. A model of adaptive disinhibitory gating has been proposed to explain how unexpected stimuli trigger VIP-mediated dynamically modulated cortical circuit functioning and plasticity to enforce behavioral adaptations<sup>21</sup>. Disinhibition induces rapid modulation of cortical output in response to stimuli, resulting in a transient break in the excitation/inhibition (E/I) balance<sup>22</sup>. The resulting break in inhibition on PYs briefly allows for synaptic integration, selective amplification of PY response and coincidence detection<sup>21</sup>, resulting in reinforcement of associative learning.

## 1.2 EXECUTIVE FUNCTION

The mPFC receives diverse input from many different brain areas, which convey information such as emotional state and sensory information, which the cortex uses to modify behavior and make decisions<sup>23</sup>. The mPFC can control behavior through distinct mechanisms, including:

- (1) Cognitive inhibition, or focus, in which the mPFC is responsible for filtering out unimportant or non-relevant stimuli from the environment to maintain goal-directed behavior<sup>24-26</sup>.
- (2) Inhibitory control, or self-control, in which the mPFC is responsible for inhibiting impulses triggered by either external or internal cues<sup>25,27,28</sup>.
- (3) Working memory, in which the mPFC has been implicated in the ability to hold information temporarily to be retrieved in the near future<sup>29-31</sup>.
- (4) Cognitive flexibility, in which the mPFC allows for appropriate adaptation of action according to new information from the environment<sup>31-33</sup>.
- (5) Risk assessment, in which the mPFC balances the reward outcome of a behavior with the effort, in order to allow for avoidance of high risk, low reward situations while prioritizing low risk, high reward behavior<sup>34-36</sup>.

Through its control of attention and decision-making, the mPFC maintains goal-directed behavior by relaying information to various brain areas.

### 1.2.1 Impulsivity and novelty-Seeking

Impulsivity, or a lack of inhibitory control, is defined broadly as an inability to withhold from or stop a response despite a known negative consequence. Impulsive behavior can include an inability to delay gratification, acting without forethought, or preferring a small reward immediately rather than waiting for a larger reward later<sup>37</sup>. During decision making processes, neurotypical individuals will face impulsive thoughts or triggering stimuli but

normally functioning cognitive control will inhibit neuronal responses to maintain goal-directed behavior (**Figure 1-2**). Individuals with increased impulsivity, however, either lack or have decreased inhibition of the resulting impulse from triggering stimuli and thus will engage in an impulsive action, even when aware of a negative outcome (**Figure 1-2**)<sup>37</sup>. Impulsivity is comorbid with novelty-seeking, a trait that drives an increase in investigatory behavior in response to a novel stimulus. While increased novelty- or sensation-seeking increases risk taking or thrill-seeking in the search for novel and stimulating sensations (colloquially described as recklessness or spontaneity), impulsivity involves a failure to inhibit spontaneous or unplanned behavior (colloquially described as carelessness or capriciousness)<sup>38,39</sup>.

Impulsivity is a hallmark of a group of psychological disorders classified as impulse-control disorders (ICD), such as attention-deficit/hyperactivity disorder (ADHD), obsessive-compulsive disorder (OCD), and behavioral addictions (e.g., kleptomania, pathological gambling, binge eating disorder, compulsive sexual behavior)<sup>40-46</sup>. According to the fourth edition of the Diagnostic and Statistical Manual of Mental Disorders (DSM-IV), about 10.5% of the U.S. population suffers from an impulse-control disorder such as ADHD, OCD, and behavioral addictions<sup>46</sup>.

Both increased impulsivity and novelty-seeking are key indicators in addiction and are prominent behavioral markers across all phases of SUD<sup>47-49</sup>, placing individuals with an ICD at an increased risk to develop a SUD (**Figure 1-3**)<sup>50-55</sup>. Both impulsivity and novelty-seeking are strongly associated with both the development and maintenance of a substance use disorder (SUD)<sup>56,57</sup> and even moderate the efficacy of SUD treatment<sup>58,59</sup>. Current research indicates that increased novelty-seeking is a predictor of an individual's vulnerability to first use drugs, with high novelty seekers experimenting with drugs at an earlier age and using more types of drugs<sup>60,61</sup>. Increased impulsivity, however, is a predictor of the development of a SUD and of increased vulnerability to relapse during periods of sobriety<sup>39,62,63</sup>. SUDs have been found to increase impulsivity, facilitating further and more varied drug use<sup>64,65</sup>. Thus, continued study of the cognitive underpinnings of aberrant impulsivity and novelty-seeking is vital in improving pharmacological treatment for both ICDs and SUD.

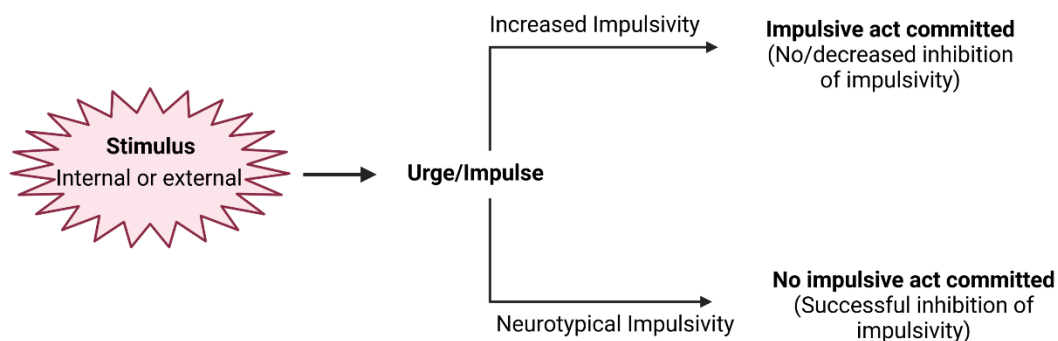


**Figure 1-2: Model of impulsivity as a lack of cortical inhibition.** Impulsivity is triggered by a stimulus, which can be either internal or external. Internal stimuli can include impulsive thoughts or a specific emotional state. External stimuli can include triggering physical events or situational variables. In a situation where the inhibitory process is fully functional, the urge to perform an impulsive action would be inhibited, while in individuals with increased baseline impulsivity, the individual will perform the impulsive act even if aware of the negative implications. Thus, inability to inhibit impulsive action due to stimuli is at the crux of both addiction and impulse-control psychopathologies. Adapted from Bari and Robbins<sup>37</sup>. Figure created with BioRender.com.

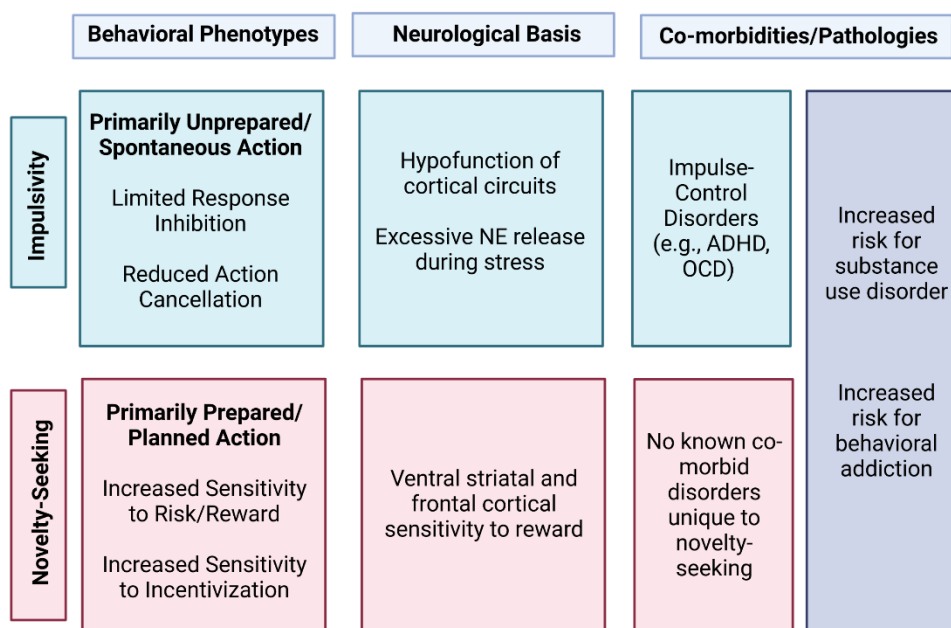


**Figure 1-3: Trait impulsivity and novelty-seeking and their associated psychological effects.** Increased trait impulsivity in individuals leads to limited response inhibition and reduced action cancellation specifically when tasked with decision-making that is spontaneous<sup>66,67</sup>. These behavioral phenotypes can often result in uncontrolled self-administration of a drug or harmful behavior<sup>68</sup>. Current research has determined that this is due to hypofunction in the cortex<sup>48,69</sup>, in part due to excessive noradrenaline release that occurs during a stimulus that triggers impulsive action<sup>5,70-74</sup>. Increased novelty- or sensation-seeking results in increased sensitivity to both risk and reward, and increased sensitivity to the reinforcing properties of that reward. Together, these traits make individuals with heightened novelty-seeking experience greater reward from a drug or harmful behavior, thus reinforcing addiction<sup>75,76</sup>. Current data implicates increased ventral striatal activity, possibly due to increased dopamine release during rewarding activities<sup>77,78</sup>. Adapted from Vassileva and Conrod<sup>55</sup> and Castellanos-Ryan and Conrod<sup>68</sup>. Created with BioRender.com.

### 1.3 MOLECULAR CONTROL OF BEHAVIOR

While impulsive action and novelty-seeking are implicated in almost all addictive disorders and other impulse-control psychopathologies, the biological causes of these behavioral aberrations have still not been fully elucidated. Impulsivity has been largely attributed to hypofunction in the prefrontal cortex (PFC)<sup>48,69</sup>, leading to reduced inhibition of impulsive responding, but very little is known about the molecular mechanisms or neural communication systems that contribute to this phenotype. Two major brain pathways that converge onto the PFC – dorsal and median raphe serotonergic innervation and locus coeruleus adrenergic innervation- have been implicated in the control of impulsivity and novelty-seeking. Cholinergic innervation from the basal forebrain and local cortical production of acetylcholine have been shown to have some control over impulsive action but have been more greatly implicated in the control of attention. Dopamine (DA) synergistically interacts with these pathways, resulting in distinct but parallel aberrations in behavior that are also implicated in ICDs and SUD. Additionally, while the following discussions of the pathways that mediate PFC function will be described as if they operate in isolation for the sake of clarity, it bears mentioning that these pathways are highly interconnected and have behavioral implications beyond the scope of impulse control and novelty-seeking though not described here.

#### 1.3.1 Dopaminergic control of cognitive function

While the mesocortical pathway is often implicated in disorders of cognitive control, there is not a strong body of evidence indicating that direct dopaminergic activation from the ventral tegmental area (VTA) onto the mPFC is responsible for the maladaptive neuronal changes modifying the motivational drive or “craving” to consume a drug of choice. Rather, increasing evidence indicates that PFC dysfunction is due to DA effecting behavioral control via the mesolimbic pathway, where the nucleus accumbens (NAc) processes rewarding (inherent or conditioned pleasure) and reinforcing (facilitates survival, i.e. food and water) stimuli<sup>79-81</sup>.

Cools, *et al.* posit that the NAc modulates motivational drive according to a cost-benefit analysis that is biased towards decreased cognitive load<sup>82</sup>. Because cognitive control is inherently “costly” (reviewed in<sup>83</sup>), healthy individuals will tend to choose a less cognitively-demanding task, due to a behavioral phenomenon called cognitive effort discounting (COD)<sup>83-86</sup>. Thus, if a goal-mediated behavior is deemed too cognitively taxing or has an accompanying reward that is not deemed to be sufficiently rewarding, the NAc assigns low motivational value to the behavior and employs a dopamine-dependent decision to not exert control over the PFC<sup>87</sup>. In this model of cortical control, dopamine does not directly modulate PFC function, but rather enhances or impairs the motivational value attached to a behavior and therefore affects the willingness to exert cognitive control<sup>82</sup>. Therefore, aberrations in sensation- or novelty-seeking may be primarily activated by dopaminergic pathways.

To determine how dopamine affects COD, adults were tested using a cognitive effort discounting paradigm (COG-ED), in which participants were tasked with choosing between a low-effort task for a small reward or a high-effort task for a larger reward<sup>86,88</sup>. After a practice phase, participants are then asked to choose between repeating a high-

effort task for more money or a low-effort task for less money<sup>86,88</sup>. While the higher reward remained fixed, the reward for the lower-effort task increased after choosing a high-reward task and decreased after choosing a low-reward task<sup>88</sup>. Adult participants showed clear discounting of the reward in a difficulty-dependent manner, where participants were willing to be paid less money to avoid a more cognitively engaging task<sup>86,88</sup>. To further query the neuronal control mechanisms of COD, healthy older adults were administered tyrosine to determine the effects of increased dopamine in COG-ED. Consumption of tyrosine, the precursor of DA and noradrenaline, has been linked with enhanced cognitive performance, possibly through increased synthesis and release of catecholamines<sup>89,90</sup>. To determine how baseline cognitive differences may affect COG-ED choices, subjective values (SV) were measured against trait impulsivity scores (Barratt Impulsiveness Scale). SV of rewards indicate the level of value depreciation related to the amount of effort required to complete the task, with SV decreasing linearly with increased effort<sup>86</sup>. It was determined that tyrosine administration resulted in SV depreciation across all effort levels as a function of increased trait impulsivity<sup>88</sup>. These results indicated that in individuals with higher trait impulsivity, increased dopamine reduces the motivational value of cognitive control.

This model of decreased motivational value of cognitive control during increased DA in impulsive individuals could underpin ADHD pathologies. It is possible that maladaptation of dopaminergic pathways in ICDs such as ADHD causes high motivational value to be attached to highly stimulating behaviors (i.e., high-thrill activities, high-novelty experiences, illegal activities, rebelliousness) and low motivational value to be attached to uninteresting or unstimulating behaviors, especially ones that require high cognitive demand (i.e., schoolwork, sustained attention during school/work/church, cleaning)<sup>91</sup>. This atypical assignment of motivation results in the distinct pathologies of impulse control disorders such as ADHD.

NAC control of reinforcement learning also plays a significant role in addiction. Repeated drug use results in the sensitization of the mesolimbic pathway and can be permanent<sup>79</sup>. The incentive-sensitization theory of addiction posits that individuals will continually increase drug use, even while pleasure obtained decreases, due to mesolimbic sensitization<sup>79,80</sup>. Because dopaminergic action attaches motivational significance to a reward, increased sensitization results in hyper-reactivity to drug cues, triggering intense cravings<sup>79</sup>. In individuals with SUD, these cravings increase vulnerability to relapse and therefore will continue to further sensitize the mesolimbic system through a maladaptive feed-forward mechanism. While aberrations in impulse control also predict increased vulnerability to relapse<sup>39,62,63</sup>, the lack of evidence linking dopaminergic action to cortical control of impulsive behavior implicates a negative synergistic effect between (1) SUD- or ICD-mediated neuroadaptations of serotonergic, cholinergic or noradrenergic innervation onto the PFC leading to increased impulsivity, and (2) increased mesolimbic sensitization due to a SUD-mediated maladaptive feed-forward mechanism, leading to intense cravings when faced with drug cues. Thus, when an individual experiences intense drug cravings, the concomitant lack of impulse inhibition results in an even higher likelihood to capitulate and engage in drug use.

### 1.3.2 Cholinergic control of cognitive function

Acetylcholine (ACh) release in the mPFC primarily originates in the basal forebrain (BF) and is also present in small populations of cortical interneurons<sup>92–96</sup>. There are two forms of ACh receptors – nicotinic (nAChR) and muscarinic (mAChR), which are functionally distinct. The nAChRs are ligand-gated cation-selective channels while mAChRs are G-protein coupled receptors<sup>97</sup>. nAChRs are made up of five subunits arranged symmetrically around a central pore. There are twelve neuronal subunits ( $\alpha 2 - \alpha 10$  and  $\beta 2 - \beta 4$ ), resulting in a large variety of receptor subtypes<sup>98</sup>. In the cortex, only two main types of receptors are present – homopentameric receptors comprised of five  $\alpha 7$  subunits and heteromeric receptors comprised of two  $\alpha 4$  subunits, two  $\beta 2$  subunits and either an  $\alpha 4$ ,  $\beta 4$  or  $\alpha 5$  subunit (**Figure 1-4**)<sup>99,100</sup>. There are five different subtypes of mAChRs, all of which are G-coupled protein receptors (GPCRs)<sup>101</sup>. In the cortex, M1, M2 and M4 receptors are present, with M1 interacting with Gq/11 proteins, while M2 and M4 receptors interact with Gi/o proteins (**Figure 1-4**)<sup>102,103</sup>. Through intracellular signaling cascades, ACh binding to mAChRs affects primarily potassium and calcium channels to affect membrane polarization<sup>104</sup>.

Choline acetyltransferase (ChAT), an acetylcholine synthesizing enzyme, has been shown to be primarily expressed in VIP-expressing interneurons<sup>94</sup>. Approximately 30% of VIP interneurons are ChAT positive (VIP<sup>+</sup>/ChAT<sup>+</sup>), making VIP<sup>+</sup>/ChAT<sup>+</sup> interneurons only approximately 0.5% of the cortical neuron population<sup>105–108</sup>. These neurons have been found to release both ACh and GABA, indicating their ability to modulate cortical activity via different transmitter mechanisms<sup>109</sup>. In contrast to other VIP-expressing interneurons, VIP<sup>+</sup>/ChAT<sup>+</sup> interneurons do not disinhibit pyramidal neurons<sup>109</sup>. It is believed that cholinergic activity from the BF is responsible for early phases of attentional control while activity of local VIP<sup>+</sup>/ChAT<sup>+</sup> interneurons is responsible for later attentional control<sup>109–113</sup>.

While it has been well-established that cholinergic signaling in the cortex primarily controls attention (reviewed in <sup>97</sup>), a small body of literature has indicated that ACh signaling in the cortex may additionally affect impulsivity. Both human and animal studies have shown that nicotine administration is sufficient to produce increased impulsive action, primarily through the heteromeric subtypes of nAChRs<sup>114–119</sup>. Additionally, one group had found that administration of a heteromeric nAChR antagonist was sufficient to suppress impulsive behavior even in the absence of nicotine<sup>120</sup>. Of particular interest is that this control of impulsive action via heteromeric nAChRs in the cortex has been shown to occur primarily in the IL<sup>116</sup>, further implicating the distinct roles of the cortical subareas in the control of behavior. Beyond this data, however, the role of cholinergic signaling in the control of impulsivity remains vastly understudied, making it difficult to hypothesize how cholinergic signaling may differentially modulate the cortical microcircuit.

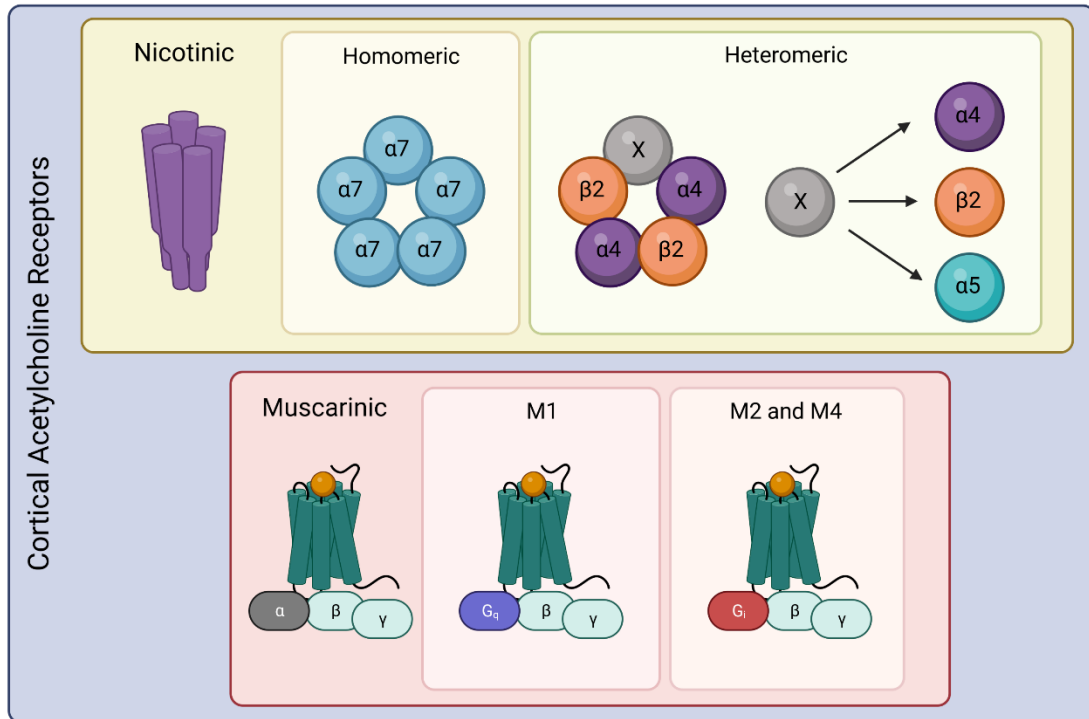


**Figure 1-4: Types of acetylcholine receptors.** There are two forms of acetylcholine receptors – nicotinic and muscarinic. Nicotinic receptors are ligand-gated cation-selective channels that are made up of five subunits arranged symmetrically around a central pore. In the cortex, only two main types of receptors are present – homopentameric receptors comprised of five  $\alpha 7$  subunits and heteromeric receptors comprised of two  $\alpha 4$  subunits, two  $\beta 2$  subunits and either an  $\alpha 4$ ,  $\beta 4$  or  $\alpha 5$  subunit<sup>99,100</sup>. Muscarinic receptors are G-protein coupled receptors. In the cortex, M1, M2 and M4 receptors are present, with M1 interacting with  $G_q/11$  proteins, while M2 and M4 receptors interact with  $G_i/o$  proteins<sup>102,103</sup>. Created with BioRender.com.

### 1.3.3 Serotonergic control of cognitive function

Serotonergic input to the cortex is primarily provided by ventrally-located serotonergic neurons in the dorsal raphe (DR)<sup>91</sup>. The PFC also sends reciprocal projections to the DR, which mediate PFC top-down control of motivated behavior such as impulsivity<sup>121–123</sup>. Serotonin receptors (5-HTRs) consist of seven subfamilies, 5-HT<sub>1</sub> to 5-HT<sub>7</sub>, all of which are G-coupled protein receptors, apart from 5-HT<sub>3</sub>, which is a ligand-gated cation channel. Serotonergic neurotransmission has been implicated in diseases caused by altered cognitive function, such as major depressive disorder (MDD), schizophrenia, and OCD<sup>124</sup>. In the mPFC, pyramidal neurons and PV and SST inhibitory interneurons primarily express 5-HT<sub>1A</sub>R and 5-HT<sub>2A</sub>R, but VIP inhibitory interneurons additionally express 5-HT<sub>3A</sub>R<sup>10,125</sup>. Further characterization via *in situ* hybridization revealed that two separate populations of PV interneurons express either 5-HT<sub>1A</sub>R or 5-HT<sub>2A</sub>R, but not in the same neuron<sup>126</sup>.

#### 1.3.3.1 5-HT<sub>1</sub> Receptors

The 5-HT<sub>1</sub> family of receptors are G<sub>i</sub>/G<sub>o</sub>-coupled and when activated, hyperpolarize neuronal membranes via the downstream activation of G-coupled inwardly rectifying K<sup>+</sup> channels (GIRKs)<sup>127</sup>. Across models and measurements of altered impulsivity, 5-HT<sub>1A</sub>R agonists have been shown to exhibit a biphasic response, in which low doses and high doses of an agonist have opposing effects on behavior. For example, biphasic HT<sub>1A</sub>R has been represented in a variable consecutive number (VCN) model in which animals are trained to respond on one lever until cued to respond on a second lever<sup>128</sup>. Correct cue-directed responding is reinforced via reward delivery, while premature/impulsive responding results in a 5 s timeout and task reset. Animals that were given 8-OH-DPAT, a selective 5-HT<sub>1A</sub>R agonist, exhibited increased impulsivity as measured by reduced accuracy during VCN at low doses of 8-OH-DPAT. At high doses, animals demonstrated significantly decreased impulsivity and even achieved perfect accuracy at the highest dose of 8-OH-DPAT<sup>128</sup>.

Biphasic response of 5-HT<sub>1A</sub>R agonism is due to both presynaptic (autoreceptor) and postsynaptic functions<sup>129</sup>. 5-HT<sub>1A</sub>R autoreceptors located on the soma and dendrites of DR-localized serotonergic neurons maintain serotonergic tone via an autoregulatory feedback response during heightened local concentration of serotonin. The autoreceptors thus function to suppress serotonin synthesis, turnover, and release at terminal projections through direct, autonomous inhibition<sup>129–132</sup>. At low agonist concentrations, 5-HT<sub>1A</sub>R autoreceptors are activated and decreases serotonin release into the PFC, thus increasing impulsivity. At high agonist concentrations, PFC 5-HT<sub>1A</sub>R is directly activated regardless of DR-mediated changes in activation and successfully decreases impulsivity.

Translationally, impaired 5-HT<sub>1A</sub>R function is implicated in individuals with impulse aggression, characterized by explosive reactions to situations that exceed the “normal” level of emotion<sup>133</sup>. Participants were administered oral ipsapirone, a selective partial 5-HT<sub>1A</sub> receptor agonist, and 5-HT<sub>1A</sub>R function was determined via analysis of plasma cortisol and plasma prolactin. Under a normally functioning 5-HT<sub>1A</sub>R, agonism should result in increased serum cortisol and prolactin. Analysis of cortisol and prolactin levels post-ipsapirone indicated that impulsivity was the sole significant predictor of both decreased cortisol and prolactin release<sup>134</sup>. Measurement of 5-HT<sub>1A</sub>R-mediated hormone release indirectly implicates decreased 5-HT<sub>1A</sub>R function in the control of increased

impulsivity. One genome-wide association study (GWAS) has enabled broader investigation into possible genetic variants of the 5-HT<sub>1A</sub>R gene (*HTR1A*) and found that common variants in the *IPO11-HTR1A* region were significantly associated with alcohol and nicotine co-dependence at genome wide-significance level, while rare variants were only associated with ADHD<sup>135</sup>. Variants were closely located in the same region, lending genetic evidence to observed co-morbidity of ADHD and substance abuse<sup>135</sup>. Further functional analysis into variations of 5-HT<sub>1A</sub>R is necessary to enable further understanding of the genetic and molecular underpinnings initiating altered 5-HT<sub>1A</sub>R function.

### 1.3.3.2 5-HT<sub>2</sub> Receptors

Receptors in the 5-HT<sub>2</sub> family are G<sub>q</sub>/G<sub>11</sub>-coupled and when activated, increase cellular levels of IP<sub>3</sub> and DAG, leading to an excitatory action potential. Knockdown of 5-HT<sub>2C</sub>R in the mPFC is sufficient to increase motor impulsivity as measured by a 1-choice serial reaction time task (1-CSRTT)<sup>136</sup>. In brief (serial reaction time tasks are discussed more in depth in Chapter 2), this behavioral assay trains rodents to correctly identify and respond to a visual cue within a set time (5 seconds). Premature responses, in which the animal responds before the visual cue appears, are considered an indicator of motor impulsivity. In rodents trained on a 5-choice serial reaction time task (5-CSRTT), the 5-HT<sub>2A</sub>R antagonists ketanserin and M100907 decreased premature responding and increased the number of omissions, while the 5-HT<sub>2C</sub>R antagonist SB242084 increased premature responding and slightly reduced response accuracy<sup>137,138</sup>. These data demonstrate that both mPFC 5-HT<sub>2C</sub>R and 5-HT<sub>2A</sub>R specific activation are sufficient to modulate impulsivity behavior through serotonergic action.

5-HT<sub>2A</sub>R and 5-HT<sub>2C</sub>R regulate the excitatory/inhibitory balance in the mPFC and are thought to interact under compensatory mechanisms. Selective 5-HT<sub>2C</sub>R knockdown results in a compensatory upregulation of 5-HT<sub>2A</sub>R protein expression and selective 5-HT<sub>2A</sub>R antagonism via M100907 in 5-HT<sub>2C</sub>R knockdown animals decreased motor impulsivity as measured by a 1-choice serial reaction time task (1-CSRTT)<sup>136</sup>. The compensatory action of the 5-HT<sub>2A</sub> and 5-HT<sub>2C</sub> receptors seems to be vital in maintaining optimal serotonergic tone across various profiles of PY neuron engagement.

Because hallucinogens mimic features of early-stage schizophrenia like cortical hypofrontality, researchers argue that the molecular mechanisms driving a hallucinogenic state mirror neurobiological abnormalities in early-stage schizophrenia<sup>139</sup>. This hypothesis has been supported by data showing higher proportion of active conformation 5-HT<sub>2A</sub>R in the PFC of schizophrenic individuals, resulting in increased activation of 5-HT<sub>2A</sub>R due to preferential binding to the receptor in its active conformation<sup>140</sup>. This phenotype is mirrored by psilocybin-mediated 5-HT<sub>2A</sub> receptor activation leading to serotonergic hyperactivity<sup>141</sup>. Thus, hallucinogens serve as a useful tool to better understand the causality behind the pathophysiology of schizophrenia and the possible mechanisms regulating the accompanying dysregulated impulse control. Hallucinogens such as DOI (2,5-dimethoxy-4-iodoamphetamine) increase impulsive decision making as measured by a delay discounting task (DDT), in which animals are required to choose a delayed, large reward or an immediate, small reward<sup>142</sup>. Animals given DOI demonstrated a choice preference for the immediate, small reward in a dose-dependent manner<sup>142</sup>. When schizophrenic individuals were tasked with a DDT, they chose the immediate, smaller reward more often than healthy patients<sup>143</sup> Together, this evidence strongly indicates that

5-HT<sub>2A</sub>R hyperfunction is responsible for driving impulsivity in both schizophrenia and hallucinogenic drug use.

5-HT<sub>2C</sub>R signaling is fundamentally altered in individuals with the 5-HT<sub>2C</sub>R cys23ser polymorphism, which is prevalent in 12-30% of individuals, depending on ancestral background<sup>144</sup>. The serine variant of the 5-HT<sub>2C</sub>R is associated with depression, bipolar disorder, and high sensitivity to drug-related cues<sup>145-147</sup> and has been loosely tied to increased impulsivity in males<sup>148</sup>. The cys23ser polymorphism reduces 5-HT binding affinity, attenuates agonist-induced intracellular signaling, and has lower plasma membrane expression than the wild-type variant<sup>144,149,150</sup>. Since 5-HT<sub>2C</sub>R antagonism increases impulsive responding in rodents, it can be extrapolated that the polymorphism-mediated decrease in intracellular signaling results in similar behavioral phenotypes<sup>137</sup>. While this is a compelling hypothesis, further experimentation should be done to examine motor impulsivity with a 5-CSRTT in both 5-HT<sub>2C</sub>R knockout animals and animals with a knock-in point mutation to mimic the naturally occurring 5-HT<sub>2C</sub>R cys23ser polymorphism. This will also enable further query into the whether the 5-HT<sub>2C</sub>R cys23ser polymorphism is sufficient to drive compensatory expression of 5-HT<sub>2A</sub>R to further elucidate how these receptors may contribute to impulse-control aberrations.

### 1.3.4 Noradrenergic control of cognitive function

It has been hypothesized that locus coeruleus (LC) innervation into the PFC is at least partially responsible for the control of impulsive action. While the PFC receives information from a myriad of brain locations, it receives the densest noradrenergic innervation from the LC, which is involved in the stress and panic response<sup>151</sup>. Researchers have proposed that through noradrenaline (NA) release in the mPFC, phasic burst firing in LC-PFC projections is able to activate attention, maintain focus, and optimize task performance, likely due to an evolutionary-conserved mechanism to improve cognitive function when faced with a threatening stimulus<sup>152-156</sup>.

Varied levels of neuronal excitability in response to NA release are achieved through the variety of adrenergic receptors (AR) present in the cortex. Adrenergic receptors are a class of G protein-coupled receptors, which signal through different subtypes of G-proteins. To be engaged,  $\beta$ -adrenergic receptors ( $\beta$ -AR) require high NA concentrations ([NA]) due to their low affinity to NA ( $K_i = 3570-26,400$  nM)<sup>157</sup>. When bound to NA,  $\beta$ -AR initiates the adenylyl cyclase/cyclic AMP (cAMP) signaling pathway through the  $G_s$  protein, which impairs PFC function<sup>158,159</sup>. Alpha-1-adrenergic receptors ( $\alpha_1$ -AR) require moderate [NA] (moderate NA affinity,  $K_i = 56-990$  nM)<sup>160</sup> and activate the phospholipase C/IP<sub>3</sub>/DAG signaling pathway through the  $G_q$  subunit. Alpha-2A adrenergic receptors ( $\alpha_2A$ -AR) require the lowest [NA] (high NA affinity,  $K_i = 5.56-5.87$  nM)<sup>161</sup> and inhibit the adenylyl cyclase/cAMP signaling pathway<sup>162</sup>. The varying affinities of the ARs allow for gain amplification, thus affecting cortical functioning under different [NA] (**Figure 1-5**).

Auto-receptors for NA serve as gain modifiers to regulate [NA] at both high and low local levels of NA. Pre-synaptic  $\alpha_2A$ -AR will inhibit NA release under low to moderate [NA]<sup>163-166</sup>, while pre-synaptic  $\beta$ -ARs amplify NA release when activated by high levels of NA<sup>167</sup>. Alpha2-ARs are also voltage-dependent, and during neuron depolarization will lose their affinity for NA, thus removing their inhibitory effect as local [NA] increases during times

of high stress, further biasing neuronal response towards increased NA release<sup>168</sup>. At saturating levels of NA,  $\alpha$ 2-ARs regain their affinity for NA, allowing for a return to homeostasis after a response to a stimulus has occurred<sup>168</sup>. Through these feedback loops, moderate [NA] is maintained to facilitate optimal cognitive functioning, while also working as gain modulators to further increase or decrease incoming adrenergic signals<sup>169,170</sup>.

It has been established that NA transmission is altered in individuals with ADHD<sup>171–173</sup> and several pharmacological interventions have been successful in decreasing impulsive response. Atomoxetine, a selective NA reuptake inhibitor, improves response inhibition in both humans and rats when administered systemically (orally or i.p, respectively)<sup>174–177</sup>. No studies have been done to determine if atomoxetine administered intracerebrally into the PFC would be sufficient to drive this phenotype. Guanfacine, an FDA-approved ADHD medication, is a selective  $\alpha$ 2-adrenoreceptor agonist and has been found to strengthen working memory, increase behavioral inhibition, and improve attention, both when administered systemically and infused directly into the PFC<sup>178–182</sup>. Guanfacine-mediated increased cognitive function via  $\alpha$ 2-AR agonism implicates increased adenylyl cyclase/cAMP in decreased cognitive function. Blockade of  $\beta$ 1-ARs via betaxolol, a specific  $\beta$ 1-AR antagonist, was found to increase cognitive function as measured by improved working memory performance<sup>183</sup>. Conversely, activation of  $\beta$ 2-ARs via clenbuterol, a  $\beta$ 2-AR agonist, improved working memory, but only in animals already experiencing cognitive deficits due to aging<sup>184</sup>. Because adrenergic receptors have both unique binding affinities and varied responses to NA binding, the LC can exert control over PFC functioning by affecting local [NA].

Both excitatory and inhibitory neurons in each layer of the PFC express at least one adrenergic receptor<sup>185–196</sup> and similar proportions of both cortical PY and inhibitory interneurons (VIP, SST, PV) are contacted by LC-NA afferents<sup>197</sup>. Toussay *et al.* found that LC-NA innervation primarily activated PV and SST interneurons (~36% of each population) and activated significantly fewer VIP interneurons (~16%) and PY neurons (22%)<sup>197</sup>. This response was ameliorated via cortical NA denervation with DSP-4, a neurotoxin that is selective for noradrenergic neurons<sup>197</sup>. The lack of data directly characterizing the adrenergic receptor profile of specific sub-classes of PFC neurons along with the broad LC-NA innervation of the PFC across all subtypes of neurons makes it difficult to hypothesize the differential effects that NA signaling has on interactions within the microcircuitry of the mPFC. Further research examining the role of NA in disrupting “typical” communication in the mPFC is necessary to be able to fully understand how mPFC AR signaling can improve cognitive function and reduce impulsive action.

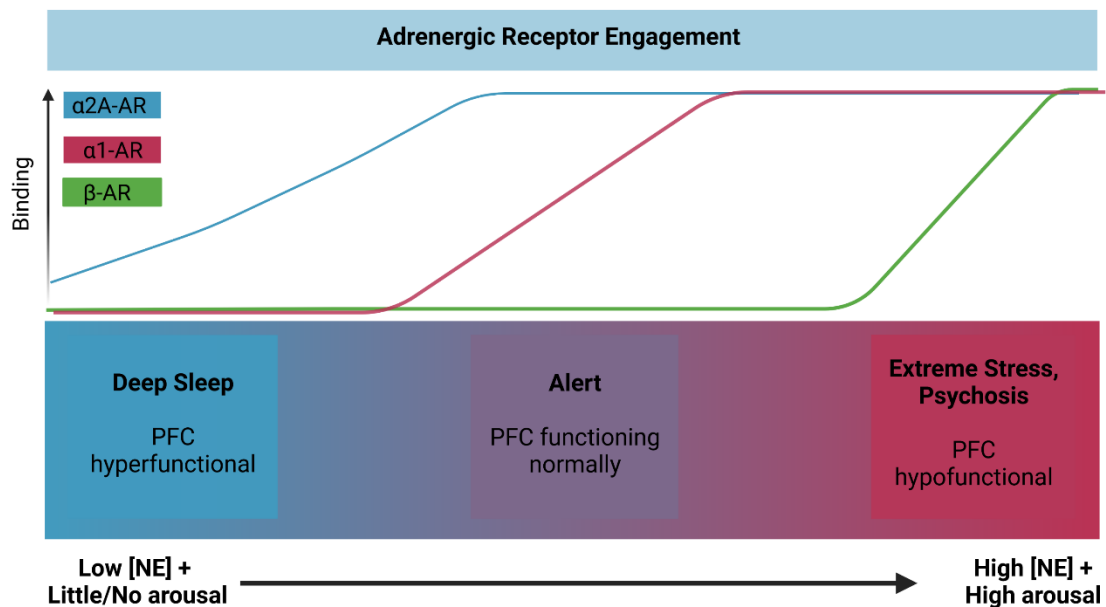


**Figure 1-5: Model of adrenergic receptor engagement relies on different binding affinities to affect behavior.** The various adrenergic receptors (AR) located on cortical neurons allow for NA-mediated gain modulation to further decrease the activity of neurons receiving inhibitory input, and further increase the activity of neurons receiving excitatory input. This modulation is achieved through the differential affinities of each AR, which are engaged differentially according to the local levels of NA. Thus, NA from the LC can regulate cortical brain function to prioritize action that is most beneficial to the host according to outside stimuli. Created with BioRender.com.

## 2 CHAPTER 2: VIP INTERNEURONS AND THEIR CONTROL OF BEHAVIOR

---

### 2.1 ABSTRACT

It has been well-established that novelty-seeking and impulsivity are significant risk factors for the development of psychological disorders, including substance use disorder and behavioral addictions. While dysfunction in the prefrontal cortex is at the crux of these disorders, little is known at the cellular level about how alterations in neuron activity can drive changes in impulsivity and novelty seeking. We harnessed a cre-dependent caspase-3 ablation in both male and female mice to selectively ablate vasoactive intestinal peptide (VIP)-expressing interneurons in the prefrontal cortex to better explore how this microcircuit functions during specific behavioral tasks. Caspase-ablated animals had no changes in anxiety-like behaviors or hedonic food intake but had a specific increase in impulsive responding during longer trials in the three-choice serial reaction time test. Together, these data suggest a circuit-level mechanism in which VIP interneurons function as a gate to selectively respond during periods of high expectation.

### 2.2 INTRODUCTION

In both humans and mice, the medial prefrontal cortex (mPFC) bidirectionally regulates goal-seeking behavior, such as novelty-seeking and impulsivity<sup>198</sup>. Various studies have demonstrated abnormal activity of the mPFC in patients with substance use disorder (SUD) or behavioral addictions (e.g., pathological gambling, kleptomania, binge eating, compulsive sexual behavior)<sup>25,42,53,199–206</sup>. Additionally, impulsivity and novelty-seeking are strongly associated with both the development and maintenance of SUD<sup>56,57</sup>, and even moderate the efficacy of SUD treatment<sup>59,207,208</sup>. While dysfunction in the mPFC may underpin conditions that are often characterized by alterations in reward pursuit in both males and females<sup>209–211</sup>, very little is known about how specific neuronal populations in the mPFC regulate these behaviors.

Extra-cortical glutamatergic, serotonergic, and cholinergic inputs converge onto vasoactive intestinal peptide (VIP)-expressing interneurons in the mPFC<sup>15–18</sup>, placing them at an ideal position to serve as a mediator between long-range inputs and local cortical processing. VIP interneurons are associated with behavioral modification, especially following reward presentation<sup>19,20</sup>, implicating their role in novelty-seeking and impulsivity phenotypes. By providing inhibitory input onto somatostatin (SST) interneurons that innervate pyramidal (PY) neurons, VIP interneurons provide indirect, disinhibitory input onto PY neurons. Because of their unique position to regulate novelty-seeking and impulsivity, through both their myriad of inputs as well as their local circuit control, it is of particular interest to better understand how VIP interneurons function in the control of behavior.

The rodent mPFC is composed of three primary subareas – the anterior cingulate cortex (ACC), the prelimbic cortex (PL), and the infralimbic cortex (IL). Studies have suggested these mPFC subregions have differential and specialized roles in behavior, including the control of social interaction, palatable food intake, and novel object investigatory behavior

<sup>2-6</sup>. These roles result from the distinct projections that each mPFC subarea receives from various other brain areas, which primarily converge onto VIP interneurons<sup>7-9,212</sup>. As such, we hypothesized that selective ablation of VIP interneurons in the IL would be sufficient to modulate both impulsive responding as measured by a three-choice serial reaction time task and novelty-seeking as measured by novel animal investigation. Using an adeno-associated virus (AAV) construct encoding a cre-dependent caspase-3, we were able to investigate whether VIP interneuron control is necessary in the modulation of behavior. VIP ablation in the mPFC led to a specific increase in impulsive responding during long-delay trials, with no non-specific effects on anxiety-like behaviors or food-related motivation, revealing a novel role of VIP neurons in the control of impulsive behavior.

## 2.3 RESULTS

### 2.3.1 VIP-driven caspase-3 AAV injection into rodent mPFC selectively ablates VIP-expressing neurons

Various studies have described the differential and specialized roles the mPFC subregions have in the control of social behavior. For example, Huang, *et al.* found that activation of projections from the PL to the basolateral amygdala (BLA) impaired social interaction, while inhibition of IL-BLA projections also impaired social interaction<sup>2</sup>. This is most likely due to the distinct projections that each subarea receives, as well as the differences in the areas that each subarea innervates<sup>7-9</sup>. Additional studies have directly implicated the PL and IL in behavioral inhibition, indicating that inhibition of PL neurons increased premature responses, while inhibition of IL neurons decreased premature responses in a response preparation task<sup>4</sup>. Because VIP neurons are the primary convergence point of projections into the mPFC, we hypothesized that VIP neurons would be an important gateway point for behavioral modification. Therefore, we aimed to resolve the contribution of IL VIP neurons to the control of impulsive behavior, as measured by a three-choice serial reaction time task (3CSRTT). To evaluate this contribution, we measured 3CSRTT reaction times in mice wherein IL VIP neurons were ablated. In order to visualize VIP neurons, we created a VIP::ZsGreen mouse line in which a VIP-cre drives a floxed ZsGreen reporter to specifically label VIP neurons. Ablation of the VIP interneurons was achieved via a bilateral injection of a cre-dependent Caspase 3 into the border of the IL and dorsal peduncular cortex (DP) of VIP::ZsGreen mice, thus causing apoptosis of cre-expressing VIP neurons (Figure 2-1A). Sham animals were given an identical injection of sterile saline. We confirmed VIP-specific ablation through the specific loss of ZsGreen-expressing neurons (unpaired t-test,  $p = 0.0164$ , Figure 2-1B). Cre-dependent ablation was also confirmed to be primarily contained to the IL region versus the PL region of the mPFC (Figure 2-2).

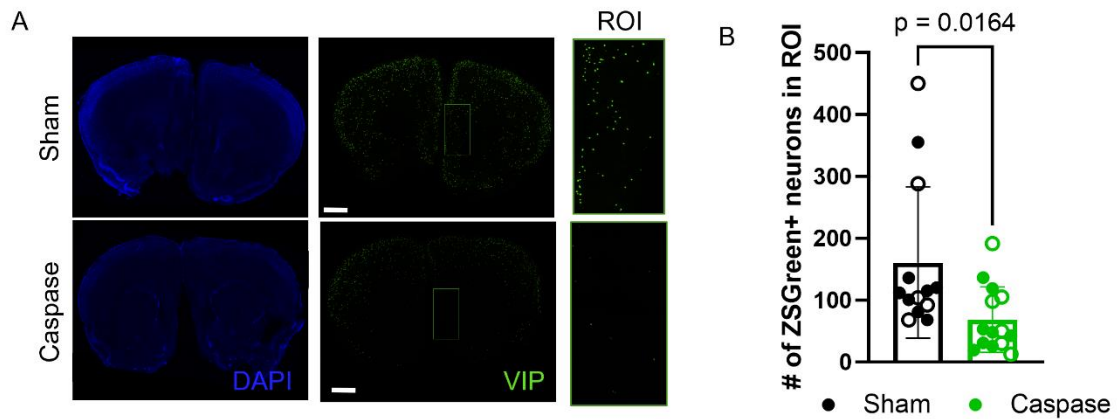


**Figure 2-1: Caspase ablation localized to the IL and DP.** (A) AAV-drive cre-dependent caspase ablation of VIP interneurons was successful in selectively ablating VIP interneurons, as indicated by loss of ZsGreen fluorescence. Scale bar: 1 mm. (B) Successful ablation of VIP interneurons was observed in all study animals (unpaired t-test,  $p = 0.0164$ ), between +1.10 mm and +1.98 mm rostral of the bregma, corresponding to panels 14 to 22 in Paxinos and Franklin<sup>213</sup>. ROI was decided using pilot animals to determine spread of AAV and then centered around injection coordinates. Open circles = male, closed circles = female.

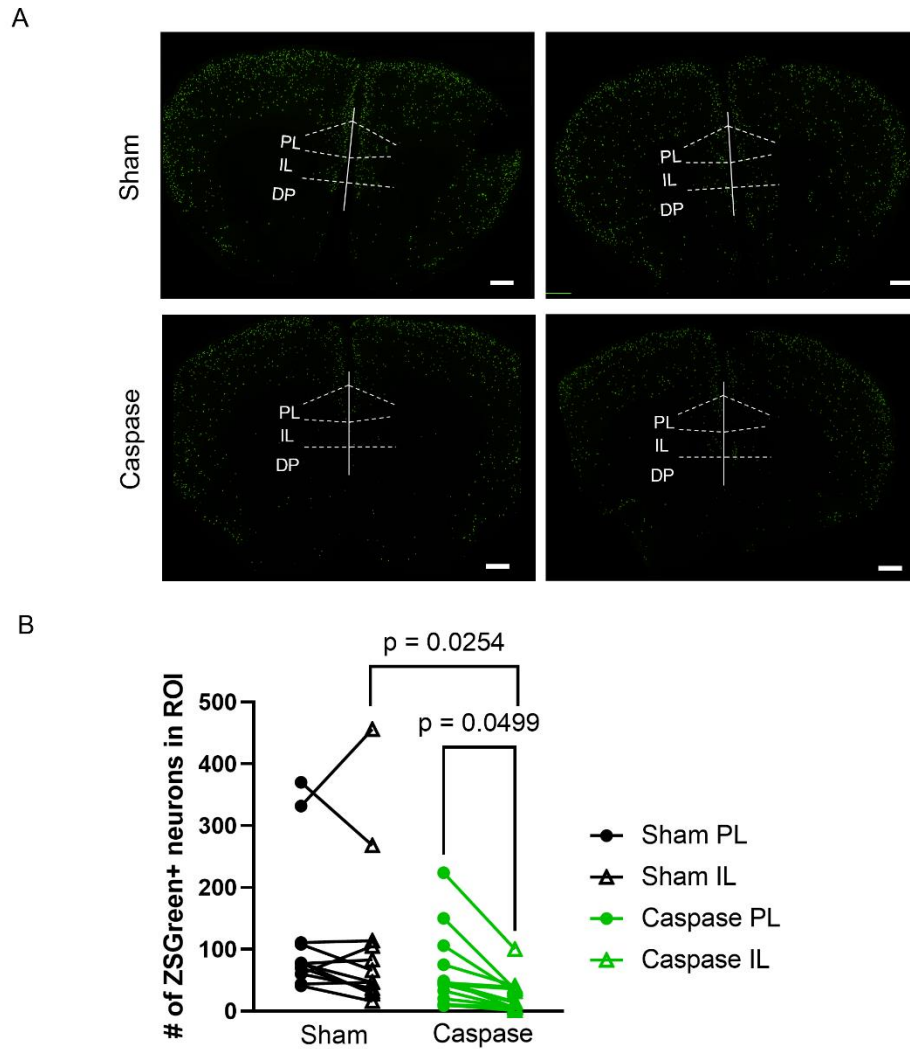


**Figure 2-2: Caspase ablation of VIP interneurons is primarily localized to the IL.** (A) Representative images of the spread of caspase-3 AAV. PL = prelimbic, IL = infralimbic, DP = dorsal peduncular cortex. (B) Quantitative analysis of ablation of VIP interneurons in the PL vs IL. Caspase ablation was localized to the IL, as indicated by a significant decrease of VIP interneurons (represented by ZsGreen expression) in the IL ( $p_{IL} = 0.0254$ ) but not in the PL ( $p_{PL} = 0.1092$ ). Additionally, there are significantly fewer VIP interneurons in the IL of caspase animals ( $p_{caspase} = 0.0499$ ) but not in the sham animals ( $p_{sham} = 0.8284$ ), indicating specific ablation of VIP interneurons in the IL.

### 2.3.2 Ablation of VIP interneurons increases impulsive responding in long-delay trials

The 3CSRTT is designed to measure motor impulsivity as a characteristic of prefrontal cortex activity<sup>214</sup>. In this task, the mouse is trained to recognize an illuminated nose poke hole and must poke within a 5 second window of time to receive a reward. Four distinct behaviors are measured during this task: (1) omission, in which the mouse does not respond to the cue within 5 seconds, (2) incorrect, in which the mouse pokes in the incorrect hole, (3), correct, in which the mouse pokes in the correct hole, and (4) premature, in which the mouse pokes during the intertrial interval (ITI) that occurs between the response time and the following cue. The number of premature responses serves as an indicator of impulsive action. We trained both VIP-ablated and sham mice in the 3CSRTT (Figure 2-3A). While there was not a statistically significant difference in premature, correct, or incorrect responding between sham and caspase-treated animals when all ITIs were sampled together, there was a trend towards ablated mice having an increased proportion of premature responses (unpaired t-test,  $p = 0.093$ , Figure 2-3B). Based on data indicating that the infralimbic area is responsible specifically for behavioral control of long-delay trials<sup>4</sup>, we then separated trials by the ITI and found that ablated animals had a significant increase in premature responses exclusively when the ITI was set to 12.5 s ( $p = 0.004$ , Figure 2-3C). This observation was similar across both male and female populations, with no significant differences between the sexes (Figure 2-4, Tables 2-1 and 2-2).

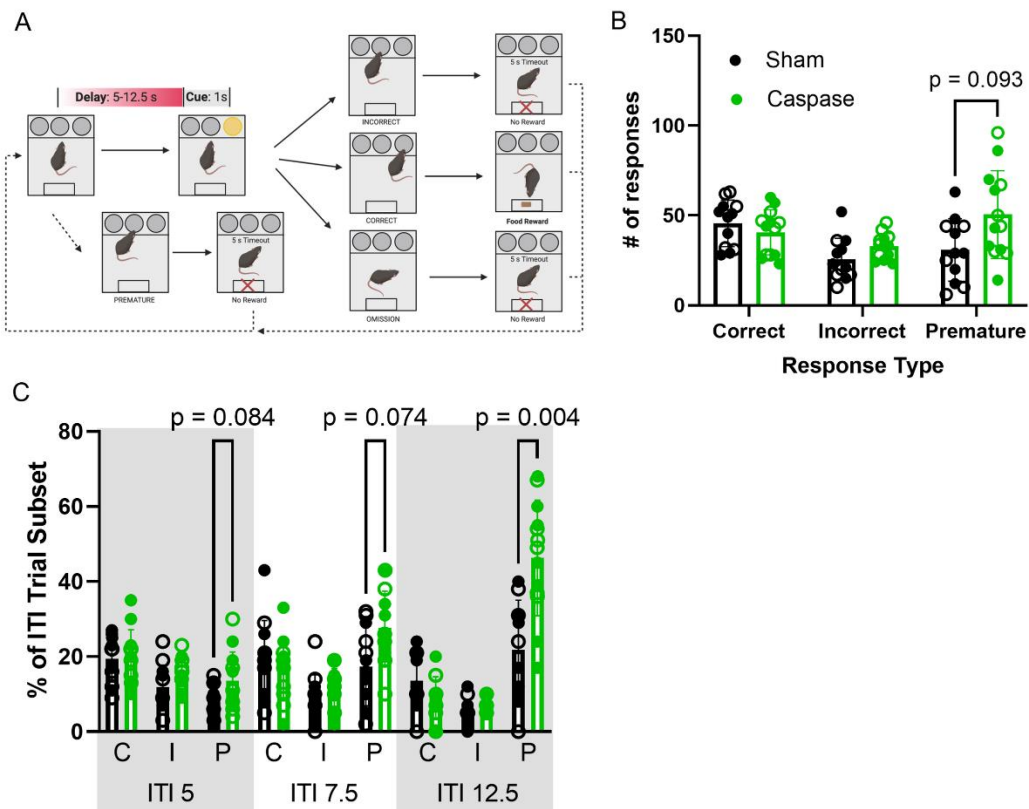


**Figure 2-3: Caspase ablation of IL VIP interneurons results in an increase in long-delay premature responses as measured by 3CSRTT.** (A) Task schematic of three-choice serial reaction time task. Created with Biorender.com. (B) VIP ablation in the IL results in a slight increase in premature responses across all inter-trial intervals. A two-way ANOVA revealed there was a statistically significant interaction between treatment and response type ( $F(2,29) = 4.011$ ,  $p = 0.0225$ ; unpaired t-tests,  $p_{\text{correct}} = 0.344$ ,  $p_{\text{incorrect}} = 0.108$ ,  $p_{\text{premature}} = 0.093$ ). (C) When separated into discrete ITI categories, a two-way ANOVA demonstrates that there is a statistically significant interaction between treatment and ITI-dependent response type ( $F(8,206) = 7.056$ ,  $p < 0.0001$ ; unpaired t-tests,  $p_{\text{correct ITI5}} = 0.662$ ,  $p_{\text{incorrect ITI5}} = 0.112$ ,  $p_{\text{premature ITI5}} = 0.084$ ,  $p_{\text{correct ITI7.5}} = 0.503$ ,  $p_{\text{incorrect ITI7.5}} = 0.303$ ,  $p_{\text{premature ITI7.5}} = 0.074$ ,  $p_{\text{correct ITI12.5}} = 0.133$ ,  $p_{\text{incorrect ITI12.5}} = 0.303$ ,  $p_{\text{premature ITI12.5}} = 0.004$ ). C = correct, I = Incorrect, P = premature. Open circles = male, closed circles = female.

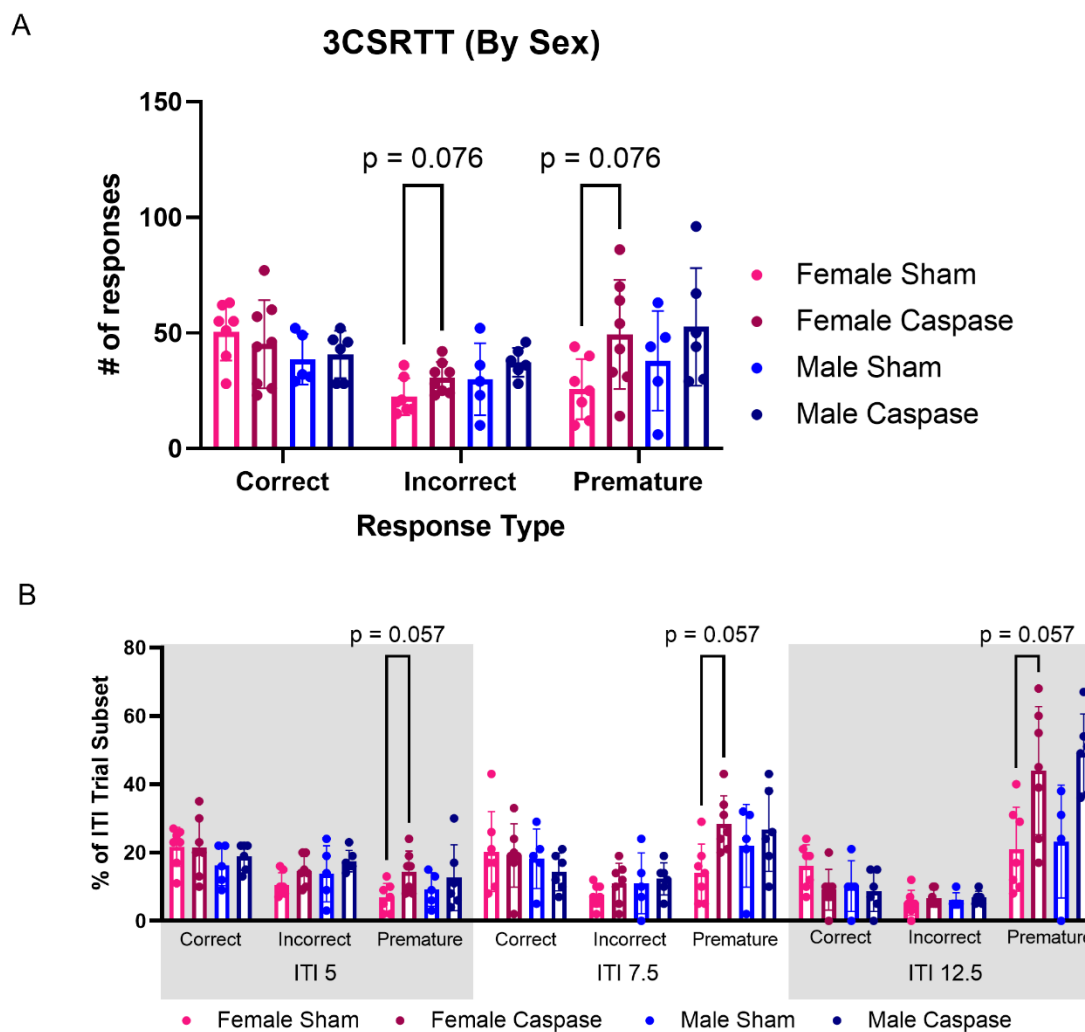


**Figure 2-4: Caspase ablation of IL VIP interneurons does not cause discriminate impulsive behavior in males vs females.** (A) Caspase ablation results in a trend of increased premature responding in both male and female mice, with a stronger increase in female animals, while not significant. No significant differences between male and female animals. (B) ITI length corresponds to an increase in premature responses in both males and females but is not significant. No significant differences between male and female animals. Statistics summarized in Tables 2-1 and 2-2.

3-way ANOVA	Sum of Squares	df	Mean Square	F (DFn, Dfd)	P value
Response Type	2557	2	1279	F (2, 69) = 5.332	P=0.0070
Sex	84.62	1	84.62	F (1, 69) = 0.3529	P=0.5544
Treatment	1416	1	1416	F (1, 69) = 5.906	P=0.0177
Response Type x Sex	988.8	2	494.4	F (2, 69) = 2.062	P=0.1350
Response Type x Treatment	1422	2	711	F (2, 69) = 2.965	P=0.0582
Sex x Treatment	5.565	1	5.565	F (1, 69) = 0.02321	P=0.8794
Response Type x Sex x Treatment	231.7	2	115.8	F (2, 69) = 0.4830	P=0.6190
<b>Multiple unpaired t-tests with Welch's correction and FDR</b>					
<i>Group 1</i>	Female Sham	Female Sham	Male Sham	Male Caspase	
<i>Group 2</i>	Female Caspase	Male Sham	Male Caspase	Female Caspase	
Correct	p = 0.455	p = 0.338	p = 0.764	p = 0.800	
Incorrect	p = 0.045	p = 0.364	p = 0.557	p = 0.534	
Premature	p = 0.045	p = 0.364	p = 0.557	p = 0.800	

**Table 2-1: Statistics summary for Figure 2-5A.**

3-way ANOVA								
		Sum of Squares	df	Mean Square	F (DFn, DFd)	P value		
Response Type		13617	8	1702	F (8, 206) = 23.62	P<0.0001		
Sex		43.29	1	43.29	F (1, 206) = 0.6009	P=0.4391		
Treatment		906.5	1	906.5	F (1, 206) = 12.58	P=0.0005		
Response Type x Sex		484.6	8	60.58	F (8, 206) = 0.8408	P=0.5677		
Response Type x Treatment		3278	8	409.8	F (8, 206) = 5.688	P<0.0001		
Sex x Treatment		1.101	1	1.101	F (1, 206) = 0.01528	P=0.9017		
Response Type x Sex x Treatment		247.8	8	30.98	F (8, 206) = 0.4299	P=0.9022		
<b>Multiple unpaired t-tests with FDR</b>								
<i>Group 1</i>		Female Sham	Female Sham	Male Sham	Male Caspase			
<i>Group 2</i>		Female Caspase	Male Sham	Male Caspase	Female Caspase			
Correct (ITI 5)		p = 0.789	p = 0.593	p = 0.703	p = 0.995			
Incorrect (ITI 5)		p = 0.112	p = 0.593	p = 0.703	p = 0.995			
Premature (ITI 5)		p = 0.113	p = 0.593	p = 0.703	p = 0.995			
Correct (ITI 7.5)		p = 0.555	p = 0.810	p = 0.703	p = 0.995			
Incorrect (ITI 7.5)		p = 0.295	p = 0.593	p = 0.764	p = 0.995			
Premature (ITI 7.5)		p = 0.112	p = 0.593	p = 0.703	p = 0.995			
Correct (ITI 12.5)		p = 0.112	p = 0.593	p = 0.764	p = 0.995			
Incorrect (ITI 12.5)		p = 0.555	p = 0.810	p = 0.703	p = 0.995			
Premature (ITI 12.5)		p = 0.112	p = 0.810	p = 0.173	p = 0.995			

Table 2-2: Statistics summary for Figure 2-5B.

### 2.3.3 Ablation of VIP interneurons does not affect interest in novel animals

Previous studies demonstrate that activation of IL VIP neurons reduces novel animal investigation<sup>6</sup>, implicating a role of IL VIP neurons in the control of novelty seeking behavior. To evaluate this role, we tested mice on a novel social interaction assay, as previously described<sup>215</sup>. In this assay, mice were given 150 s to explore an open field with two restrainers, and then 150 s to explore the open field with a novel mouse in one of the restrainers (Figure 2-5A). Mice that underwent VIP ablation did not spend significantly more time exploring the novel mouse (unpaired t test,  $p = 0.5532$ , 95% C.I. = [-24.79, 13.59]) and did not make first contact with the novel animal at significantly different times from the sham animals (unpaired t test,  $p = 0.5929$ , 95% C.I. = [-43.73, 25.52], Figure 2-5B). These findings were consistent in both male and female populations, with no significant changes between sexes (Table 2-3, Figure 2-6A). However, caspase-ablated males showed a trend towards approaching a novel animal much faster than their sham counterparts (Table 2-3, Figure 2-6A).

### 2.3.4 VIP Interneuron ablation does not increase spatial anxiety-like behavior

Because our behavioral tests revealed that VIP neuron ablation selectively increases impulsivity behavior (i.e., an increase in the number of impulsive responses as measured by the 3CSRTT), we tested the hypothesis that the observed increase in impulsivity may be a non-specific effect of an overall change in behavior. To assess this possibility, animals were subjected to an open field assay to determine any changes in spatial anxiety-like behavior. Spatial anxiety-like behavior was quantified by measuring the amount of time that an animal spent in the center of the open field, with the expectation that animals with higher levels of spatial anxiety will spend less time in the center of the open field. VIP neuron ablation did not affect time spent in the center of the open field, suggesting that ablation does not increase anxiety-like behavior (unpaired t test,  $p = 0.2851$ , 95% C.I. = [-26.19, 8.036], Figure 2-5C). These findings were consistent across both male and female populations, with no differences between sexes (Figure 2-6B, Table 3). Ablation of VIP neurons in the IL did not significantly affect overall locomotion when compared to sham animals (unpaired t test,  $p = 0.7447$ , 95% C.I. = [-5751, 4166], Figure 2-5C). A two-way ANOVA revealed that caspase ablation did not have a statistically significant effect on overall distance travelled, but sex was a statistically significant factor in the overall distance traveled (Figure 2-6C, Table 2-3).

### 2.3.5 Ablation of VIP interneurons does not increase palatable food intake

Because of the effect of VIP ablation on impulsive responding, it is possible that VIP ablation creates a general effect on novelty seeking, causing an increased motivation for non-chow food and a resulting increase in impulsive responses. Studies have demonstrated that optogenetic manipulation of the mPFC can alter free feeding<sup>216-218</sup>, and that activation of the IL VIP interneurons is sufficient to increase palatable food intake<sup>6</sup>. We therefore evaluated the effect of VIP neuron ablation of hedonic food intake. In this assay, mice are given a pre-weighed nugget of high-fat diet (Teklad TD.88137, 15.2% kcal from protein, 42.7% kcal from carbohydrate, and 42% kcal from fat) and allowed to eat freely for 30 minutes. We consider food intake during this time period, conducted just prior to the start

of the light cycle, to be driven primarily by hedonic mechanisms, as our prior work has shown animals consume minimal amounts of food in this assay when tested with home cage dietary chow (Teklad 2013, 4% fat, 17% protein, 48% carbohydrate, no sucrose, 2.9 kcal/g) <sup>6</sup>. Ablation of VIP interneurons in the IL was not sufficient to produce a significant change in palatable food intake over a 30 min period (unpaired t test,  $p = 0.8128$ , 95% C.I. = [-0.2789, 0.3523, Figure 2-5D). These findings were consistent in both male and female animals, with no significant differences between sexes (Figure 2-6C, Table 2-3).

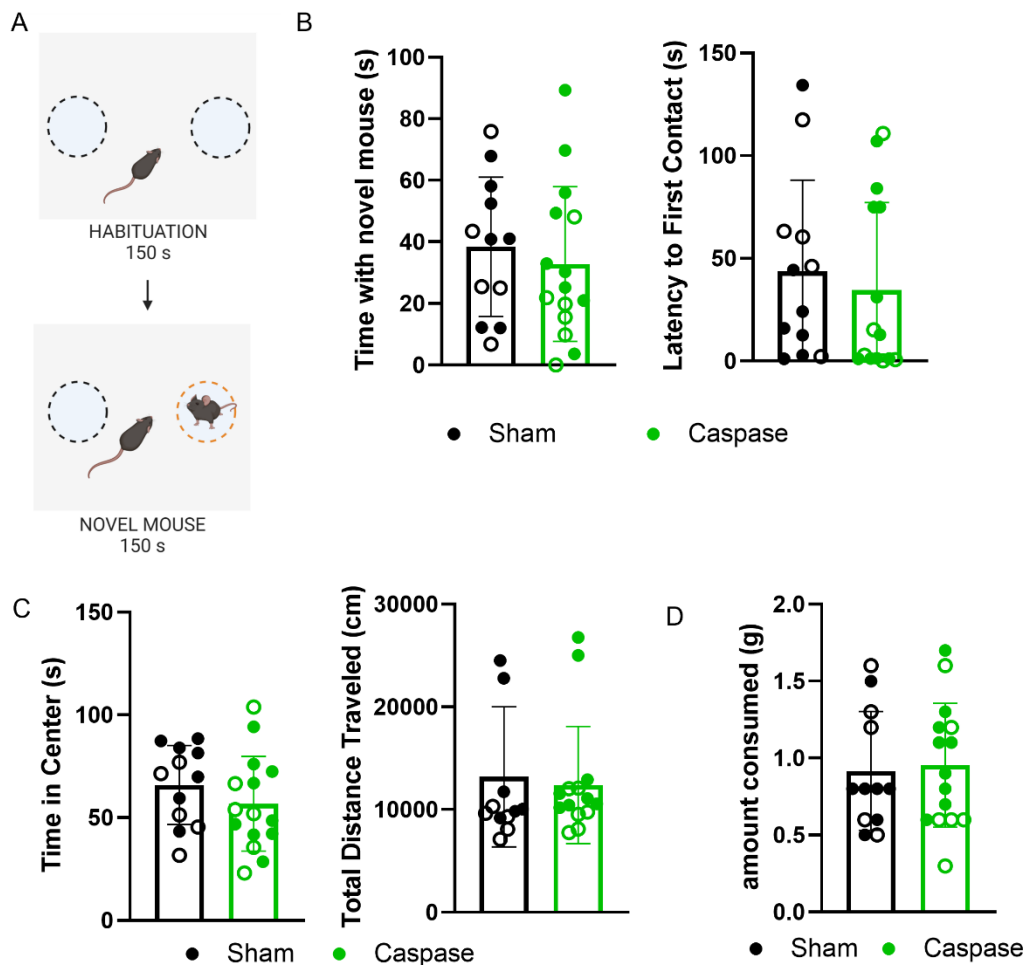


**Figure 2-5: Caspase ablation of IL VIP interneurons does not influence novelty-seeking or anxiety behaviors.** (A) Task schematic of novel social interaction assay. Created with Biorender.com. (B) VIP ablation in the IL does not affect time spent exploring a novel animal (unpaired t-test,  $p = 0.5532$ ) or latency to approach a novel animal (unpaired t-test,  $p = 0.5929$ ), (C) spatial anxiety-like behavior as measured by time spend in the center of an open field (unpaired t-test,  $p = 0.2851$ ) and overall locomotion in an open field (unpaired t-test,  $p = 0.7447$ ) or (D) amount of high-fat diet consumed (unpaired t-test,  $p = 0.8128$ ). Open circles = male, closed circles = female.

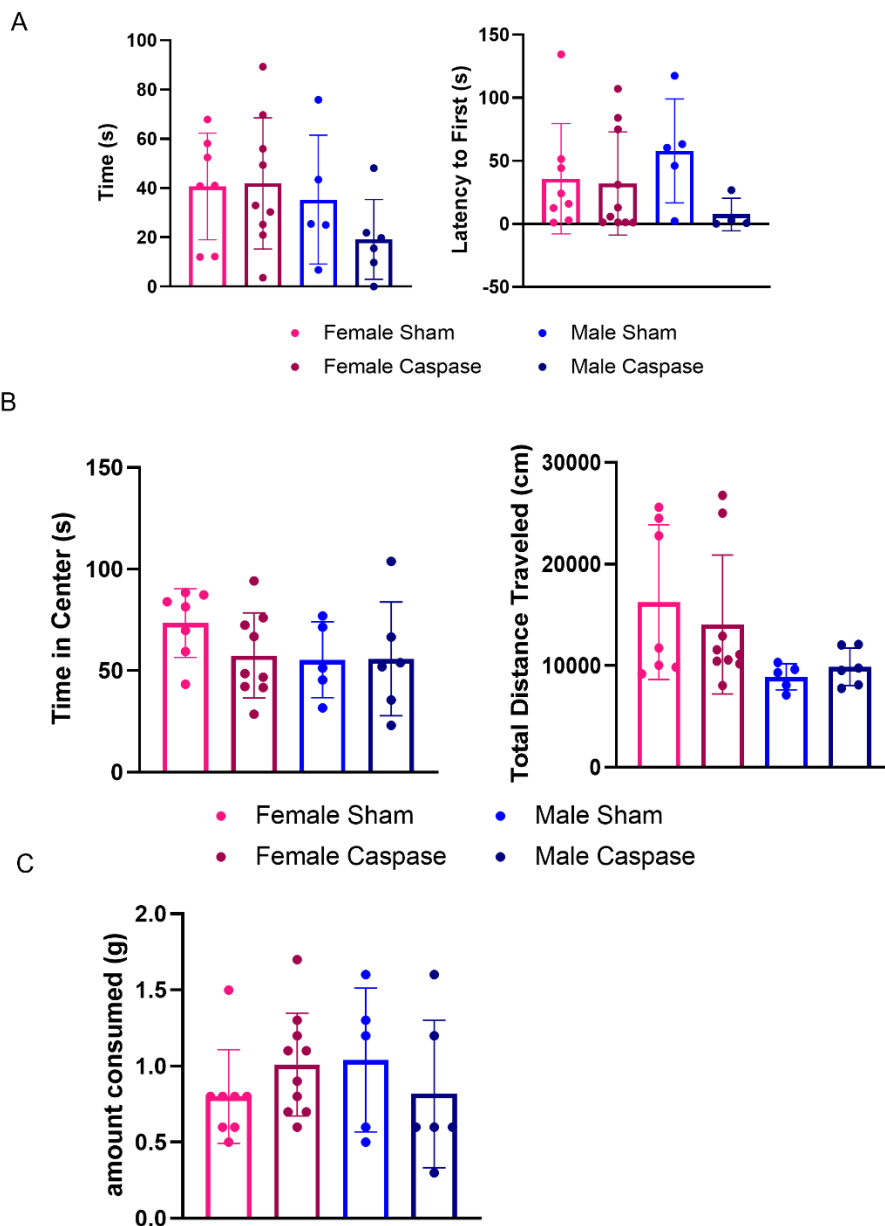


**Figure 2-6: Caspase ablation of IL VIP interneurons does not cause discriminate novelty-seeking or anxiety-related behaviors in males vs. females.** (A) Caspase ablation does not affect novelty-seeking behavior as measured by novel social assay in either males or females. No significant differences between male and female animals. (B) Caspase ablation does not affect anxiety-related behavior as measured by time spent in center of open field and overall locomotion in either males or females. No significant differences between male and female animals. (C) Caspase ablation does not affect binge-like food intake in either males or females. No significant differences between male and female animals. Statistics summarized in Table 2-3.

<b>2-way ANOVA (Time Spent with novel animal)</b>					
	Sum of Squares	df	Mean Square	F (DFn, DFd)	P value
Sex x Treatment	486.8	1	486.8	F (1, 23) = 0.8934	P=0.3544
Sex	1270	1	1270	F (1, 23) = 2.331	P=0.1405
Treatment	355.7	1	355.7	F (1, 23) = 0.6528	P=0.4274
<b>2-way ANOVA (Latency to approach novel animal)</b>					
	Sum of Squares	df	Mean Square	F (DFn, DFd)	P value
Sex x Treatment	3211	1	3211	F (1, 23) = 2.065	P=0.1641
Sex	8.729	1	8.729	F (1, 23) = 0.005614	P=0.9409
Treatment	4331	1	4332	F (1,23) = 2.786	P=0.1086
<b>2-way ANOVA (Cumulative time in center of open field)</b>					
	Sum of Squares	df	Mean Square	F (DFn, DFd)	P value
Sex x Treatment	434.1	1	434.1	F (1, 23) = 0.9471	P=0.3406
Sex	627	1	627	F (1, 23) = 1.368	P=0.2542
Treatment	385.7	1	385.7	F (1, 23) = 0.8414	P=0.3685
<b>2-way ANOVA (Total distance traveled)</b>					
	Sum of Squares	Df	Mean Square	F (DFn, DFd)	P value
Sex x Treatment	16245363	1	16245363	F (1, 23) = 0.5010	P=0.4862
Sex	214056079	1	214056079	F (1, 23) = 6.602	P=0.0171
Treatment	2301648	1	2301648	F (1, 23) = 0.07099	P=0.7923
<b>Multiple unpaired t-tests with FDR (Total distance traveled)</b>					
Female Sham vs Male Sham	P = 0.0612				
Female Caspase vs Male Caspase	P = 0.1723				
<b>2-way ANOVA (Amount of HFD consumed)</b>					
	Sum of Squares	df	Mean Square	F (DFn, DFd)	P value
Sex x Treatment	0.3174	1	0.3174	F (1, 25) = 2.116	P=0.1582
Sex	0.0003005	1	0.0003005	F (1, 25) = 0.002003	P=0.5393
Treatment	0.003681	1	0.003681	F (1, 25) = 0.02454	P=0.8768

**Table 2-3: Statistics summary for Figure 2-6.**

## 2.4 DISCUSSION

The data presented here indicate that ablation of VIP interneurons in the IL is sufficient to drive impulsivity without increasing novelty-seeking or anxiety-like behaviors. We demonstrate here that VIP interneurons are necessary for control over impulsive responding specifically during long-delay trials. These behavioral changes occur without increasing anxiety-like behavior or palatable food intake, implicating VIP IL interneurons in the specific control of impulsive responding. To our knowledge, this marks the first behavioral exploration of IL-VIP interneuron ablation and further elucidates their role in the control of behavior.

Previous studies demonstrate that excitation of mPFC PY neurons with a Gq-coupled DREADD does not alter binge-like feeding or anxiety-like behavior but reduces impulsivity on the 3CRSTT task, but only after a high dose of CNO<sup>215</sup>, consistent with our findings. In contrast, Hardung *et al.* found that optogenetic IL inhibition in rats suppresses early responses<sup>4</sup>, which we did not find in our model of VIP ablation in mice. The differences in our findings likely result from differences in inhibition – while they chose to inhibit entire areas of the mPFC without distinction for neuron type, which would primarily target PY neurons, we have directly manipulated only VIP neurons. However, our findings indicate that VIP ablation in the IL only increased impulsive responding during long-delay trials, consistent with the findings of Hardung *et al.* insofar that the IL is implicated specifically in long-delay trials.

Though we found VIP ablation in the IL was sufficient to drive increased premature responding during long-delay trials, there is not sufficient power to determine if this phenomenon is sex-specific. We observed in S2 Fig. that there was a strong trend in both sexes towards increased premature responding in long-delay trials, but these remain non-significant based on our set statistical significance threshold ( $p_{\text{female}} = 0.112$ ,  $p_{\text{male}} = 0.173$ ). Additionally, while none of the behavioral assays indicate sex-specific differences, it is possible that these would become more apparent if our study had greater statistical power to detect these potential sex dependent effects.

While we have previously demonstrated that VIP stimulation via a cre-dependent stabilized step-function opsin (SSFO) expressed in VIP-cre animals was sufficient to suppress high calorie food intake and decrease overall locomotion, we found no effect on food intake during this experiment<sup>6</sup>. It is possible that this selective effect on animal behavior results is driven by the population of VIP interneurons that synapse directly onto PY neurons<sup>15,16</sup>. Thus, direct activation of VIP interneurons would directly suppress novelty-seeking while ablation of the VIP interneurons could be compensated for by additional inhibitory output from parvalbumin (PV) and SST neurons. Additionally, recent research has shown that VIP neurons act as a type of gate, allowing us to also hypothesize that direct stimulation of the VIP neurons is sufficient to “open” the gate, while ablation results in the gate continuing to remain “closed” and have no effect on novelty-seeking behavior<sup>21</sup>.

A mechanism of adaptive disinhibitory gating would additionally explain why VIP-specific ablation had an effect only in long ITI trials. Krabbe, *et al.* found that VIP interneuron activation was strongly modulated by outcome expectations, revealing a novel form of disinhibitory gating in the control of learning and behavior<sup>21</sup>. We can therefore hypothesize that VIP interneurons are similarly affected by changing ITIs in our model of impulsivity

and are activated specifically during longer periods of waiting. When VIP interneurons are ablated, this adaptive gate is absent, thus resulting in increased impulsive responding during longer ITIs. One study examining the role of serotonin receptor (5-HTR) antagonism in the control of impulsivity found that while antagonism of 5-HT<sub>2A</sub>R and 5-HT<sub>2B</sub>R had no effect on premature responding during a 5-CSRTT, antagonism of 5-HT<sub>2C</sub>R increased premature responding in an ITI-dependent manner<sup>137</sup>. As 5-HT<sub>2C</sub>R are almost exclusively expressed on VIP interneurons<sup>219</sup>, we can extrapolate that serotonergic innervation of VIP interneurons is responsible for this phenotype of motor impulsivity. Finally, our findings are also consistent with the role that the mPFC plays in the control of appropriately timed reactions<sup>27,220,221</sup>, as well as the role that the IL specifically plays in response inhibition<sup>222-224</sup>, and sheds new light on the role of VIP interneurons in the control of the timing of this inhibition.

## 2.5 EXPERIMENTAL METHODS

### 2.5.1 Experimental animals.

All studies were approved by the University of Virginia's Animal Care and Use Committee. Twelve-week-old adult male and female VIP-IRES-Cre (VIP-Cre, Strain # 010908) and B6.Cg-Gt(ROSA)26Sor<sup>tm6(CAG-ZsGreen1)Hze/J</sup> (Ai6, Strain # 007906) were purchased from The Jackson Laboratory. Ai6 contains a floxed STOP-cassette resulting in ZsGreen expression only in cre-expressing cells. Mice were housed in the Pinn Hall vivarium at the University of Virginia on a 12h light: 12h dark cycle (lights off at 21:00) with *ad libitum* access to food (Teklad 2013, 4% fat, 17% protein, 48% carbohydrate, no sucrose, 2.9 kcal/g) and water, unless otherwise stated. Both lines have been backcrossed to C57Bl6/j animals for at least 7 generations. We generated heterozygous VIP::ZsGreen animals through two subsequent crosses: (1) crossing VIP-cre homozygous females with Ai6 homozygous males and (2) crossing the resulting heterozygous VIP<sup>cre/+</sup>/Ai6<sup>fl/+</sup> offspring (referred to as VIP::ZsGreen throughout). This strategy results in ZsGreen expression localized to VIP-expressing neurons. Animals (N = 27, N<sup>F,sham</sup> = 7, N<sup>F,caspase</sup> = 9, N<sup>M,sham</sup> = 5, N<sup>M,caspase</sup> = 6) were transferred to a flipped light cycle room (12h light: 12h dark, lights off at 10:00, on at 22:00) 1 week before surgery and throughout the remainder of behavioral experimentation to allow for all behavioral experiments to occur during Zeitgeber Time (ZT) 12-14hr, during a time of heightened animal activity and alertness. Animals were genotyped using the following primer sets: (1) for VIP-Cre: Mutant (Mut) Forward 5'-CCC CCT GAA CCT GAA ACA TA - 3', Common 5'-GCA CAC AGT AAG GGC ACA CA - 3', Wild Type (WT) Forward 5'-TCC TTG GAA CAT TCC TCA GC - 3' and (2) for Ai6: WT Forward 5' -AAG GGA GCT GCA GTG GAG TA - 3', WT Reverse 5' - CCG AAA ATC TGT GGG AAG TC - 3', Mut Reverse 5' - GGC ATT AAA GCA GCG TAT CC - 3', Mut Forward 5' - AAC CAG AAG TGG CAC CTG AC - 3'.

### 2.5.2 Adeno-associated viral vector and stereotaxic viral injections.

Mice were anesthetized with Ketaset (60 mg/kg, i.p., Zoetis, Parsippany, NJ, US) and Dexdomitor (0.45 mg/kg, i.p., Zoetis) and given Normasol (500 uL, s.c., Mölnlycke, Göteborg, Sweden), which we found to decrease surgical deaths. All injections were performed using Neurostar StereoDrive (Tübingen, Germany). VIP neurons were targeted using a Cre-dependent Caspase 3 virus, pAAV-flex-taCasp3-TEVp from Addgene<sup>225</sup>. We injected 400 nL of virus bilaterally into the boundary of the infralimbic cortex (IL) and the dorsal peduncular cortex (DP) of 8-10-week-old male and female VIP::ZsGreen mice using coordinates based on Franklin and Paxinos<sup>213</sup> (+1.54 mm from bregma, ±0.3 mm lateral of midline, and 3.3 mm ventral of the dura). A Hamilton syringe fitted with a 26G needle was inserted to a depth of -3.3 mm and 400 nL of virus was delivered via pressure injection over a period of 12 minutes. To prevent delivery of the virus to more dorsal areas, the needle was left *in situ* for 10 minutes and then slowly removed. Control mice received sham surgery, wherein 400 nL of sterile saline was delivered bilaterally in the same manner as the AAV. Mice were given ketoprofen (5 mg/kg, i.p.), antisedan (1mg/kg, i.p., Zoetis) and Normasol (500 uL, s.c.) to accelerate post-surgical awakening. After surgery, mice were singly housed throughout the duration of the experiments. After 14 days to allow for

sufficient levels of viral vector expression and to allow the animals to fully recover from surgery, mice underwent behavioral assays.

### **2.5.3 Brain tissue preparation.**

Mice were euthanized using 100  $\mu$ L of Euthasol euthanasia solution (Virbac AH, Inc., Carros, France). Once mice no longer responded to a toe pinch, mice were first flushed with chilled phosphate-buffered saline, followed by perfusion with chilled 4% paraformaldehyde in 0.1-M phosphate buffer (4% PFA). Brains were kept in 4% PFA overnight and then transferred into 1X PBS until sectioning took place. Brains were dissected and sectioned at 40- $\mu$ m thickness on a compresstome (Precisionary Instruments, Natick, MA, USA). Sections were mounted in sequential order, air-dried, and coverslipped in Vectashield hard-set mounting medium with DAPI (Vector Laboratories, Newark, CA, USA).

### **2.5.4 Quantitative analysis of VIP ablation by caspase.**

Six 40  $\mu$ m sections from +1.10 and +1.98 rostral of bregma were taken, corresponding to panels 14 to 22 in Paxinos and Franklin<sup>213</sup>. All slices were imaged at 4X magnification using an Olympus BX61 using manual tiling function. Neurons were counted within a pre-determined ROI from previous pilot experiments using ImageJ. All quantitative analysis of VIP ablation was performed in animals used in behavioral animals. Two animals (one sham female and one caspase-injected female) were removed from analysis because of non-specific expression of ZsGreen that was evident during analysis.

### **2.5.5 Three-choice serial reaction time task.**

Behavioral assays were performed in the following order: (1) 3CSRTT, (2) open field test, (3) social interaction test, and (4) binge eating test. Behavioral training and testing occurred during the animal's dark cycle (ZT12-24) in a red-light lit behavioral room. Behavioral acquisition training is split into 13 stages and is performed in operant chambers (Med Associates, Inc, St. Albans, VT, USA). Briefly, in stage 1, all nose poke holes are illuminated and a nose poke in any hole results in reward delivery (Banana Flavor Pellets, #F06727, Bio-Serv, Flemington, NJ, USA). Subsequently, in stage 2, only the center hole is illuminated, and only pokes in this hole result in reward delivery. As training progresses, the duration of nose poke hole illumination is progressively reduced, ultimately reaching 0.5 seconds (s), and nose poke holes are illuminated in a pseudo-random order. During all stages of training and testing, mice must refrain from poking until the hole is illuminated and must wait 5 s to identify the correctly lit nose poke hole prior to poking. A premature poke or lack of response will result in a 5 s timeout and no reward. After completion of stage 13 of training, the intertrial interval (ITI, the time between the illumination of the nose poke holes) is lengthened to 7 s to produce a slight elevation in impulsive responding to allow improved data collection. During testing, the animals undergo 250 trials, in which the ITI is randomized between 5 s, 7.5 s, and 12.5 s in order to increase impulsive responding during longer ITI trials. Both training and testing are self-paced and conducted over a 12-hour period each day, in *ad libitum* fed animals. A typical animal will finish training within 7-10 days (84 to 120 hours) and testing between 14-20 hours.

### **2.5.6 Open Field Test.**

All behavioral testing occurred in a dedicated behavior room, separate from the home room, as conducted previously<sup>6,215</sup>. The behavioral room is lit only by red light, allowing for minimal interruptions of the animals' circadian cycle during behavioral testing<sup>226</sup>. Two days after 3SCSRTT testing, mice were brought to the behavioral room and allowed to acclimate for 1 hour before testing began. Mice were placed into the PhenoTyper (Noldus, Wageningen, the Netherlands) and allowed to explore for 15 minutes while movement was recorded using EthoVision XT tracking software (Noldus). The PhenoTyper was cleaned between each mouse with Minncare disinfectant to remove residual odors. We waited 5 minutes between each animal to allow for any residual odor from the cleaning agent to dissipate. During testing, a yellow light was turned on in the PhenoTyper, to provide consistent illumination of the arena. To ensure that arena novelty was not a confounding variable during the social interaction assay, all mice underwent this experiment before all other experiments conducted in the PhenoTyper.

### **2.5.7 Social interaction.**

The social interaction task was performed in the PhenoTyper, as previously described<sup>6,227</sup>. Before the social interaction test, all mice were brought to the behavior room and allowed to acclimate for at least 1 hour. To allow for habituation, the chamber was first prepared with two empty restrainers on opposite sides of the PhenoTyper. The test mouse was placed in the center of the PhenoTyper and allowed to explore for 150 seconds. The test mouse was then returned to its home cage for 30 s while the restrainers were cleaned with Minncare and replaced. A novel mouse of the same sex was then placed in one restrainer and the test mouse was returned to the center of the chamber and allowed to explore for 150 s. The side of the chamber the novel mouse was placed on was randomized to minimize confounding variables due to lingering smells. The chamber was cleaned between each mouse with Minncare and allowed to air out for 5 minutes to remove residual odors. Mouse movement was recorded using Ethovision.

### **2.5.8 Binge-like eating assay.**

Measurement of palatable food intake was performed as previously described<sup>6,228</sup>. On the night before testing, mice received a small (<0.2 g) sample of the high calorie diet (Teklad TD.88137, 15.2% kcal from protein, 42.7% kcal from carbohydrate, and 42% kcal from fat, Envigo, Dublin, VA, USA), delivered into their home cage. At ZT 20:00, all food was removed, and mice were challenged with approximately 3g of pre-weighed high fat diet and allowed to consume freely. After 30 minutes, the food was removed and weighed, and mice were returned to *ab libitum* chow feeding conditions.

### **2.5.9 Statistical analysis.**

All statistical analyses were performed in Prism 9 (GraphPad, Boston, MA, USA). Multiple comparisons were corrected for false positives using a false discovery rate correction (FDR) with a desired FDR set at 1.00%.

**DISCLAIMER**

This chapter is a reprint of: **Hatter, J. A.**, & Scott, M. M. (2023). Selective ablation of VIP interneurons in the rodent prefrontal cortex results in increased impulsivity. *PLOS ONE*, 18(6), e0286209.

**AUTHOR CONTRIBUTIONS**

The studies were designed by Dr. Michael Scott and Jessica Hatter. Experimental work, data analysis and initial manuscript preparation were performed by Jessica Hatter. Manuscript editing was performed by Jessica Hatter, Dr. Michael Scott, and Dr. Mark Beenhakker.

## **3 CHAPTER 4: INTRODUCTION TO GLUCAGON NEURONS AND THE HINDBRAIN**

---

Bi-directional communication between the central nervous system (CNS) and enteric nervous system (ENS) via the vagal nerve serves as a powerful regulator of energy homeostasis, glucose metabolism, and hunger<sup>229</sup>. Gut-brain communication is achieved through various hormones and peptides that are transmitted to the brain in response to peripheral cues. These neurotransmitters have become subjects of increased interest as pharmacological interventions targeting these pathways have been successful in the treatment of various metabolic pathologies.

### **3.1 OBESITY**

#### **3.1.1 Obesity and Co-Morbid Pathologies**

Using the body mass index formula ( $BMI = \text{weight (kg)}/\text{height (m)}^2$ ), obesity is defined as a BMI of 30 or higher<sup>230</sup>. Obesity is significantly associated with mortality rates, and as BMI increases, so does overall mortality and co-morbid diabetes-related mortality rates<sup>231</sup>. In 2013, the National Health and Nutrition Survey estimated that in the United States, 1 in 3 adults were considered obese (body mass index/BMI  $\geq 30$ ) and obesity accounted for 18% of deaths among Americans between the ages of 40 and 85<sup>232,233</sup>. Obesity risk has been determined to be significantly affected by thirteen specific factors that are co-morbid in individuals with obesity<sup>234</sup>. The thirteen specific factors are as follows: type-2 diabetes (T2D), cardiovascular disease, breathing/airway abnormalities, kidney abnormalities, nonalcoholic fatty liver disease (NAFLD) and cirrhosis, altered hormonal profiles, gastroesophageal reflux disease (GERD), cancer, increased intake of medication, impairment of physical functioning, depression, body image, and financial impacts<sup>234</sup>. Cancer and cardiovascular disease are the factors that primarily influence obesity-related mortality.

#### **3.1.2 Economic Impacts**

In the United States, it has been estimated that annual medical spending attributable to an obese individual was \$1901 in 2014, resulting in a \$149.4 billion economic burden at a national level<sup>235</sup>. The two significant drivers in increased incremental costs of obesity were age (obese adults have higher incremental costs of obesity than the nonobese population, but this is not seen in obese versus nonobese children) and obesity-related conditions, indicating that most of the costs are caused by co-morbid conditions of obesity<sup>235</sup>.

#### **3.1.3 Metabolic adaptation during obesity**

While rising obesity is often attributed to an increase in access to calorie-dense food and a decrease in physical activity<sup>236–238</sup>, obesity is not simply an imbalance between energy intake and energy expenditure<sup>239</sup>. While public health surrounding obesity tends to advise

reduced calorie intake to lose weight<sup>239</sup>, many studies have indicated that reductions in calorie intake are not sufficient to control or reverse weight gain<sup>239–243</sup>. In fact, reduction in calorie intake is much more likely to result in metabolic adaptations such as increased fat deposition, increased appetite, and reduced energy expenditure<sup>240,243,244</sup>. Metabolic adaptations have been found to persist for years after initial weight-loss and will even continually depress energy expenditure, making continued weight loss increasingly difficult despite reduced caloric intake and increased physical activity<sup>243,244</sup>. This has led to a theory of a metabolic “set point” or a homeostat, in which metabolic adaptations are primed to defend an individual’s current weight against perturbations, but this theory is controversial and experimental evidence is contradictory<sup>245–249</sup>.

### ***3.1.3.1 Discrete metabolic profiles of metabolic adaptation through the lens of bariatric surgery***

Bariatric surgeries such as Roux-en-Y gastric bypass (RYGB), vertical sleeve gastrectomy (VSG), and laposcopic adjustable band (LAGB) remain the most effective interventions against obesity<sup>250</sup>. RYGB is performed by creating and attaching a small gastric pouch to a loop of the mid-jejunum, thus causing ingested food to completely bypass most of the stomach and small intestine. While it was initially believed that RYGB-mediated weight loss was purely due to the purely mechanical restriction of food intake and decreased nutrient absorption (restrictive-malabsorptive), more recent research indicates that RYGB alters appetite-regulating pathways<sup>251,252</sup>. Similarly, VSG, which removes approximately 80% of the stomach, has been shown to have effects on whole-body metabolism beyond the effects of calorie restriction<sup>253</sup>.

By comparing RYGB- and VSG-mediated changes in physiology with those that occur during calorie restriction, possible mechanisms of metabolic action can be determined<sup>254</sup>. Analysis of metabolic profiles after RYGB-, VSG- and low-calorie diet (LCD)- mediated weight loss showed decreased resting metabolic rate (RMR) in all three groups that was sustained up to a year<sup>254</sup>. At 8 weeks post-surgical and dietary interventions, RYGB- and LCD had induced the least amount of metabolic adaptation, while VSG had significantly decreased RMR compared to RYGB and LCD. At one year post-intervention, continued LCD had further depressed RMR when compared to 8 weeks, RYGB had no significant difference between time points, and VSG patients had increased RMR when compared to the early time point<sup>254</sup>. These results indicate that metabolic adaptation occurs in both surgical and dietary interventions, despite bariatric surgeries maintaining weight loss with greater efficacy than dietary intervention<sup>255</sup>.

Analysis of circulating metabolic markers between groups revealed differences in metabolic signaling profiles (summarized in Table 3-1) that could explain this difference in response to suppressed RMR<sup>254</sup>. Comparison of general metabolic markers such as circulating glucose and HOMA-IR (a measure of insulin resistance<sup>256</sup>) indicate that despite sustained decreases in RMR across all groups, RYGB and VSG either maintained or further decreased initial decreases in circulating glucose, insulin levels, insulin resistance as

measured by HOMA-IR, and circulating triglycerides, while LCD intervention was not able to maintain these decreases long-term<sup>254</sup>.

Previous research has implicated decreased circulating leptin in metabolic adaptation during weight loss<sup>257–259</sup> and has shown that reversal of circulating leptin levels to pre-weight-loss levels reverses metabolic adaptation<sup>260</sup>. Leptin levels in surgical-intervention groups were decreased at both time points, while caloric intervention initially decreased leptin, but was returned to baseline levels at one year post-intervention (**Table 3-1**)<sup>254</sup>. Thyroid function, which is known to regulate metabolism<sup>261</sup>, can be determined indirectly via measurement of thyroid hormones triiodothyronine (T<sub>3</sub>) and thyroxine (T<sub>4</sub>). While differential regulation of thyroid hormone was observed between surgical-intervention and caloric-intervention groups (summarized in **Table 3-1**), thyroid regulation of metabolism operates through many distinct mechanisms<sup>261</sup>, making it difficult to attribute specific causation between decreased RMR and decreased T<sub>3</sub> and T<sub>4</sub> levels<sup>254</sup>. Additionally, while T<sub>3</sub> and T<sub>4</sub> levels are decreased, they remain within normal range, making it difficult to determine if these changes are functionally relevant to this model of metabolic adaptation<sup>262</sup>.

### 3.1.3.2 Summary

Together, these results indicate that metabolic adaptation in response to weight loss can be essentially “over-ruled” by specific gut-hindbrain signaling that is increased after RYGB. Based on these findings, weight loss can theoretically be mediated under two distinct mechanisms:

- (1) Compensatory metabolic activation results in weight plateau and weight cycling. Resting metabolic rate is decreased in response to decreased energy intake (either caloric restriction/LCD or mechanical restriction of food intake/RYGB), resulting in compensatory action to restore balance between energy intake and energy expenditure<sup>239–241,244</sup>. This is hypothesized due to too-low energy intake or too-low protein intake<sup>263–265</sup>, in response to too-rapid weight loss<sup>266</sup>, or when adiposity is too low<sup>267</sup>. In addition to decreasing energy expenditure, metabolic adaptation increases appetite<sup>240,243,244</sup>, making adherence to an LCD more difficult. The subsequent weight-loss plateau and increased appetite result in weight cycling<sup>240</sup>.
- (2) Gut-hindbrain communication selectively modulates feeding-related circuits to maintain sustained weight loss despite metabolic adaptation. Vagal-mediated gut-hindbrain communication has been shown to mediate success of RYGB<sup>268</sup>. Animals that received a celiac branch vagotomy and a RYGB lost significantly less body weight in the first 40 days post-RYGB, compared to RYGB animals with intact vagal signaling<sup>268</sup>. Additionally, postprandial circulating peptide YY (PYY) and glucagon-like peptide 1 (GLP-1) measured in patients post-RYGB begin to rise as early as 2 days post-surgery and effect measurable changes in appetite<sup>269</sup>. These findings, along with many others (reviewed in Hankir, *et al.*<sup>252</sup>), have revealed that RYGB weight-loss is controlled through diverse systems activated by gut-

hindbrain communication, including those implicated in homeostatic control of feeding, such as melanocortinergic and serotonergic systems, and those implicated in hedonic control of feeding, such as dopaminergic and opioidergic systems. Activation of these systems is achieved through gut-mediated release of gut hormones, microbiota products, and leptin<sup>252</sup>.

Gut-hindbrain communication has been well-established in the control of hedonic eating behavior and energy balance<sup>252,270,271</sup>, with GLP-1 acting as one of the most robust effectors of this communication, as discussed in the following section. However, a large body of research has indicated that the gut-hindbrain communication has effects on motivation and higher cognitive functions<sup>272-279</sup>. Additional research has emerged that implicates gut dysbiosis in the control of behavior in response to drugs of abuse, as well as in affecting emotional state<sup>280-282</sup>. This is explored further in the discussion, as a vital link between mPFC neurobiology and the gut.

			<b>RYGB</b>	<b>VSG</b>	<b>LCD</b>
Metabolic markers	Plasma glucose (mg/dL)	Δ 8 weeks	Decreased	Decreased	Decreased
		Δ 1 year	Sustained	Sustained	Reversal; return to baseline levels
	Insulin (mU/mL)	Δ 8 weeks	Decreased	Decreased	Decreased
		Δ 1 year	Sustained	Further decreased	Increased
	HOMA-IR score	Δ 8 weeks	Decreased	Decreased	Decreased
		Δ 1 year	Sustained	Further decreased	Increased
Triglycerides (mg/dL)	Δ 8 weeks	Decreased	Decreased	Decreased	
	Δ 1 year	Further decreased	Further decreased	Reversal; return to baseline levels	
Total cholesterol (mg/dL)	Δ 8 weeks	Decreased	Decreased	Decreased	
	Δ 1 year	Reversal; return to baseline levels	Reversal; return to baseline levels	Reversal; trending towards increase above baseline	
Markers of metabolic adaptation	Leptin (ng/mL)	Δ 8 weeks	Decreased	Decreased	Decreased
		Δ 1 year	Further decreased	Further decreased	Reversal; return to baseline levels
	Triiodothyronine (T <sub>3</sub> , ng/dL)	Δ 8 weeks	Decreased	Decreased	Decreased
		Δ 1 year	Further decreased	Further decreased	Sustained
	Thyroxine (T <sub>4</sub> , μg/dL)	Δ 8 weeks	Decreased	Decreased	No change
		Δ 1 year	Sustained	Slight further decrease	No change
	Thyroid stimulating hormone (TSH, μIU/mL)	Δ 8 weeks	No change	No change	No change
		Δ 1 year	Slight decrease	No change	No change

**Table 3-1: A summary of changes in circulating metabolic markers in both surgical and dietary interventions.** Table is adapted from data in Tam, *et al.* for clarity<sup>254</sup>. Data labeled Δ 8 weeks describe changes in metabolic marker between pre-intervention baseline and 8 weeks post-intervention. Data labeled Δ 1 year describe changes in metabolic marker between 8 weeks post-intervention and one year post-intervention. These changes enable discrimination of weight-loss mechanisms purely due to calorie deficit (LCD) and weight-loss mechanisms dependent on changes in molecular physiology (RYGB, VSG).

## 3.2 GLP-1 IN THE CONTROL OF APPETITE

### 3.2.1 Gene expression and posttranslational processing

GLP-1 is encoded by *GCG* within the larger precursor protein, preproglucagon (PPG). Preproglucagon is cleaved by prohormone convertases to produce a diverse group of signaling molecules (**Figure 3-1**)<sup>283</sup>. While prohormone convertase (PC2) is expressed in the hindbrain, only trace amounts of glucagon have been detected in this part of the brain, which has led researchers to believe that prohormone convertase (PC1/3) is primarily responsible for CNS processing of PPG<sup>284,285</sup>. The half-life of GLP-1 is approximately 1-2 minutes due to cleavage by dipeptidyl-peptidase-4 (DPP-4)<sup>286</sup>.

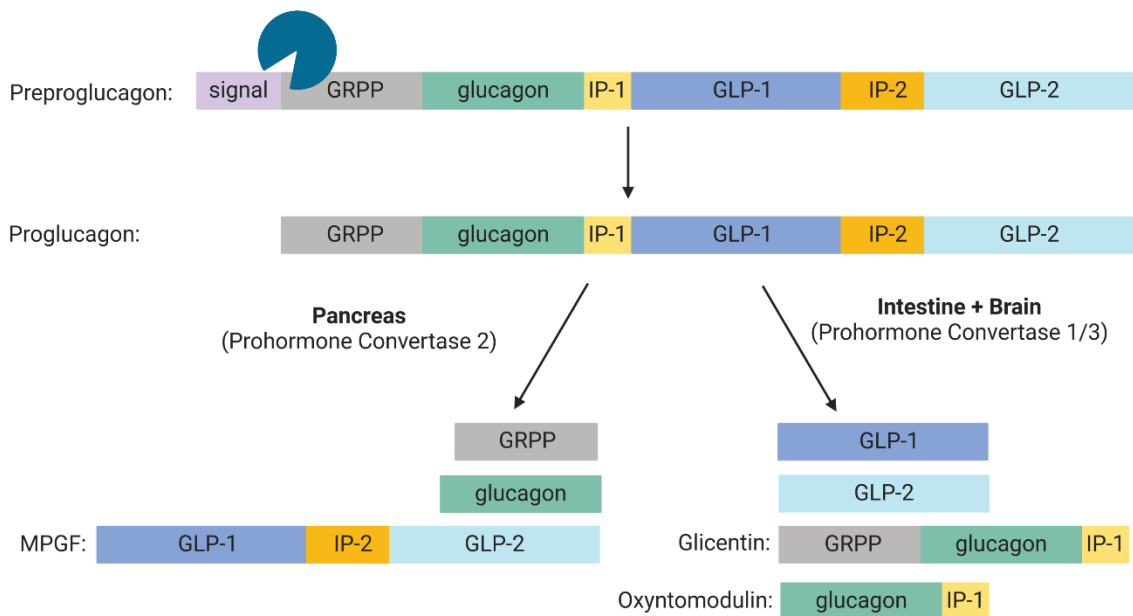


**Figure 3-1: GLP-1 is produced as a product of posttranslational processing of preproglucagon.** Differential cleaving of proglucagon is mediated by organ-specific expression of prohormone convertases. Processing occurring in the intestines and brain produces GLP-1, GLP-2, glicentin, and oxyntomodulin, which have been implicated in the regulation of food intake. Processing in the pancreas produces glicentin-related pancreatic polypeptide (GRPP), glucagon, and the Major Proglucagon Fragment (MPGF).

### 3.2.2 GLP-1-mediated activation of appetite-regulatory networks

*Gcg*-expressing (GCG) neurons that release GLP-1 are primarily located in the nucleus of the solitary tract (NTS)<sup>287</sup>. When GCG neurons were ablated bilaterally via a cre-dependent diphtheria toxin injection into the NTS of glucagon-cre animals, there was significant loss of GLP-1 in the brainstem, hypothalamus, and spinal cord<sup>287</sup>. Therefore, it was determined that GCG neurons in the NTS are a major contributor to the release of GLP-1 in those areas. In addition to GLP-1, GCG neurons have been established to contain GLP-2, oxyntomodulin, and glicentin<sup>285</sup>.

In response to gut-mediated vagal excitation, NTS-GCG neurons release GLP-1 in multiple brain regions, including the paraventricular nucleus (PVN), arcuate nucleus (ARC) and ventromedial nucleus (VMH)<sup>288-290</sup>. It has been established that NTS-GCG projections onto the PVN enhance glutamatergic synaptic transmission, which suppresses food intake, while specific ablation of GLP-1R in the PVN causes overeating and obesity<sup>289</sup>. NTS-GCG projections onto ARC neurons directly activates POMC neurons and indirectly inhibits NPY neurons through GABAergic interneurons (**Figure 3-2**)<sup>291</sup>. Additionally, the ARC has direct access to circulating metabolic hormones such as GLP-1 due to fenestrated vessels that pass through the brain area<sup>292,293</sup>, indicating that vagal-mediated GLP-1 signaling is not necessary for its control of appetite.

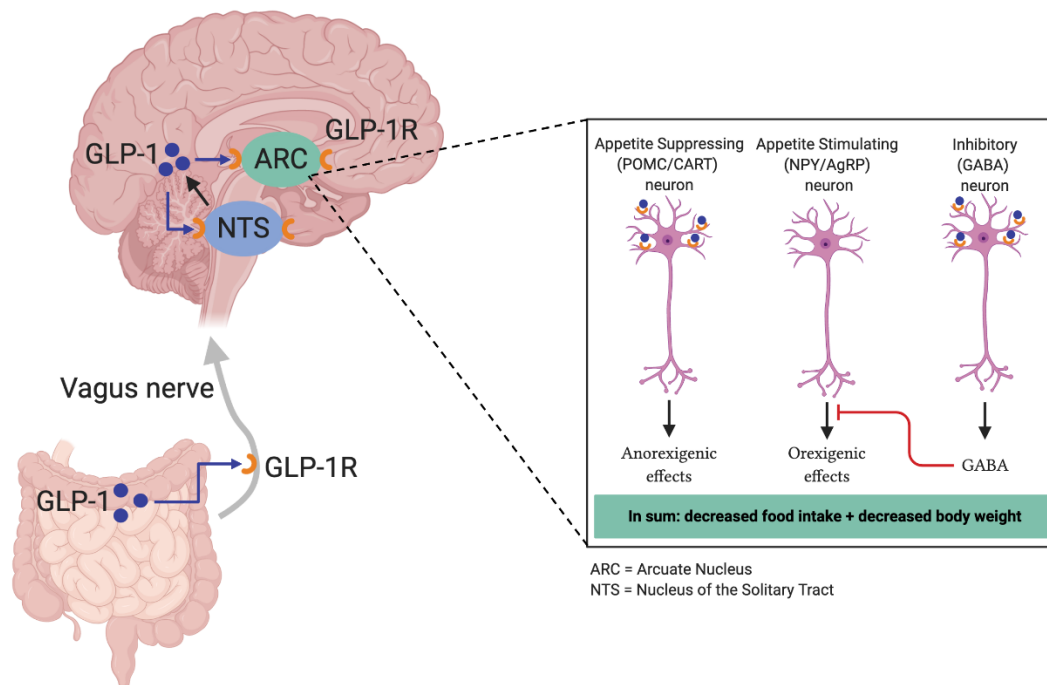


**Figure 3-2: Proglucagon-expressing (GCG) neurons modulate arcuate nucleus function via GLP-1 transmission.** Signals elicited via gut-generated GLP-1 binding to GLP-1 receptors (GLP-1R) on vagal afferents converge onto the nucleus of the solitary tract (NTS). Vagal activation of NTS *Gcg*-expressing neurons results in release of GLP-1 onto neurons in the arcuate nucleus (ARC). GLP-1 binding with GLP-1R directly activates POMC/CART neuronal transmission, while GLP-1 binding on GABAergic interneurons results in indirect inhibition of NPY/AgRP output. Thus, GLP-1 binding collectively results in decreased food intake and as a result, decreased body weight. Adapted from Baggio and Drucker<sup>291</sup>. Created with BioRender.com.

### 3.2.3 GLP-1R agonists and emerging combinatorial therapies in the control of obesity and type 2 diabetes

Mice on HFD have been shown to have decreased basal circulating GLP-1 levels, indicating that decreased GLP-1 may be a driver of metabolic adaptation seen in obesity<sup>294</sup>. Thus, GLP-1 receptor agonists (GLP-1RAs) have been explored as possible pharmaceutical targets for the treatment of obesity. GLP-1RAs are an emerging class of drugs that are used in the treatment of type 2 diabetes (T2D)<sup>295</sup>. The primary pharmacological function of GLP-1RAs is to promote insulin secretion via GLP-1's functions in the pancreas<sup>295</sup>. However, because of the wide distribution of GLP-1Rs, the agonists have positive off-target effects in other tissues. For example, liraglutide, an FDA-approved treatment for T2D, has been found to increase survival in patients with co-morbid T2D and high cardiovascular risk as indicated by decreased all-cause deaths in patients given liraglutide when compared to placebo<sup>296</sup>. In general, the class of GLP-1RAs have been indicated to have therapeutic effects beyond their role in T2D treatment, including but not limited to NAFLD, polycystic ovary syndrome (PCOS), Alzheimer's disease (AD), Parkinson's disease (PD), stroke, and certain tumors<sup>295</sup>.

Liraglutide has also been established to promote weight loss in T2D subjects<sup>297</sup>. It is evident that GLP-1R agonists are highly effective drivers of GLP-1R action and can be powerful tools in the treatment of obesity and diabetes. However, GLP-1R monotherapies often result in a weight loss plateau, in which both rodents and humans cease to lose weight after a variable amount of time<sup>298,299</sup>, thought to occur due to increased tolerance to the drug due to changes in receptor number or function, or some unknown homeostatic adaptation through compensatory metabolic-control pathways. This has necessitated the search for additional agonists that can be used in combination with GLP-1R agonists to improve initial weight loss and prevent homeostatic adaptation by targeting additional metabolic pathways. Some possible targets for combination therapies are explored below.

#### 3.2.3.1 *Growth differentiation factor 15*

Growth differential factor 15 (GDF15) has been shown to bind specifically to the GDNF family receptor  $\alpha$ -like (GFRAL) and has been shown to decrease appetite and body weight in obese animals<sup>300,301</sup>. GFRAL-expressing neurons in the area postrema (AP) have been shown to primarily innervate the NTS and parabrachial nucleus (PBN) and are sufficient to drive decreased HFD intake and body weight via DREADD excitation<sup>302</sup>. Recent studies have indicated that GLP-1R/GFRAL dual agonists induce reductions in body weight, food intake, insulin, and fasting glucose with higher efficacy than GLP-1R agonist liraglutide alone<sup>303</sup>. This synergistic improvement in metabolic indicators is thought to occur through separate pathways, as indicated by continued GLP-1R reduction in food intake even in the absence of GFRAL expression<sup>304</sup>.

#### 3.2.3.2 *Amylin*

Amylin is a peptide hormone that is co-secreted with insulin from the pancreas<sup>305</sup> and has also been shown to control energy expenditure and body weight through the excitation of

AP neurons<sup>306-312</sup>. However, amylin function has been difficult to parse out, as the amylin receptor consists of a heterodimer of the calcitonin receptor (CTR) core protein paired with one or more receptor activity modifying proteins (RAMPs), which create several different types of amylin receptors<sup>313-316</sup>. Additionally, individual neurons within the hindbrain have been shown to express more than one type of RAMP, which further increases the differential action of amylin in each neuron<sup>317</sup>. While amylin action has been highly implicated in the control of metabolism<sup>309,313,318,319</sup>, its mechanistic action is still largely unknown due to the lack of selective agonists/antagonists to target specific RAMP/CRT receptor complexes that mediate amylin signaling<sup>313</sup>.

Despite the lack of information surrounding the mechanistic effects of amylin, amylin agonist pramlintide has been successful in the treatment of T2D and has also been shown to mediate weight loss in T2D patients<sup>320,321</sup>, similarly to liraglutide. Several reports have shown that combination therapies of synthetic amylin analogs and GLP-1R agonists produce additive reductions of body weight and food intake in animals<sup>322-324</sup>. Additional research showed that the weight loss plateau associated with typical pharmacotherapies could be overcome through a stepwise combinatorial therapy wherein animals received amylin treatment for one week, liraglutide the next, and then combined amylin and liraglutide for two more weeks<sup>322</sup>. Through the examination of cFos-immuno-positive neurons in the AP and NTS, Liberini, *et al.* were additionally able to determine that amylin seemed to activate neurons equally in both the NTS and AP, while liraglutide primarily activated neurons located in the NTS<sup>322</sup>. Combination therapy increased cFos expression in both brain areas, suggesting that amylin and GLP-1 may activate a set of overlapping circuits to create synergistic reductions in food intake and body weight when activated together.

### 3.2.3.3 Adipokines: leptin, adiponectin, and interleukin-6

Bioactive molecules released from adipose tissue, known as adipokines, have been implicated in homeostatic control of metabolism<sup>325</sup>. During obesity, adipose tissue undergoes extensive remodeling and subsequently increases its release of pro-inflammatory adipokines and decreases its release of anti-inflammatory adipokines<sup>325</sup>. Additionally, GLP-1 has been found to limit inflammation in adipocytes, thus possibly mediating adipokine contribution to obesity<sup>326</sup>. Here, I'll discuss three adipokines that have been implicated in GLP-1 control of obesity – leptin, adiponectin, and interleukin-6.

#### 3.2.3.3.1 Leptin

Leptin has long been established to decrease appetite and increase energy expenditure through its actions in the ARC, acting through a similar mechanism as described in **Figure 3-2**<sup>327</sup>. As circulating leptin levels increase with increased adipose tissue mass, it is expected that leptin signaling would aid in increased fat loss<sup>328</sup>. However, leptin resistance, or impaired leptin functioning, is one of the hallmarks of obesity, although its cause is a subject of controversy<sup>329,330</sup>. Although leptin monotherapies have not been successful in causing weight loss<sup>331-333</sup>, some have hypothesized that leptin may modulate GLP-1 action or secretion, due to their overlapping actions in the ARC. Leptin has also been shown to

stimulate GLP-1 secretion from rodent and human intestinal L cells<sup>294</sup>. It has been established in both humans and rodents that low doses of GLP-1R agonists and leptin additively reduce food intake and body weight, while increasing doses of leptin had no additive effects on GLP-1R agonism<sup>334,335</sup>. Additionally, GLP-1R agonism reduced expression levels of protein tyrosine phosphatase 1B (PTP1B), a negative regulator of leptin receptor signaling, indicating a GLP-1-mediated effect on leptin signaling pathways that increase leptin sensitivity<sup>335</sup>.

In addition to its direct effects on the ARC, leptin receptors have been shown to be present on GCG neurons<sup>336</sup>, and functional studies have shown that leptin activates GCG neurons in the hindbrain<sup>337</sup>. Centrally administered leptin is also sufficient to mediate proglucagon expression and GLP-1 release in the hindbrain, as indicated by *Gcg* mRNA levels in the NTS and hypothalamic GLP-1 levels<sup>338</sup>.

#### *3.2.3.3.2 Adiponectin*

Adiponectin, though primarily produced in adipocytes, can be released by various other tissues and organs<sup>339</sup>. In both humans and rodents, adiponectin has been shown to increase insulin sensitivity, reduce inflammation, and decrease body weight<sup>340</sup>. Patients with obesity and T2D have been reported to have low adiponectin levels<sup>341</sup>, and GLP-1R agonists have been shown to increase adiponectin expression in both rodents and humans<sup>342,343</sup>. However, very little research has been done exploring how GLP-1R signaling mediates adiponectin release.

#### *3.2.3.3.3 Interleukin-6 (IL-6)*

Interleukin-6 (IL-6) is released by adipocytes, especially during adipose tissue expansion, causing its levels to be much higher in obese individuals<sup>344,345</sup>. One group found that GLP-1R agonism increases IL-6 circulating levels in both humans and mice, and that increased IL-6 signaling induced adipose tissue browning and thermogenesis<sup>346</sup>. In adipose-specific IL-6 receptor knockout mice, GLP-1R agonism still induced weight loss, but did not induce browning or metabolic alterations<sup>346</sup>. This indicates a synergistic effect between GLP-1 and IL-6, in which GLP-1 is primarily responsible for inducing weight loss, while IL-6 induces adipose tissue browning to improve glucose homeostasis and increase metabolism.

### **3.2.3.4 Endocrine-released hormones**

#### *3.2.3.4.1 Ghrelin*

Ghrelin is secreted primarily in the gut and stimulates food intake in a dose-dependent manner<sup>347</sup>. When functioning typically, ghrelin rises before a meal and decreases after a meal, with levels decreasing proportionally to the number of calories consumed<sup>348</sup>. However, in obese individuals, ghrelin levels were not proportional to caloric load, and were also reduced less post-prandially when compared to control subjects<sup>349</sup>. Ghrelin action occurs in the ARC, where its receptor is expressed on the orexigenic NPY/AgRP neurons<sup>350</sup>. It has been hypothesized that ghrelin, leptin and GLP-1 action in the ARC act

to balance the appetite modulating effects of each other and serve to enable more selective control of appetite<sup>351,352</sup>.

#### 3.2.3.4.2 *Glucose-dependent insulintropic polypeptide*

Glucose-dependent insulintropic polypeptide (GIP) is synthesized and released in the gut, and like GLP-1, belongs to the class of hormones known as incretins<sup>353</sup>. GIP receptor (GIPR)/GLP-1 receptor (GLP-1R) co-agonists have shown potential results in improving glucose tolerance and increasing weight loss beyond the effects of GLP-1R alone<sup>354–356</sup>. GIP mechanisms in the control of obesity, however, are still under debate, as agonism of GIPR has been shown to increase glucagon secretion and even inhibit the appetite-suppressing effects of GLP-1<sup>357,358</sup>. One possible mechanism explaining the improved effects of GIPR/GLP-1R co-agonism in the face of this is that GIPR is removed from the membrane after an initial GIPR stimulation, thus desensitizing further GIP metabolic action<sup>359</sup>.

#### 3.2.3.4.3 *Other PPG-derived hormones: GLP-2, glicentin, and oxyntomodulin*

GLP-2, like GLP-1, is released post-prandially from endocrine L cells and is also released by GCG neurons, though there is a paucity of research surrounding CNS GLP-2. It has been shown to induce anorexia not caused by taste aversion when injected intracranially<sup>360</sup>. However, its interactions with GLP-1 remain contentious, with one group finding that antagonism of GLP-1R abolished GLP-2 induced anorexia<sup>360</sup>, and another finding increased anorectic effects of GLP-2 in GLP-1R knockout mice<sup>361</sup>.

Both glicentin and oxyntomodulin are also released post-prandially from L cells and are thought to be released from GCG neurons in the hindbrain. Oxyntomodulin (OXM) is a dual agonist for the glucagon receptor (GCGR) and GLP-1R and is thought to mediate decreased food intake and increased energy expenditure via binding to GCGR and improved glucose homeostasis via binding to GLP-1R<sup>362–365</sup>. Three clinical trials (one ongoing) have formed to study the efficacy of a synthetic OXM analog LY3305677 in obesity and T2D, with one indicating weight loss measured up to 12 weeks in obese patients<sup>366–368</sup>. To my knowledge, there are no known effects of NTS-derived glicentin, and its receptor remains unknown.

#### 3.2.3.4.4 *Post-prandially released hormones: peptide YY and cholecystokinin*

Peptide YY (PYY), cholecystokinin (CCK) and GLP-1 are all released post-prandially and function as satiety signals. After entering the gastrointestinal lumen, nutrients trigger the secretion of these peptides from endocrine L cells, which then activate vagal afferents to the NTS<sup>369</sup>. PYY has been shown to be released post-prandially in amounts dependent on caloric load and reduces food intake and prolongs inter-meal intervals<sup>370–373</sup>. In obese individuals, fasting levels of PYY are lower and postprandial levels are lowered, despite not exhibiting resistance to the appetite-mediating effects of PYY<sup>374,375</sup>. CCK also dose-dependently reduces food intake in both rodents and humans, and reduced sensitivity to

CCK is a hallmark of diet-induced obesity<sup>376</sup>. Two different dual GLP-1/CCK hybrid peptides decreased body weight in DIO mice over GLP-1R agonism alone, indicating there may be synergistic effects that they play in the control of food intake and satiety<sup>377,378</sup>.

## 4 CHAPTER 4: TRANSCRIPTIONAL PROFILING OF HINDBRAIN NEURONS OF ANIMALS ON CHRONIC HIGH-FAT DIET

---

### 4.1 ABSTRACT

It has been well-established that GLP-1 is a central mediator in the control of food intake and body weight, making it a primary target in the pharmacological treatment of obesity. While GLP-1 receptor agonists have shown promising weight loss in obese patients, these pharmacotherapies often result in a weight loss plateau. This loss in efficacy has necessitated the search for additional targets that can be used in combination with GLP-1 receptor agonists to further improve weight loss and reduce tolerance to the therapy. This chapter explores our efforts to establish a single-nuclei isolation technique for the hindbrain and a pilot experiment to investigate differential GLP-1 signaling in obese mice. Finally, I will explore emerging data in the field and how it has changed the dogma around GLP-1 signaling.

### 4.2 INTRODUCTION

GLP-1 is directly linked to appetite suppression and been implicated in mediating weight loss, which has made it a target of interest in the control of obesity<sup>295</sup>. Obesity is significantly associated with increased mortality rates, and as body mass index (BMI) increases, so does overall mortality and co-morbid diabetes-related mortality rates<sup>231</sup>. In 2013, the National Health and Nutrition Survey estimated that in the United States, 1 in 3 adults were considered obese (body mass index/BMI  $\geq 30$ ) and obesity accounted for 18% of deaths among Americans between the ages of 40 and 85<sup>232,233</sup>. While bariatric surgery remains the most effective intervention in the treatment of obesity<sup>379</sup>, it is still only efficacious in approximately 80% of patients<sup>380</sup>, underlining a vital need for the creation of safe and effective pharmacotherapies in the treatment of obesity.

GLP-1 receptor (GLP-1R) agonists are an emerging class of drugs that have been FDA-approved in the treatment of obesity<sup>295</sup>. While initially GLP-1R agonists were explored for their promotion of insulin secretion in the treatment of type 2 diabetes (T2D), the agonists have also shown promising results in promoting weight loss in obese patients<sup>297,381,382</sup>. It has become increasingly evident that GLP-1R agonists are highly effective drivers of appetite suppression and weight loss. However, GLP-1R monotherapies often result in a weight loss plateau, in which both rodents and humans reach a point of weight loss where continued or increased drug administration ceases to decrease weight<sup>298,299</sup>. This has necessitated the search for additional therapies that can be combined with GLP-1R agonists to both improve weight loss and prevent compensatory action in other brain areas that may affect the continued effects of GLP-1R agonism.

A study by Gaykema, *et al.* compared the selective activation of GCG neurons in both lean and obese animals by injecting a cre-dependent Gq-coupled DREADD (designer receptor exclusively activated by designer drugs) into the NTS of a *Gcg*-cre expressing mouse. Excitation of *Gcg*-expressing (GCG) neurons via CNO injections was sufficient to reduce food intake in both lean and obese animals but stimulated rapid, significant weight loss exclusively in obese animals<sup>383</sup>. The rapid weight loss potentiated by GCG activation by DREADDs makes it unlikely that the DREADD-mediated GCG activation is causing transcriptional changes, necessitating that obesity and/or a chronic high-fat diet has driven changes that regulate how GCG stimulation affects body weight.

This selective regulation of weight loss suggests that there may be transcriptional changes that are differentially regulated between lean and obese animals. Identification of these transcriptional changes could lead to more efficacious treatment of obesity by establishing likely candidates for co-agonism with other established GLP-1R agonists such as liraglutide.

Based on current literature about GLP-1 action and obesity, I developed three distinct hypotheses that describe possible ways that obesity may regulate GLP action in the hindbrain to help direct analysis of transcriptional data:

- (1) GCG bias toward local or distant control depending on nutritional state. GCG neurons under different nutritional states could possibly be biased towards either glutamatergic or GLP-1 mediated action and affect different brain areas. Local NTS GCG innervation relies on glutamatergic signaling to facilitate recruitment of GLP-1 neuronal populations<sup>384</sup> while NTS GCG projections outside the NTS function through the release of GLP-1 to suppress appetite. These two modalities of NTS GCG action could explain why DREADD activation of GCG neurons in obese animals triggers such rapid weight loss, as it may activate the local circuit through glutamatergic action and function as a gain amplifier. Differential regulation of GCG and glutamate transcripts could address this hypothesis.
- (2) Co-transmission. As discussed in “Section 3.2.3: GLP-1R agonists and emerging combinatorial therapies in the control of obesity and type 2 diabetes”, there are several molecules that are released alongside of GLP-1 or are implicated in the regulation of GLP-1 action. Of particular interest is GFRAL activation, as GFRAL activation by DREADDs initiates rapid body weight loss in the most similar fashion to what was seen with DREADD activation of GCG neurons but was also paired with aversion to water and food<sup>302</sup>, indicating that the rapid weight loss caused by GFRAL activation was caused by a precipitous drop in water intake, rather than loss of fat mass. This is contrasted however, with the selective activation of GCG neurons, which caused rapid weight loss (~2 grams in 48 hours) which was accompanied by decreased adipose mass<sup>383</sup>.

- (3) Vagal remodeling and microbiome dysbiosis. Increasing evidence has implicated diet-induced microbiome dysbiosis in vagal remodeling and neuroinflammation. One study found that four weeks of HFD is sufficient to induce microbiome dysbiosis and chronically increased plasma lipopolysaccharide (LPS), which is a potent activator of the immune system<sup>385,386</sup>. Chronic low-dose administration of LPS inhibited CCK-mediated signaling and accompanying satiation response, indicating a loss or decrease of vagal afferent function, which leads to alterations in the frequency and amplitude of glutamate release in the NTS<sup>387</sup>. A decrease of vagal innervation onto the NTS is also seen in animals given a HFD, indicating that diet-mediated dysbiosis initiates vagal withdrawal from the hindbrain<sup>386</sup>. Together, these findings implicate microbiome dysbiosis in the control and maintenance of obesity. Reduced vagal innervation of GCG neurons could be explored through analysis of transcripts related to vagal signaling. GCG-negative populations could also reveal possible differences in astrocytic function, which has also been implicated in the control of neuroinflammation.

To query the role of differential regulation of GCG-mediated firing across nutritional states, we established a workflow (**Figure 4-1**) wherein animals expressing *Gcg*-driven ZSGreen are kept on either normal chow (NC) or high fat diet (HFD) for 5 months to induce obesity. After hindbrain isolation and dissociation, single-cell suspensions are sorted with Fluorescence-Activated Cell Sorting (FACs) according to ZSGreen status as an indicator of *Gcg* expression. Single-cell RNA-seq of *Gcg*-expressing and non-expressing neurons in both NC and HFD animals allows for comparison of transcriptomes to highlight possible functional differences in GCG-regulated signaling across nutritional states.

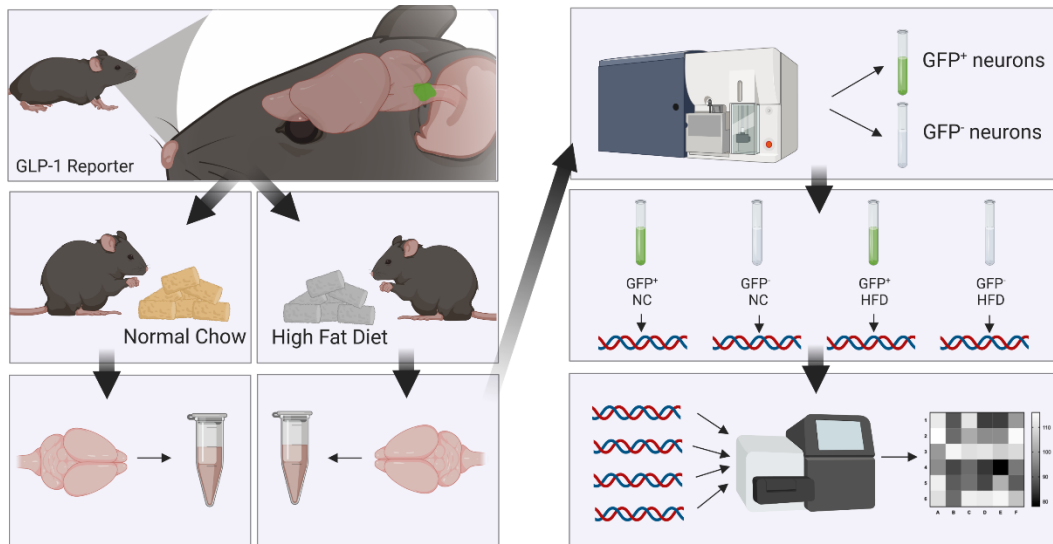


**Figure 4-1: Proposed experimental workflow to assess differential regulation in GCG neurons across nutritional states.** By driving selective expression of ZSGreen through GCG-cre, we can use FACs sorting to isolate GCG populations of neurons in both NC and HFD animals. Single-cell analysis can then reveal possible transcriptomic differences in the HFD sample of animals that could regulate differences in GLP-1 mediated signaling.

## 4.3 RESULTS

### 4.3.1 Established single-cell isolation techniques do not yield sufficient numbers of neurons

Because GCG neurons are present at very low levels in the hindbrain, we required a single-cell isolation protocol that produced high yields of cells. Typical methods of isolation, such as sucrose gradients, can result in up to 70% loss of the total cells. Based on published protocols, we first attempted a protease-mediated method of dissociation in live cells<sup>388-391</sup>. These methods resulted primarily in insufficient digestion of hindbrain slices, which we believed to be due to the high amounts of myelin present in the hindbrain that are not present in other brain areas.

Based on research indicating that fixation of cells does not substantially reduce RNA quality at the gene level<sup>392,393</sup>, we decided to fix cells with 3,3'-dithiobis(sulfosuccinimidyl propionate) (DTSSP), a water-soluble amine-reactive crosslinker, to prevent RNA degradation during isolation. Additionally, we pivoted to collecting single-nuclei rather than single-cells based on data indicating that transcript levels are similar for nuclei and cells across approximately three orders of magnitude, and conserved marker gene expression confirmed that the same 11 cell types were identified with nuclei and cells<sup>394,395</sup>. The combination of these two changes allowed us to use physical methods of dissociation, which improved the cell clumping that we experienced with the protease digestion.

### 4.3.2 Significant levels of cellular debris during nuclear isolation prevents selective isolation

Our adapted protocol resulted in successful isolation of single nuclei from the mouse hindbrain, but also resulted in significant cellular debris which made selective isolation of nuclei difficult and increased contamination (**Figure 4-2**). To address this issue, we tested several methods of enrichment, which we hoped would allow us to both concentrate nuclei and decrease contaminants that were created during dissociation. Trials included myelination removal, selective pulldown with an anti-nuclear pore complex (NPC) antibody, a gum Arabic + octanol wash<sup>396,397</sup>, size-mediated filtration, and two successive FACs sorts (trials and results summarized in **Table 4-1**). All attempted methods, however, resulted in significant loss of nuclei, rendering them incompatible with our downstream applications as well as reducing an already small population of the neurons of interest.

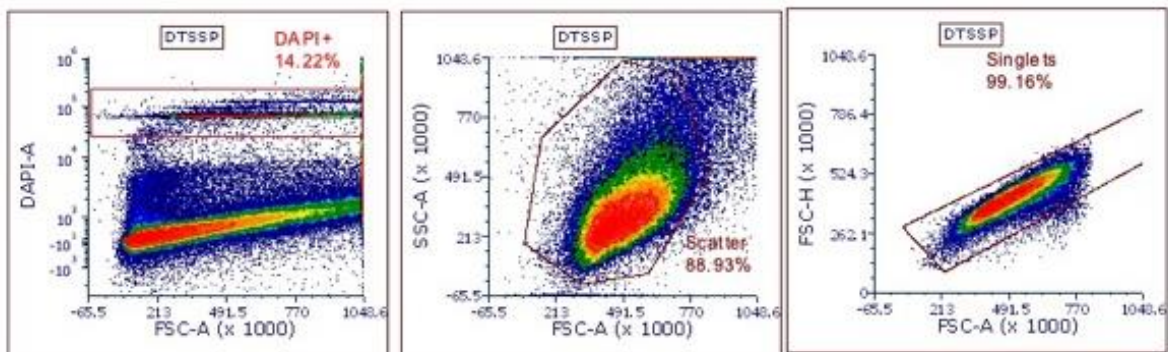


**Figure 4-2: Excessive amounts of debris during nuclear isolation prevents selective isolation of nuclei.** Representative image showing that hindbrain samples contained high amounts of debris as indicated by the large percentage of non-DAPI<sup>+</sup> events. Brain tissue obtained from the hindbrain was isolated using manual dissociation with a plastic pestle, fixed using DTSSP, and stained with DAPI. Samples shown here did not undergo any further manipulation after nuclei isolation protocol and were run on an Attune NxT Flow Cytometer (ThermoFisher). DTSSP = 3,3'-dithiobis(sulfosuccinimidyl propionate))

	Basic Protocol	Adjustments/Combinations	Results
<b>Myelin Removal</b>	Followed protocol included with Myelin Removal Beads II (Miltenyi Biotec, Bergisch Gladbach, Germany, #130-096-731)		<b>Myelin Removal</b> – 43.8 nuclei/uL <b>No myelin removal</b> – 756 nuclei/uL
<b>Selective pulldown</b>	Using a DSB-X Biotin Protein Labeling Kit (Invitrogen, # D20655), added a DSB-X biotin receptor to a purified anti-NPC antibody (BioLegend, Clone #Mab414, Cat #902902). After single nuclei isolation, add DSB-X-NPC antibody to nuclei and incubate for 30 min with rotation. Wash and add streptavidin-conjugated magnetic beads (Bioclone Inc, Cat# MM1-105) to nuclear slurry and incubate for 20 min with rotation. Add biotin release buffer (50 mM D-biotin in 10 mM sodium carbonate, Invitrogen, Cat#E20656) and incubate for 10 min to release nuclei from beads. Cell counts were determined via DAPI staining and counted nuclei using a hemacytometer and ImageJ.	Adjusted bead amounts (75 uL, 100 uL, 150 uL) with 10 ug/10 <sup>7</sup> nuclei, 1 mL release buffer Adjusted antibody added (10 ug/10 <sup>7</sup> nuclei or 25 ug/10 <sup>7</sup> nuclei) to 75 uL of beads Adjusted at what step fixative was added (before antibody, with antibody, with beads, with biotin release buffer)	75 uL: 1.07 x 10 <sup>6</sup> nuclei (45% of input) 150 uL: 1.95 x 10 <sup>6</sup> nuclei (57% of input) 10 ug Ab/10 <sup>7</sup> nuclei: 7.43 x 10 <sup>5</sup> nuclei (33% of input) 25 ug/10 <sup>7</sup> nuclei: 7.65 x 10 x 10 <sup>5</sup> nuclei (32% of input)
<b>Gum Arabic + Octanol</b>	This protocol worked, until we purchased a different lot of streptavidin-coated magnetic beads, and then we could not get the antibody to release from the beads. Followed two different protocols by Cummings and Fomey in which nuclei are added to a gum-arabic/octanol buffer before adding to beads for selective pulldown protocol	Multiple release steps (using 10 ug Ab/10 <sup>7</sup> nuclei, 75 ug beads, 1 mL release buffer)	One release: 1.07 x 10 <sup>6</sup> nuclei (45% of input) Two sequential releases: 1.74 x 10 <sup>6</sup> nuclei (74% of input)
<b>Size-Restricted Filtration</b>	Filtered nuclei with three different sizes of filters: 0.45 um, 1.2 um and 3.0 um	Combined with selective pulldown to further reduce debris using 10 ug Ab/10 <sup>7</sup> nuclei, 75 ug beads, 1 mL release buffer	Original buffer: 3.81 x 10 <sup>5</sup> nuclei (8% of input) Fomey: 1.4 x 10 <sup>6</sup> nuclei (16% of input) Cummings: 3.33 x 10 <sup>6</sup> nuclei (48% of input)
<b>Successive FACs sorting</b>	After selective pulldown protocol, sorted nuclei first on DAPI and then sorted the nuclei collected from that sort again on ZSGreen, collecting both ZSGreen <sup>+</sup> and ZSGreen <sup>-</sup> nuclei	Combined with selective pulldown to further reduce debris (using 10 ug Ab/10 <sup>7</sup> nuclei, 75 ug beads, 1 mL release buffer)	Unfiltered: 1.2 x 10 <sup>5</sup> nuclei 0.45 um filter: 8.7 x 10 <sup>3</sup> nuclei 1.2 um filter: 6.4 x 10 <sup>3</sup> nuclei 3 um filter: 7.9 x 10 <sup>3</sup> nuclei Sort 1: 1.16 x 10 <sup>3</sup> DAPI <sup>+</sup> nuclei/ 100000 events (1.16% of events were nuclei) Sort 2: 8.16 x 10 <sup>4</sup> DAPI <sup>+</sup> nuclei/ 100000 events (81.60% of events were nuclei)

**Table 4-1: Summary of protocols used to clear debris from nuclei slurry.** Trials include myelin removal with myelin removal beads, selective pulldown with various adjustments to different steps of the basic protocol, a gum arabic + octanol wash step<sup>396,397</sup>, size-restricted filtration, and successive FACs sorts to enrich for DAPI<sup>+</sup> nuclei. Number of nuclei were determined by counting DAPI<sup>+</sup> nuclei with a hemacytometer in ImageJ<sup>398</sup>.

### 4.3.3 Pilot experiment using microfluidics-based cellular sorting and Smart-seq

Due to our continued struggles with obtaining concentrated samples of hindbrain nuclei, we attempted a pilot experiment using the 10X Genomics (Pleasanton, CA, USA) protocol for the isolation of nuclei from tissue<sup>399</sup>, along with sorting nuclei with the Nanocollect WOLF (San Diego, CA, USA), which claims to be gentler than traditional cell sorters and to improve specificity of sorting. We found that we were able to increase the GFP<sup>+</sup> nuclei fraction and remove debris without an enrichment sort (**Figure 4-3**), which we had not previously been able to accomplish.

For this pilot experiment, one GLP:ZSGreen animal from each experimental group (HFD and NC) was harvested and had nuclei isolated, then sorted into 384-well plates containing Smart-seq capture buffer. Both ZSGreen<sup>+</sup> and ZSGreen<sup>-</sup> nuclei were collected from each animal into separate plates to examine both *Gcg*-expressing and non-expressing nuclei and non-nuclei in the hindbrain, as differential effects in obesity may be occurring outside of GCG nuclei. Ninety-six nuclei from each group (HFD DAPI<sup>+</sup>ZSGreen<sup>+</sup>, HFD DAPI<sup>+</sup>ZSGreen<sup>-</sup>, NC DAPI<sup>+</sup>ZSGreen<sup>+</sup>, and NC DAPI<sup>+</sup>ZSGreen<sup>+</sup>) were prepared by Dr. John Campbell using the Smart-Seq2 protocol and sequenced at the Functional Genomics core at Beth Israel Deaconess Medical Center.

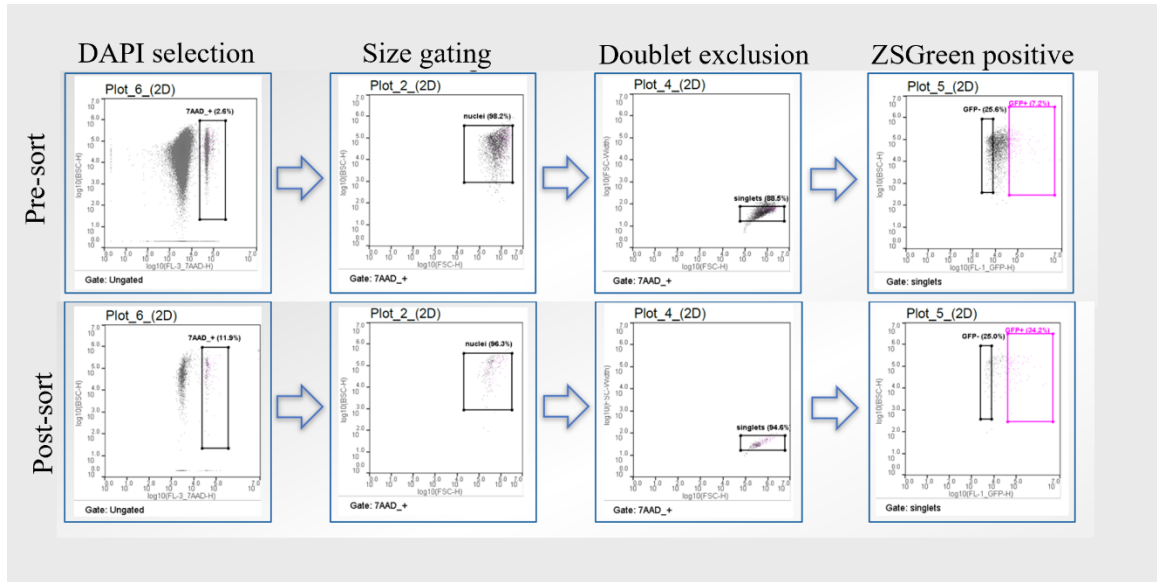


**Figure 4-3: WOLF sorter successfully enriched DAPI<sup>+</sup> nuclei and decreased levels of debris.** When observing nuclei in the pre-sorted sample, there was a significant amount of debris, which resulted in a low percentage of DAPI<sup>+</sup> nuclei in the sample. After the sort selecting for DAPI<sup>+</sup>ZSGreen<sup>+</sup> nuclei, we saw a significant increase in DAPI<sup>+</sup>ZSGreen<sup>+</sup> nuclei (post-sort), indicating successful enrichment of the target population.

#### 4.3.4 Transcriptomic analysis of single-nuclei RNA-seq

Transcriptomic analysis of single-nuclei dataset was performed using the R package Seurat<sup>400</sup>. Clustering analysis made it apparent that there were no clusters specific to treatment group (**Figure 4-4**), and that *Gcg* gene expression was present in very few of the sampled nuclei (**Figure 4-5**) and therefore was not sufficient to drive clustering of nuclei. Right away, this indicated that it was highly unlikely that this pilot experiment had revealed genes that could possibly drive differential regulation of obesity. Despite this, I examined the genes that were differentially expressed across cluster types to determine if there were other genetic markers that defined clustering that may be of interest.

Despite filtering out mitochondrial genes, Cluster 0 seemed to be driven by high expression of mitochondrial genes (**Figure 4-6**) and was also the cluster that represented the highest number of nuclei (206). Cluster 1 was defined by expression of *Rbfox1*, *Lingo2*, *Fam155a*, *Nrg3*, *Tenm2*, *Snhg11*, *Fgf14*, *Meg 3*, *Lrrtm4*, and *Kcnip4* (**Figure 4-7**). This cluster also contained the very few *Gcg*-expressing neurons that were identified (**Figure 4-5**). An examination of the functions of the genes is found in **Table 4-1**. Cluster 2 was defined by *St18*, *Plcl1*, *Arhgap23*, *Neat1*, *St6galnac3*, *Nkain2*, and *Plekhh1* (**Figure 4-8**). An examination of the functions of these genes is found in **Table 4-1**. While no trends were discovered, the expression of *Lingo2*, *Tenm2*, and *Nrg3*, which are all implicated in neuronal processes, further indicates that Cluster 1 represents a population of neurons.

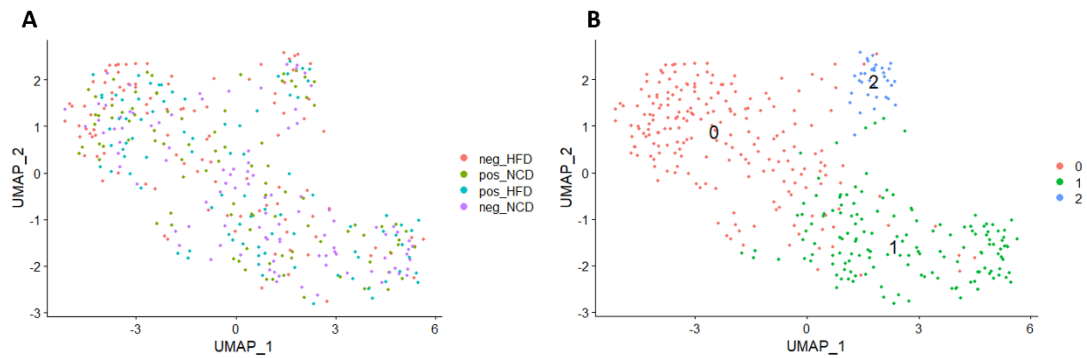


**Figure 4-4: Clustering of single-nuclei RNA-seq.** (A) When color-coded by the experimental sub-groups, it is apparent that no sub-group was transcriptionally unique, as would be expected if *Gcg* neurons experienced differential transcriptional regulation in HFD versus NC animals. (B) Clustering analysis sub-divided the nuclei into 3 distinct clusters. neg\_HFD = HFD animals, DAPI<sup>+</sup>ZSGreen<sup>-</sup> nuclei; pos\_NCD = NC animals, DAPI<sup>+</sup>ZSGreen<sup>+</sup> nuclei, pos\_HFD = HFD animals, DAPI<sup>+</sup>ZSGreen<sup>+</sup> nuclei; neg\_NCD = NC animals, DAPI<sup>+</sup>ZSGreen<sup>+</sup> nuclei

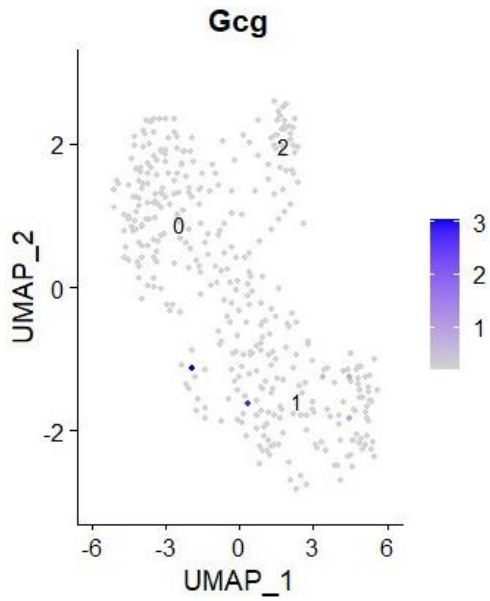


**Figure 4-5: *Gcg* gene expression was identified in very few nuclei.** *Gcg* expression was localized to Cluster 1, but was expressed in very low numbers of nuclei, indicating that either *Gcg* levels are under the level of detection, or *Gcg* neurons were not actually enriched during the sorting process.

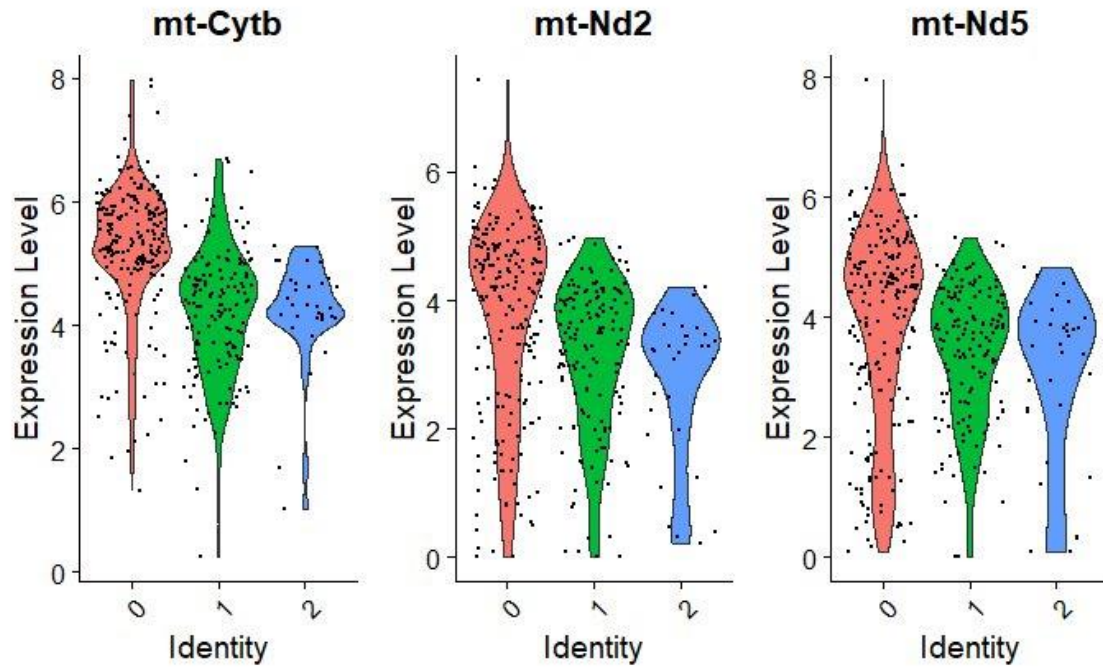


**Figure 4-6: Despite filtering, mitochondrial genes are present in all clusters.** Mitochondrial gene expression was present in every cluster at high expression levels, indicating there was a high level of mitochondrial contaminants in our sample. Cluster 1 is primarily driven by the expression of these mitochondrial genes.

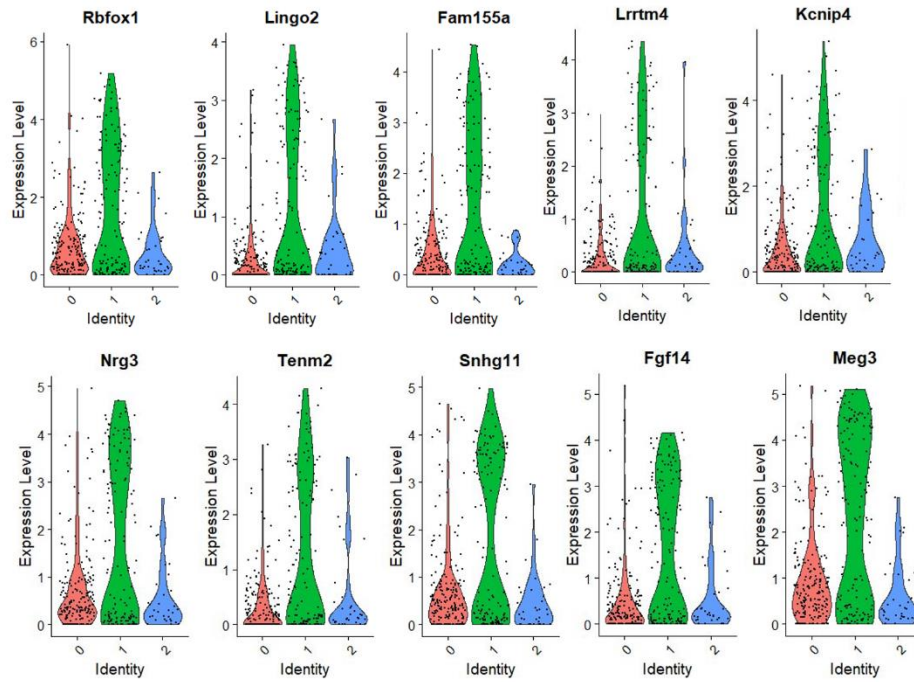


**Figure 4-7: Genes driving cluster 1.** The genes driving cluster 1 include *Rbfox1*, the gene that produces the antigen neuronal nuclei (NeuN), suggesting that this cluster represents the neuronal population.

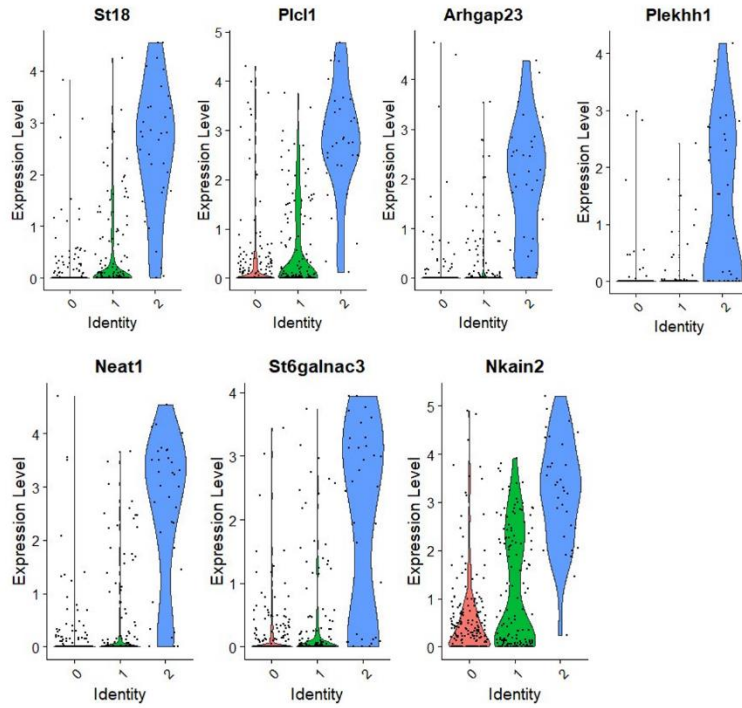


**Figure 4-8: Genes driving cluster 2.** There are no apparent identifying genes in this cluster, aside from *Plcl1* possibly indicating that this cluster represents GABAergic neurons.

Gene	Function
<b>Rbfox1</b>	Produces the neuronal nuclei (NeuN) antigen
<b>Lingo2</b>	Acts upstream of positive regulation of synapse assembly
<b>Fam155a</b>	Predicted to contribute to stretch-activated calcium-channel activity
<b>Lrrtm4</b>	Involved in regulation of synapse assembly, part of AMPA glutamate receptor complex
<b>Kcnip4</b>	Enables calcium ion binding activity and potassium channel regulator activity; part of voltage-gated potassium channel complex
<b>Nrg3</b>	Involved in intracellular signal transduction and regulation of cell migration; predicted to be active in the glutamatergic synapse
<b>Tenm2</b>	Predicted to be involved in retrograde trans-synaptic signaling by trans-synaptic protein complex; predicted to be active in neuron projection
<b>Snhg11</b>	Unknown
<b>Fgf14</b>	Predicted to enable growth factor activity and sodium channel regulatory activity
<b>Meg3</b>	Negative regulator of cell growth
<b>St18</b>	Predicted to enable DNA-binding transcription factor activity
<b>Plcl1</b>	Predicted to enable GABA receptor binding activity, regulation of GABAergic transmission, and GABA signaling pathway
<b>Arhgap23</b>	Part of RHO family of small GTPases involved in signal transduction through transmembrane receptors
<b>Plekh1</b>	Unknown
<b>Neat1</b>	Forms core structural component of the paraspeckle sub-organelles
<b>St6galnac3</b>	Predicted to be involved in oligosaccharide metabolic process and protein glycosylation
<b>Nkain2</b>	Predicted to be involved in regulation of sodium ion transport

**Table 4-1: Exploration of differentially regulated genes that drove UMAP clusters.** Functional analysis of top differentially regulated genes across clusters did not reveal any strong trends. Cluster 1 was defined by several genes involved with the glutamatergic synapse or synapse assembly in general (*Lingo2*, *Nrg3*, *Tenm2*), further indicating that it represents neurons, and possibly specifically glutamatergic neurons. Enrichment of *Plcl1* may indicate that cluster 2 contains GABAergic neurons.

#### 4.4 DISCUSSION

This study of GCG neurons in the hindbrain represents a push towards a better understanding of the mechanisms of appetite control and how they might be differentially regulated during obesity. While we attempted to establish an improved system for isolating nuclei from the hindbrain, we faced multiple obstacles due to the vast amounts of debris that are produced during tissue dissociation. This remains a primary obstacle in establishing a transcriptomic pipeline for GCG neurons and their targets specifically, as they represent a very small proportion of hindbrain neurons.

In a recent study surveying the transcriptome of mouse hindbrain neurons, 16,034 nuclei were collected from the AP and NTS of 4 animals, and only 173 expressed *Glp1r* (~1% of collected nuclei)<sup>401</sup>. Within that small population, there appeared to be even further stratification, with clustering of *Glp1r* neurons indicating that there are groups of both inhibitory and excitatory neurons that receive inputs from GCG neurons<sup>401</sup>. In terms of co-expression of receptors, 6 of the 173 *Glp1r*-expressing nuclei co-expressed *Gipr* (GIP receptor), 5 co-expressed *Calcr* (a component of amylin receptors), and 4 co-expressed *Gfral* (GDF15 receptor), indicating that there may be subsets of neurons that receive further modulation from these metabolic agonists<sup>401</sup>. As discussed in “Section 3.2.3: GLP-1R agonists and emerging combinatorial therapies in the control of obesity and type 2 diabetes”, GIP, amylin, and GDF15 are all established to work synergistically in combinatorial therapies with GLP-1R agonists<sup>304,322,354,355,358</sup>. Based on the data discussed here, it seems likely that subsets of GLP-1R neurons are co-mediated by GCG and other metabolic inputs, with little overlap<sup>401</sup>. However, it remains unclear how these synergistic effects are modulated through the lens of obesity.

A variety of research in the past decade has implicated that GLP-1 signaling operates through two distinct pathways. Two studies found that brainstem and hypothalamus knockdown of *Glp1r* did not affect glucose tolerance or food intake but did block the effects of GLP-1R agonism on both food intake and body weight<sup>402,403</sup>. In contrast, nodose ganglion-specific deletion of GLP-1R was sufficient to alter glucose tolerance and decrease food intake but did not affect GLP-1R agonism’s effects on food intake and body weight<sup>402,403</sup>. This is consistent with data showing that synthetic GLP-1R agonists are primarily found in the AP and other circumventricular organs, indicating that these agonists bypass gut-mediated signaling and instead directly activate GLP-1R neurons in the AP<sup>299</sup>. Endogenous GLP-1, in contrast, is unlikely to reach the brain due to its short half-life<sup>286</sup>. Transcriptional and functional data in obese animals treated with GLP-1R agonists also indicated that AP *Glp1r*-expressing neurons express the highest transcriptional changes after GLP-1R agonism while NTS GCG neurons were found to have no transcriptional changes after GLP-1R agonism<sup>404</sup>. In contrast, *Glp1r*-expressing neurons in the NTS were also shown to have significant levels of transcriptional changes after GLP-1R agonism, and activation of these neurons was sufficient to reduce body weight and food intake<sup>404</sup>. Together, these data indicate that GCG neurons are not necessary to mediate GLP-1R agonism through central signaling pathways, but rather through gut-vagal signaling.

A recent study implicates that central GLP-1 mediated signaling through vagal afferent neurons (VAN) does not in fact affect satiety through GCG neurons. Initially, they found that VAN-specific *Glp1r* activation was sufficient to drive a slight decrease food intake body weight without a change in energy expenditure but was also accompanied by flavor avoidance<sup>290</sup>. This contrasts with the Gaykema, *et al.* study that showed that specific activation of NTS-GCG neurons does not cause flavor avoidance or insensitivity<sup>383</sup>. Based on their findings that *Oxtr*-expressing rather than *Glp1r*-expressing VANs were the primary vagal input onto GCG neurons in the NTS, they tested food intake in the response to oxytocin and found that GCG-NTS neurons were necessary for oxytocin-mediated

reduction of food intake<sup>290</sup>. They also demonstrated that GLP-1R agonism suppresses eating and reduces body weight independently of GCG-NTS neurons, as was indicated by selective ablation of NTS-GCG neurons having no effect on the efficacy of GLP-1R agonists. However, they found that GLP-1R agonism paired with GCG-NTS activation further reduced food intake and body weight when compared with GLP-1R agonism or GCG-NTS activation alone<sup>290</sup>. Based on these findings, they hypothesized that peripheral and central GLP-1 act to affect different pathways in the NTS, with *Glp1r*-expressing vagal afferents synapsing preferentially onto non-GCG neurons and *Oxtr*-expressing vagal afferents primarily controlling GCG neuronal activation<sup>290</sup>. Importantly, they also found that GCG-NTS activation was sufficient to drive rapid weight loss in lean animals, in contrast to the findings in Gaykema, *et al*<sup>290,383</sup>.

However, these differences may allow for further insight into how these central and peripheral pathways are differentially mediated during different stages of obesity. To that end, an important distinction to make is that the “lean” population in the Gaykema, *et al* study had been on HFD for 2 weeks prior to GCG-NTS activation, while the obese population had been on HFD for 5 months<sup>383</sup>. This may indicate, therefore, that during acute HFD administration, only peripheral GLP-1 signaling is affected, possibly through differential vagal signaling in response to changes in nutrient densities or diet-induced microbial dysbiosis<sup>386,405</sup>. Because AP-mediated GLP-1R neurons may still be functioning as normal, due to their access to circulating hormones, there is still sufficient activation of GCG neurons that increasing their firing rate through DREADD activation only slightly affects satiety<sup>383</sup>. Once obesity is established, however, central and peripheral GLP-1 signaling pathways have been altered, simultaneously impairing gut-vagal signaling that would convey GLP-1-mediated signaling as well as impairing GCG-mediated signaling, possibly through synaptic changes, modulation of *Gcg* expression, alteration of vagal-AP signaling, or increased levels of oxytocin during obesity affecting vagal-GCG signaling<sup>406-410</sup>. Thus, when DREADD activation occurs, the increased excitability of the GCG neurons allows for reduced AP or vagal inputs to be able to drive an action potential, and thus restores central GLP-1 signaling pathways, which have been shown to be sufficient to decrease food intake and body weight<sup>290</sup>. However, many of these systems of GCG-mediated signaling are still poorly understood and require further investigation to fully grasp how obesity may affect both central and peripheral GLP-1 signaling.

This hypothesis of both central and peripheral mechanisms of GLP-1 being dysregulated because of obesity rather than HFD may also shed some light on some studies indicating that *Glp1r* knockouts are protected from obesity and that GLP-1R antagonism reduces weight gain on HFD<sup>411-413</sup>. In contrast to GLP-1R agonism being sufficient to drive weight loss, several studies have found that *Glp1r* knockout mice gain significantly less weight on HFD and exhibited increases in energy expenditure regardless of diet<sup>411,413</sup>. Additionally, daily injections of a GLP-1R antagonist were found to have significant metabolic effects in animals fed HFD which were not seen in NC animals. In HFD animals, GLP-1R antagonism reduced weight gain, did not affect food intake, increased energy expenditure, and did not further impair glucose tolerance, while in NC animals, GLP-1R antagonism

had no effect on weight gain, food intake, or energy expenditure but induced glucose intolerance<sup>412</sup>. The main contrast of these studies with those that studied GLP-1R agonists is the time of pharmacological or genetic intervention – agonism studies have looked at reversal of obesity (i.e., weight loss and food intake after obesity has been established) while antagonism and knockout studies have examined protection against obesity (i.e., reduced weight gain and increased energy expenditure when consuming a high calorie diet). Again, this could indicate that central and peripheral signaling pathways of GLP-1 are affected differently by high-fat diet and obesity and requires further investigation using vagal- and brain-specific interventions to fully understand the intricacies of GLP-1 signaling.

## 4.5 EXPERIMENTAL METHODS

### 4.5.1 Experimental animals

All studies were approved by the University of Virginia's Animal Care and Use Committee. GCG-cre animals were generated as previously described in Gaykema, *et al.*<sup>383</sup>. Twelve-week-old adult male and female B6.Cg-Gt(ROSA)26Sor<sup>tm6(CAG-ZsGreen1)Hze/J</sup> (Ai6, Strain # 007906) mice were purchased from The Jackson Laboratory. Ai6 contains a floxed STOP-cassette resulting in ZsGreen expression only in cre-expressing cells. Mice were housed in the Pinn Hall vivarium at the University of Virginia on a 12h light: 12h dark cycle with *ad libitum* access to normal chow (NC, Teklad 2013, 4% fat, 17% protein, 48% carbohydrate, no sucrose, 2.9 kcal/g) and water, unless otherwise stated. Both lines have been backcrossed to C57Bl6/j animals for at least 7 generations. We generated heterozygous GCG:ZsGreen animals through two subsequent crosses: (1) crossing GCG-cre homozygous females with Ai6 homozygous males and (2) crossing the resulting heterozygous GCG<sup>cre/+</sup>/Ai6<sup>fl/+</sup> offspring (referred to as GCG:ZsGreen throughout). This strategy results in ZsGreen expression localized to GCG-expressing neurons. At weaning, pups were either kept on NC or transferred onto a high-calorie diet (Teklad TD.88137, 15.2% kcal from protein, 42.7% kcal from carbohydrate, and 42% kcal from fat, Envigo, Dublin, VA, USA) in an effort to distribute sexes evenly across both NC and HFD conditions. GCG animals were genotyped with the following primers: *Cre*<sup>+</sup> 5'-GTGAAACAGCATTGCTGTAC-3', *Cre*<sup>-</sup> 5'-TGCTTCTGTCCGTTTGCCGGT-3', M176 5'-GGTCAGCCTAATTAGCTCTGTCAT and M177 5'-GATCTCCAGCTCCTCCTCTGTCT-3'. Ai6 mice were genotyped with the following primers: WT Forward 5' -AAG GGA GCT GCA GTG GAG TA - 3', WT Reverse 5' - CCG AAA ATC TGT GGG AAG TC - 3', Mut Reverse 5' - GGC ATT AAA GCA GCG TAT CC - 3', Mut Forward 5' - AAC CAG AAG TGG CAC CTG AC - 3'.

### 4.5.2 Nuclei isolation protocol used for pilot experiment

Two seven-month old GCG:ZsGreen animals, one kept on NC for 7 months and one kept on HFD for 7 months, were euthanized using 100 uL of Euthasol euthanasia solution (Virbac AH, Inc., Carros, France). Once mice no longer responded to a toe pinch, mice were decapitated as a secondary measure of euthanasia. The brains of the animals were

removed and placed in ice-cold PBS to halt heat-mediated degradation of RNA. Using two razor blades, the hindbrain was dissected by cutting caudal of the superior colliculus and rostral to the cerebellum. The following protocol is an adaptation of the 10X Genomics protocol for isolation of nuclei<sup>399</sup>. Tissue slices were placed in a 1.5 mL microfuge tube filled with 200  $\mu$ L of ice-cold 10X buffer (20 mM sodium bicarbonate buffer pH 8.2, 5 M NaCl, 1M MgCl<sub>2</sub>, 25% NP-40 brought up to 10 mL with 1X PBS). Using a sterile plastic pestle, tissue was disrupted with 10 twists of the pestle and then another 200  $\mu$ L of ice-cold 10X buffer was added to the homogenate. Homogenate was spun for ~2 sec in a tabletop minifuge to settle any non-homogenized tissue. Tissue was then further homogenized via ten more passes of the plastic pestle and 100  $\mu$ L of 10X buffer was added to homogenate. Tissue was then further homogenized using an electric homogenizer at mid-speed for 20 seconds. To fix, 0.5 mg of DTSSP (Cat # 21578, ThermoFisher, Waltham, MA, USA) was added to all samples. Samples were then incubated with rotation at 4°C for 30 min. DTSSP was quenched by 40 mM of Tris-HCl. Tissues were brought up to 1 mL total volume with 10X wash (5% BSA in 50 mL Ca<sup>2+</sup>, Mg<sup>2+</sup>- free PBS) and 1  $\mu$ L (10  $\mu$ g/mL) of 7:ADD (Cat # SML1633, Sigma Aldrich, St. Louis, MO, USA) was added to stain DNA. Tubes were incubated for at with rotation at 4°C for 10 min to allow for sufficient staining of the DNA. Tubes were spun for 7 min at 700  $\times$  g in a tabletop centrifuge and resuspended in 1 mL of 10X wash two times and then passed through a 20  $\mu$ m filter (Cat # 130-101-812, Miltenyi Biotec, Bergisch Gladbach, North Rhine-Westphalia, Germany).

#### 4.5.3 Sorting of Nuclei Using NanoCelect WOLF Cell Sorter

Nuclei sorting was achieved using the NanoCelect WOLF Cell Sorter and analysis was done through their proprietary program (NanoCelect Biomedical, San Diego, CA, USA). The sorting strategy was as follows: 7-AAD staining was used to define nuclei and discriminate debris, FSC and BSC were used to confirm nuclei, doublets were discriminated using FSC-Height versus FSC-Width, and ZSGreen populations were selected by high fluorescence in the GFP channel. Four 384-well plates were pre-prepared with 10  $\mu$ L of Smart-Seq2 sample buffer and each represented a different population of nuclei – (1) HFD-fed 7-AAD<sup>+</sup>ZSGreen<sup>-</sup>, (2) HFD-fed 7-AAD<sup>+</sup>ZSGreen<sup>+</sup>, (3) NC-fed 7-AAD<sup>+</sup>ZSGreen<sup>-</sup>, and (4) NC-fed 7-AAD<sup>+</sup>ZSGreen<sup>+</sup>. Plates were then spun down and flash frozen over dry ice.

#### 4.5.4 Transcriptomic analysis

Ninety-six nuclei from each sorted group (HFD DAPI<sup>+</sup>ZSGreen<sup>+</sup>, HFD DAPI<sup>+</sup>ZSGreen<sup>-</sup>, NC DAPI<sup>+</sup>ZSGreen<sup>+</sup>, and NC DAPI<sup>+</sup>ZSGreen<sup>-</sup>) were prepared by Dr. John Campbell using the Smart-Seq2 protocol and sequenced at the Functional Genomics core at Beth Israel Deaconess Medical Center.

Transcriptomic analysis of single-nuclei dataset was performed using the R package Seurat<sup>400</sup>, following the Satija Lab's Seurat – Guided Clustering Tutorial<sup>414</sup> and the Harvard Chan Bioinformatics Core – Introduction to Single-cell RNA-seq<sup>415</sup>. Filter thresholds were

set as follows:  $n\text{UMI} \geq 400$ ,  $n\text{Gene} \geq 200$ ,  $\log_{10}\text{GenesperUMI} > 0.6$  and  $\text{mitoRatio} < 0.2$  based on visualizations of quality metrics and established single-nuclei protocols.

#### **ACKNOWLEDGMENTS**

This research could not have been completed without Dr. John Cambell's continued technical support and assistance with Smart-Seq2. WOLF sorting was conducted by Omar Alvarado and Richard Simmerman.

## 5 CHAPTER 5: DISCUSSION AND FUTURE DIRECTIONS

---

### 5.1 SUMMARY

The present dissertation outlines an effort to better understand how behavioral aberrations arise from atypical brain function. To that end, we conducted studies to explore cortical control of behavior and to establish the transcriptomic profile of proglucagon neurons which regulate feeding behavior and metabolism. While seemingly disparate, I will later discuss a large body of research that has indicated that the hindbrain has effects on motivation and higher cognitive functions<sup>272-279</sup>, as well as research that implicates gut dysbiosis in the control of behavior in response to drugs of abuse, as well as in affecting emotional state<sup>280-282</sup>.

Based on studies that have implicated abnormal activity of the mPFC in patients with substance use disorder (SUD) or behavioral addictions (e.g., pathological gambling, kleptomania, binge eating, compulsive sexual behavior)<sup>25,42,53,199-206</sup>, we sought to better understand how specific neuronal populations in the mPFC regulate atypical behavior. We harnessed a cre-dependent caspase-3 ablation in both male and female mice to selectively ablate vasoactive intestinal peptide (VIP)-expressing interneurons in the prefrontal cortex to better explore how this microcircuit functions during specific behavioral tasks. Caspase-ablated animals had no changes in anxiety-like behaviors or hedonic food intake but had a specific increase in impulsive responding during longer trials in the three-choice serial reaction time test. Together, these data suggest a circuit-level mechanism in which VIP interneurons function as a gate to selectively respond during periods of high expectation.

To better understand how GLP-1 mediates weight loss and obesity, we attempted to establish a pipeline to isolate hindbrain neurons with minimal loss to investigate how GCG neurons may be transcriptionally regulated during obesity. Based on a previous study from our lab that showed that GCG stimulation was sufficient to drive weight loss in obese mice but not in lean mice, we hypothesized that GCG neurons underwent transcriptional changes during obesity that mediated their increased effectiveness. However, our difficulties with establishing an isolation technique that did not result in significant loss prevented us from producing robust single-nuclei sequencing data.

### 5.2 DISCUSSION

While this dissertation discusses two seemingly disparate brain areas, an emerging body of literature has indicated that gut-hindbrain signaling has effects on substance use and anxiety, which have been primarily attributed to dysfunction in the prefrontal cortex (PFC). By increasing our understanding of how these brain areas interact to produce behavior, we move towards a more integrated view of the brain, in which brain areas do not operate in isolation but are in fact affected by a multitude of signaling pathways. Here, I will review two emerging areas of research - GLP-1 receptor agonists in the treatment of addiction and microbiome mediation of behavior and addiction.

### 5.2.1 GLP-1, Addiction, and the PFC

Even though most of the literature surrounding GLP-1 primarily discusses its effects on food intake and metabolism, there is a body of research that implicates GLP-1 in modulating drug “satiety” as well as food satiety. While this dissertation has primarily focused on GCG neurons that target areas such as the ARC in the control of homeostatic feeding, these GCG neurons additionally synapse onto areas that have been implicated in hedonic responses, such as the nucleus accumbens (NAc), ventral tegmental area (VTA), and laterodorsal tegmental area (LDTg)<sup>416,417</sup>.

The VTA has long been implicated as the “control center” for rewarding and reinforcing processes and is the main source of dopaminergic inputs onto both the NAc (mesolimbic) and PFC (mesocortical). VTA neurons projecting to the NAc are modulated by excitatory inputs from the laterodorsal tegmental nucleus (LDT)<sup>418</sup>. VTA neurons also exhibit projection-specific alterations in synaptic plasticity following rewarding or aversive stimuli and in their functional role. VTA-NAc projections have an increased AMPA/NMDA ratio (indicating long-term potentiation) after a single cocaine injection and increase place preference, indicating that these neurons contribute to reward<sup>418,419</sup>. VTA-PFC projections, in contrast, show an increased AMPA/NMDA ratio after a formalin injection in the hindpaw and induce conditioned place aversion, implicating these neurons are responsible for mediating aversion responses<sup>418,419</sup>.

As explored in “Section 1.3.1: Dopaminergic control of cognitive function,” NAc control of behavioral reinforcement has ties to both ADHD and addiction and could be affected via the GLP-1-mediated modulations of VTA signaling discussed below.

#### 5.2.1.1 Cocaine

Several studies have established a link between GLP-1R modulation and cocaine use. GLP-1R agonism has been shown to reduce cocaine-induced place preference, decrease cocaine self-administration, and decrease cocaine-induced hyperlocomotion<sup>420–422</sup>. Researchers hypothesized that GLP-1 action occurs through the VTA, which is known to play a critical role in drug seeking<sup>423</sup>, based on findings that GLP-1 receptors are expressed in VTA. When exendin-4 (Ex-4), a GLP-1R agonist, was injected intra-VTA, it was found to reduce cocaine-seeking without affecting sucrose-seeking<sup>424,425</sup>, while a VTA-specific GLP-1R knockdown was sufficient to increase cocaine intake<sup>424</sup>. While VTA *Glp1r* expression was unchanged during extinction studies, NTS *Gcg* expression was significantly decreased by day 7 of extinction, which coincides with drug-seeking behavior<sup>426–428</sup>. It has been established that there is a population of monosynaptic GCG neurons in the NTS that project directly to the VTA<sup>417</sup>, thus implicating a possible NTS-VTA pathway for the control of drug-seeking. In terms of mesocorticolimbic signaling, it was found that Ex-4 infusion into the NAc was sufficient to attenuate cocaine-seeking<sup>425</sup> and peripheral Ex-4 administration prevented cocaine-induced activation of neurons in the NAc<sup>421</sup>. One study has shown that acute cocaine administration impairs reactivity of the PFC to VTA stimulation, which they hypothesize could facilitate impulsive behaviors during drug use<sup>429</sup>.

### 5.2.1.2 Amphetamines

Amphetamine-related hyperactivity, conditioned place preference and dopamine release in the NAc have all been shown to be attenuated by acute Ex-4 administration<sup>422,430</sup>. When GLP-1R was selectively ablated in the CNS, Ex-4 treatment had no effect on amphetamine-conditioned place preference, indicating that its effects are mediated through *Glp1r*-expressing neurons in the AP or NTS<sup>431</sup>. In addition, a synthetic DPP IV inhibitor was sufficient to reduce amphetamine-induced hyper-locomotion, indicating that circulating GLP-1 levels are important in the regulation of amphetamine-related behavior<sup>432</sup>. While amphetamine has been shown to induce *c-Fos* expression in the PFC<sup>433</sup>, reciprocal PFC projections to the VTA remain understudied.

### 5.2.1.3 Alcohol

Acute GLP-1R agonism both peripherally and injected directly into the NTS has been shown to be sufficient to reduce alcohol intake and preference for alcohol in alcohol-dependent male rats across multiple studies<sup>434–437</sup>. Additionally, infusion of a GLP-1R antagonist into the NTS ameliorates Ex-4 suppression of alcohol-induced locomotion, NAc dopamine release, and alcohol-conditioned place preference<sup>438</sup>. The VTA is implicated in modulating these effects, as indicated by direct injection of Ex-4 significantly reducing alcohol intake<sup>436</sup>. A clinical trial studying the use of GLP-1R agonist exenatide in reducing alcohol intake in individuals with alcohol use disorder (AUD) found that exenatide significantly reduced total alcohol intake in a subgroup of obese individuals<sup>439</sup>. In terms of mesocorticolimbic activation, it is hypothesized that acute ethanol increases spontaneous dopamine transmission to promote reward<sup>440,441</sup>, while repeated alcohol intake induces anhedonia and altered reward processing, indicating a hypodopaminergic state in the PFC and NAc<sup>442,443</sup>.

## 5.2.2 The microbiome, reward, and addiction

The role of vagal afferent (VAN) signaling has been well-established as a vital pathway for information transfer from the gut to the brain. As previously discussed, VAN activation occurs through gut-released peptides such as GLP-1, but more recently, it has been implicating in microbiome-related signaling. As microbial dysbiosis is linked to a variety of neurologic<sup>444</sup> and psychiatric<sup>445,446</sup> conditions, understanding the roles of microbial metabolites and their signaling pathways has reached heightened importance. Additionally, microbiome dysbiosis has been linked to altered behavior and reward pathways, indicating a novel target for both control of behavior (PFC-mediated) and metabolism (hindbrain-mediated)<sup>447–449</sup>.

### 5.2.2.1 Microbial metabolites and VAN activation

One microbial metabolite has shown strong indications of modulating VAN signaling. Short-chain fatty acids (SCFAs), such as acetate, butyrate and propionate, are produced by gut microbiota as a byproduct of polysaccharide digestion<sup>450</sup>. Propionate has been shown to increase VAN activity and induces *fos* expression in the NTS in a VAN-dependent

manner, indicating that SCFAs are able to mediate VAN signaling<sup>451</sup>. Oral butyrate is sufficient to decrease food intake and decrease neuronal activity in the NTS, which was abolished by a subdiaphragmatic vagotomy<sup>452</sup>. These data provide evidence that SCFAs are able to activate NTS pathways via VAN activation. Additionally, chronic elevation of lipopolysaccharide (LPS), a product of bacterial breakdown, is sufficient to induce leptin and CCK resistance in VAN<sup>453</sup>. Vagotomy experiments have further implicated microbial-VAN activation to affect signaling in the CNS<sup>454,455</sup>, while it seems that other microbes are able to alter CNS activity through non-VAN-mediated mechanisms<sup>456,457</sup>.

### ***5.2.2.2 Microbiome and drugs of abuse***

While the effects of diet on microbiota dysbiosis have been well-established<sup>458–460</sup>, the biology surrounding drugs of abuse and their impact on microbiome dysbiosis is understudied. As previously discussed, drugs of abuse “hijack” CNS reinforcement pathways by increasing dopamine (DA) release from the VTA, primarily onto the NAc. The gut microbiota has been found to additionally modulate the DA pathway, as reviewed in<sup>461</sup>, and it has therefore been hypothesized that microbes are able to mediate reward pathways in addiction. In addition, dysbiosis has been linked to a variety of neurologic disorders<sup>444,446,449,454–456,462–465</sup>, further necessitating the need to address the pathogenesis of the microbiome in the control of disease.

#### ***5.2.2.2.1 Alcohol***

Chronic alcohol intake leads to bacterial overgrowth in both the small and large intestine, increased intestinal permeability, and alterations in microbial diversity in both humans and animal models<sup>466–473</sup>. In a study which looked at the microbiota of animals selectively bred to be high alcohol drinkers found that both administration of oral antibiotics and vagotomy before allowing access to alcohol was sufficient to reduce voluntary ethanol intake by 70%<sup>474</sup>. In a model of chronic intermittent ethanol (CIE) vapor exposure, which is used to produce alcohol dependence and escalation in self-administration in rats, another group found that tigecycline, a tetracycline antibiotic, was able to reduce high alcohol consumption in both alcohol-dependent and non-dependent animals<sup>475</sup>. Perhaps most convincingly, it was shown that transplantation of microbes from mice given chronic alcohol to normal healthy controls was sufficient to drive alcohol withdrawal-induced anxiety<sup>476</sup>. In animals that were considered vulnerable to addiction based on increased impulsive and compulsive behaviors as well as increased relapse, it was found that striatal dopamine receptor expression was altered<sup>477</sup>. Together, these results implicate a microbial-dependent mechanism for the maintenance of alcohol use.

#### ***5.2.2.2.2 Cocaine***

Kiraly, *et al.* found that treatment with antibiotics for two weeks was sufficient to enhance cocaine-conditioned place preference as well as increase locomotor activity. They also found that conditioned place preference was able to be reversed via administration of

SCFAs. Antibiotic-treated animals were also shown to have cocaine-dependent alterations of dopamine- and glutamate-transcripts in the NAc<sup>478</sup>.

#### 5.2.2.2.3 Opioids

Lee, *et al.* found that both intermittent and sustained morphine administration were sufficient to induce microbial changes. Intermittent morphine administration, however, created an impaired reward response, as measured by a lack of morphine-conditioned place preference. Depletion of the gut microbiota with antibiotics was shown to recapitulate this lack of morphine-conditioned place preference, indicating that intermittent administration of morphine may have reward-related effects. Transfer of a naïve, healthy mouse's microbiome to antibiotic-treated animals was sufficient to restore morphine-conditioned place preference<sup>479</sup>.

#### 5.2.2.2.4 Nicotine

In a study by Chi, *et al.*, they examined potential sex-specific differences in nicotine's effects on microbial dysbiosis. They found that oxidative stress and DNA repair pathways were enriched in the microbiome after nicotine treatment in male mice only, and weight loss only occurred in the male mice. Additionally, they showed that both GABA and glutamate were differentially altered in female and male mice, as indicated by the fecal metabolome<sup>480</sup>.

Together, these studies implicate the role of the microbiome in the control of reward pathways and therefore in the regulation of addiction. As the microbiome is thought to act primarily by increasing DA in the NAc, this may cause sensitization of the mesolimbic pathway and add to increased reactivity of drug cues. Thus, the microbiome represents an area of novel pharmaceutical intervention in the control of addiction.

## 5.3 FUTURE DIRECTIONS

### 5.3.1 mPFC Control of Behavior

While our findings that VIP ablation in the IL is sufficient to modulate impulsive behavior in long-delay trials, there was not sufficient power to determine if this phenomenon is sex-specific. There is a strong trend in both sexes towards increased premature responding in long-delay trials but remain non-significant based on our set statistical significance threshold. Thus, investigation into sex-specific differences must be continued.

Additional measures of impulsivity that query different types of impulsivity, such as delay discounting or action cancellation during a stop-signal task would allow for improved understanding of how VIP signaling mediates impulsivity in disorders such as ADHD, which increases both motor impulsivity and delayed discounting<sup>481,482</sup>. Based on data indicating that motor impulsivity (measured through 5-CSRTT) is greater in male animals while impulsive choice (measured through delayed discounting tasks) is greater in female

animals<sup>483</sup>, we could additionally investigate these sex-specific differences and their regulation by VIP interneurons. Further stratification of VIP-mediated impulsivity will allow for improved understanding of how the mPFC controls the timing of actions as well as investigating possible sex-specific mechanisms of mPFC behavioral control.

One study examining the role of serotonin receptor (5-HTR) antagonism in the control of impulsivity found that while antagonism of 5-HT<sub>2A</sub>R and 5-HT<sub>2B</sub>R had no effect on premature responding during a 5-CSRTT, antagonism of 5-HT<sub>2C</sub>R increased premature responding in an ITI-dependent manner<sup>137</sup>. As 5-HT<sub>2C</sub>R are almost exclusively expressed on VIP interneurons<sup>219</sup>, we can extrapolate that serotonergic innervation of VIP interneurons is responsible for this phenotype of motor impulsivity. To test this hypothesis, a VIP-specific knockout of 5-HT<sub>2C</sub>R could be created by crossing the established VIP-cre line with a 5-HT<sub>2C</sub>R -floxed line. While the 5-HT<sub>2C</sub>R-floxed line is not currently available, new methods in creating floxed animals have greatly decreased the amount of time necessary to create a novel floxed mouse<sup>484</sup>. If serotonergic inputs are regulating long-delay impulsivity as hypothesized, conditional knockout mice should show similar phenotypes to those seen with VIP ablation. By examining how conditional 5-HT<sub>2C</sub>R knockout affects behavior, we would be able to better understand how serotonergic signaling affects behavior and therefore harness improved pharmacotherapies in the treatment of impulse-control disorders and addiction.

Additionally, VIP neuron populations are still poorly understood and could thus result in muddled understanding of the functions of the mPFC circuit. This is due to two distinct subtypes of VIP, which differentially target either pyramidal neurons (inhibitory) or SST neurons (disinhibitory). Functional analysis of a VIP-cre mouse line found that activation of VIP neurons initiates inhibitory postsynaptic currents from SST interneurons, which only minorly affecting the output of pyramidal neurons, indicating that the VIP-cre line preferentially targets disinhibitory VIP interneurons<sup>19</sup>. Transcriptional analysis of mPFC neurons indicated that there are two non-overlapping populations of VIP interneurons, which differentially express either calretinin or cholecystokinin<sup>219</sup>. These were determined to be interneuron-selective (VIP<sup>CR</sup>) or pyramidal neuron-selective (VIP<sup>CK</sup>).

To initially examine the differential roles of these two neuro subtypes, DREADD expression could be differentially achieved through the use of RC::FL-hM3Dq, a dual recombinase-responsive Gq-coupled DREADD<sup>485</sup> in either VIP-Flp:CR-Cre or VIP-Flp:CCK-Cre animals to result in DREADD expression localized to those subsets of VIP interneurons. Their differential effects on known VIP-modulated targets such as impulsive responding, high-calorie diet intake, novel-object investigation, and locomotion<sup>6</sup> could then be observed during CNO administration. Additionally, by examining the overlap of *c-fos* immunoreactivity and SST, PV and VGUT1/2 immunoreactivity after DREADD expression, more definitive evidence regarding the synaptic preferences of each subtype of VIP neuron would be generated. The experiments discussed here would improve understanding of mPFC control of behavior by addressing the following gaps in knowledge: (1) mPFC control during non-motor impulsivity tasks, (2) sex-specific

modulation of mPFC control during impulsivity tasks, (3) the necessity of serotonergic action to mediate the increase in long-delay impulsivity, (4) sub-type specific differences of VIP interneurons in the control of impulsive responding, and (5) VIP sub-type specific activation of downstream interneurons and pyramidal neurons. Together, these would lead to significantly increased understanding of the VIP-mPFC circuitry and its contribution to behavior.

### 5.3.2 The Role of the Hindbrain in Obesity

Based on the hypothesis discussed in “Section 4.3: Discussion,” an important experiment would be to examine the effects of an inducible, vagal- or CNS- knockout of GLP-1R during various stages of obesity. While this would necessitate a great amount of mouse breeding and creation of new mouse lines, this study would be able to further elucidate mechanisms of obesity remodeling in both the CNS and vagus. As previously discussed, GLP-1R antagonism or knockouts have been sufficient to protect against DIO, while GLP-1R agonism is sufficient to initiate weight loss in obese individuals. These disparate effects could be explored through temporal control of GLP-1R knockout in either the vagus or the CNS, in order to observe how loss of GLP-1R before HFD, during acute HFD, and during chronic HFD/obesity either centrally or peripherally affects DIO. This would also effectively decouple possible differences between diet-induced and obesity-induced metabolic adaptation and could lead to improved pharmacologic targeting.

While we failed in our efforts to generate a single-nuclei RNA-seq transcriptome of GCG neurons, three large single-nuclei datasets of hindbrain neurons now exist, enabling us to examine other possible mechanisms of GCG control<sup>401,404,486</sup>. Insights into the signaling pathways of other drivers of weight loss such as GFRAL and GIPR, the subgroups of neurons that are targeted by vagal afferents, changes in synaptic plasticity across different neuronal groups, differences in *Gcg* expression in obese versus lean animals, and more could be gleaned from further examination of these datasets. Additionally, two transcriptomic datasets exploring the molecular identities of vagal afferents have been produced<sup>487,488</sup>, enabling even further insight into the diverse enteric-brain signaling pathways mediated through the vagus, especially vagal-mediated microbial signaling. Together, these datasets represent vast amounts of information that can be harnessed to drive hypotheses and a multitude of untapped opportunities for pharmacological intervention.

Finally, based on findings indicating that *Oxtr*-expressing and not *Glp1r*-expressing VANs are responsible for mediating GCG activation<sup>290</sup> and that obese individuals have increased basal levels of oxytocin<sup>408–410</sup> implicates that the pharmacological manipulation of oxytocin may be relevant in the control of obesity. Oxytocin receptor is expressed most prominently in the hypothalamus, hippocampus, pons, and substantia nigra<sup>489</sup> and has diverse effects. Most notably, oxytocin has been found to inhibit the stress-induced activity of the hypothalamic-pituitary-adrenal (HPA) to promote reduction in cortisol levels<sup>490</sup>. Cortisol concentrations in the hair is highly associated with an increased risk in obesity and

strongly correlates with abdominal fat mass, which is considered a hallmark of excess cortisol<sup>491</sup>. Along with data showing that GLP-1R agonism affected transcriptional changes in the response to corticosterone as determined by gene ontology analysis<sup>404</sup>, these data highly implicate a reciprocal function of oxytocin and cortisol signaling in the control of obesity that has yet to be explored.

## REFERENCES

---

1. Bicks, L. K., Koike, H., Akbarian, S. & Morishita, H. Prefrontal cortex and social cognition in mouse and man. *Front Psychol* **6**, 1–15 (2015).
2. Huang, W. C., Zucca, A., Levy, J. & Page, D. T. Social Behavior Is Modulated by Valence-Encoding mPFC-Amygdala Sub-circuitry. *Cell Rep* **32**, (2020).
3. Caballero, J. P., Scarpa, G. B., Remage-Healey, L. & Moorman, D. E. Differential effects of dorsal and ventral medial prefrontal cortex inactivation during natural reward seeking, extinction, and cue-induced reinstatement. *eNeuro* **6**, (2019).
4. Hardung, S. *et al.* A Functional Gradient in the Rodent Prefrontal Cortex Supports Behavioral Inhibition. *Current Biology* **27**, 549–555 (2017).
5. Moorman, D. E., James, M. H., McGlinchey, E. M. & Aston-Jones, G. Differential roles of medial prefrontal subregions in the regulation of drug seeking. *Brain Res* **1628**, 130–146 (2015).
6. Newmyer, B. A. *et al.* VIPergic neurons of the infralimbic and prelimbic cortices control palatable food intake through separate cognitive pathways. *JCI Insight* **4**, (2019).
7. Heidbreder, C. A. & Groenewegen, H. J. The medial prefrontal cortex in the rat: Evidence for a dorso-ventral distinction based upon functional and anatomical characteristics. *Neurosci Biobehav Rev* **27**, 555–579 (2003).
8. Vertes, R. P. Differential projections of the infralimbic and prelimbic cortex in the rat. *Synapse* **51**, 32–58 (2004).
9. Vertes, R. P. Interactions among the medial prefrontal cortex, hippocampus and midline thalamus in emotional and cognitive processing in the rat. *Neuroscience* **142**, 1–20 (2006).
10. Rudy, B., Fishell, G., Lee, S. H. & Hjerling-Leffler, J. Three groups of interneurons account for nearly 100% of neocortical GABAergic neurons. *Dev Neurobiol* **71**, 45–61 (2011).
11. Tremblay, R., Lee, S. & Rudy, B. GABAergic Interneurons in the Neocortex: From Cellular Properties to Circuits. *Neuron* **91**, 260–292 (2016).
12. Wang, X. J. & Yang, G. R. A disinhibitory circuit motif and flexible information routing in the brain. *Curr Opin Neurobiol* **49**, 75–83 (2018).
13. Benes, F. M. & Berretta, S. GABAergic Interneurons: Implications for Understanding Schizophrenia and Bipolar Disorder. *Neuropsychopharmacology* *2001 25:1* **25**, 1–27 (2001).

14. Apicella, A. junior & Marchionni, I. VIP-Expressing GABAergic Neurons: Disinhibitory vs. Inhibitory Motif and Its Role in Communication Across Neocortical Areas. *Front Cell Neurosci* **16**, 1 (2022).
15. Lee, S., Kruglikov, I., Huang, Z. J., Fishell, G. & Rudy, B. A disinhibitory circuit mediates motor integration in the somatosensory cortex. *Nat Neurosci* **16**, 1662–1670 (2013).
16. Chandler, D. J., Lamperski, C. S. & Waterhouse, B. D. Identification and distribution of projections from monoaminergic and cholinergic nuclei to functionally differentiated subregions of prefrontal cortex. *Brain Res* **1522**, 38–58 (2013).
17. Arroyo, S., Bennett, C., Aziz, D., Brown, S. P. & Hestrin, S. Prolonged disynaptic inhibition in the cortex mediated by slow, non- $\alpha 7$  nicotinic excitation of a specific subset of cortical interneurons. *J Neurosci* **32**, 3859–64 (2012).
18. Wall, N. R. *et al.* Brain-Wide Maps of Synaptic Input to Cortical Interneurons. *J Neurosci* **36**, 4000–4009 (2016).
19. Huang, Z. J. *et al.* Cortical interneurons that specialize in disinhibitory control. *Nature* **503**, 521–524 (2013).
20. Pinto, L. & Dan, Y. Cell-Type-Specific Activity in Prefrontal Cortex during Goal-Directed Behavior. *Neuron* **87**, 437–450 (2015).
21. Krabbe, S. *et al.* Adaptive disinhibitory gating by VIP interneurons permits associative learning. *Nat Neurosci* **22**, 1834–1843 (2019).
22. Letzkus, J. J., Wolff, S. B. E. & Lüthi, A. Disinhibition, a Circuit Mechanism for Associative Learning and Memory. *Neuron* **88**, 264–276 (2015).
23. Anastasiades, P. G. & Carter, A. G. Circuit organization of the rodent medial prefrontal cortex. *Trends Neurosci* **44**, 550 (2021).
24. Aron, A. R. & Poldrack, R. A. The Cognitive Neuroscience of Response Inhibition: Relevance for Genetic Research in Attention-Deficit/Hyperactivity Disorder. *Biol Psychiatry* **57**, 1285–1292 (2005).
25. Miller, E. K. The prefrontal cortex and cognitive control. *Nat Rev Neurosci* **1**, 59–65 (2000).
26. Kirshner, H. S. *Cognitive Neuroscience of Memory. Cognitive and behavioral neurology : official journal of the Society for Behavioral and Cognitive Neurology* vol. 33 (2020).
27. Chambers, C. D., Garavan, H. & Bellgrove, M. A. Insights into the neural basis of response inhibition from cognitive and clinical neuroscience. *Neurosci Biobehav Rev* **33**, 631–646 (2009).

28. Miller, E. K. The prefrontal cortex: Complex neural properties for complex behavior. *Neuron* **22**, 15–17 (1999).
29. Clark, K. L. & Noudoost, B. The role of prefrontal catecholamines in attention and working memory. *Front Neural Circuits* **8**, 33 (2014).
30. Kim, D. *et al.* Distinct Roles of Parvalbumin- and Somatostatin-Expressing Interneurons in Working Memory. *Neuron* **92**, 902–915 (2016).
31. Murray, A. J. *et al.* Parvalbumin-positive interneurons of the prefrontal cortex support working memory and cognitive flexibility. *Sci Rep* **5**, 16778 (2015).
32. Klune, C. B., Jin, B. & Denardo, L. A. Linking mPFC circuit maturation to the developmental regulation of emotional memory and cognitive flexibility. *Elife* **10**, (2021).
33. Kehagia, A. A., Murray, G. K. & Robbins, T. W. Learning and cognitive flexibility: frontostriatal function and monoaminergic modulation. *Curr Opin Neurobiol* **20**, 199–204 (2010).
34. Bechara, A. Risky business: Emotion, decision-making, and addiction. *J Gambl Stud* **19**, 23–51 (2003).
35. Bush, G. *et al.* Dorsal anterior cingulate cortex: A role in reward-based decision making. *Proc Natl Acad Sci U S A* **99**, 523–528 (2002).
36. Ferenczi, E. A. *et al.* Prefrontal cortical regulation of brainwide circuit dynamics and reward-related behavior. *Science (1979)* **351**, (2016).
37. Bari, A. & Robbins, T. W. Inhibition and impulsivity: Behavioral and neural basis of response control. *Prog Neurobiol* **108**, 44–79 (2013).
38. Zuckerman, M. & Glicksohn, J. Hans Eysenck's personality model and the constructs of sensation seeking and impulsivity. *Pers Individ Dif* **103**, 48–52 (2016).
39. Magid, V., MacLean, M. G. & Colder, C. R. Differentiating between sensation seeking and impulsivity through their mediated relations with alcohol use and problems. *Addictive behaviors* **32**, 2046 (2007).
40. Winstanley, C. A., Eagle, D. M. & Robbins, T. W. Behavioral models of impulsivity in relation to ADHD: Translation between clinical and preclinical studies. *Clin Psychol Rev* **26**, 379–395 (2006).
41. Chamberlain, S. R. *et al.* Impaired Cognitive Flexibility and Motor Inhibition in Unaffected First-Degree Relatives of Patients with Obsessive-Compulsive Disorder. *Am J Psychiatry* **164**, 335 (2007).
42. Choi, J. S. *et al.* Altered Brain Activity during Reward Anticipation in Pathological Gambling and Obsessive-Compulsive Disorder. *PLoS One* (2012) doi:10.1371/journal.pone.0045938.

43. Castellanos, F. X., Sonuga-Barke, E. J. S., Milham, M. P. & Tannock, R. Characterizing cognition in ADHD: beyond executive dysfunction. *Trends Cogn Sci* **10**, 117–123 (2006).
44. Clark, L. *et al.* Association Between Response Inhibition and Working Memory in Adult ADHD: A Link to Right Frontal Cortex Pathology? *Biol Psychiatry* **61**, 1395–1401 (2007).
45. Gut-Fayand, A. *et al.* Substance abuse and suicidality in schizophrenia: a common risk factor linked to impulsivity. *Psychiatry Res* **102**, 65–72 (2001).
46. American Psychiatric Association. *Diagnostic and Statistical Manual of Mental Disorders: DSM-IV*. (1994).
47. Jupp, B. & Dalley, J. W. Behavioral endophenotypes of drug addiction: Etiological insights from neuroimaging studies. *Neuropharmacology* **76 Pt B**, 487–497 (2014).
48. Goldstein, R. Z. & Volkow, N. D. Drug addiction and its underlying neurobiological basis: neuroimaging evidence for the involvement of the frontal cortex. *Am J Psychiatry* **159**, 1642–1652 (2002).
49. De Wit, H. Impulsivity as a determinant and consequence of drug use: a review of underlying processes. *Addiction biology* **14**, 22–31 (2009).
50. Jentsch, J. D. *et al.* Dissecting impulsivity and its relationships to drug addictions. *Ann N Y Acad Sci* **1327**, 1–26 (2014).
51. Mitchell, M. R. & Potenza, M. N. Addictions and Personality Traits: Impulsivity and Related Constructs. *Curr Behav Neurosci Rep* **1**, 1–12 (2014).
52. Lorains, F. K., Cowlishaw, S. & Thomas, S. A. Prevalence of comorbid disorders in problem and pathological gambling: Systematic review and meta-analysis of population surveys. *Addiction* vol. 106 490–498 Preprint at <https://doi.org/10.1111/j.1360-0443.2010.03300.x> (2011).
53. Black, D. W., Shaw, M., McCormick, B., Bayless, J. D. & Allen, J. Neuropsychological performance, impulsivity, ADHD symptoms, and novelty seeking in compulsive buying disorder. *Psychiatry Res* **200**, 581–587 (2012).
54. Wang, B. qian, Yao, N. qi, Zhou, X., Liu, J. & Lv, Z. tao. The association between attention deficit/hyperactivity disorder and internet addiction: a systematic review and meta-analysis. *BMC Psychiatry* **17**, (2017).
55. Vassileva, J., Conrod, P. J., Justine, S. & Montreal, C. Impulsivities and addictions: a multidimensional integrative framework informing assessment and interventions for substance use disorders. *Philosophical Transactions of the Royal Society B* **374**, 20180137 (2019).

56. Littlefield, A. K. & Sher, K. J. The Multiple, Distinct Ways that Personality Contributes to Alcohol Use Disorders. *Soc Personal Psychol Compass* (2010) doi:10.1111/j.1751-9004.2010.00296.x.
57. Verdejo-García, A., Lawrence, A. J. & Clark, L. Impulsivity as a vulnerability marker for substance-use disorders: Review of findings from high-risk research, problem gamblers and genetic association studies. *Neurosci Biobehav Rev* **32**, 777–810 (2008).
58. Stevens, L. *et al.* Impulsivity as a vulnerability factor for poor addiction treatment outcomes: A review of neurocognitive findings among individuals with substance use disorders. *J Subst Abuse Treat* (2014) doi:10.1016/j.jsat.2014.01.008.
59. Hutchison, K. E. Substance Use Disorders: Realizing the Promise of Pharmacogenomics and Personalized Medicine. *Annu Rev Clin Psychol* (2010) doi:10.1146/annurev.clinpsy.121208.131441.
60. Robert Cloninger, C. Neurogenetic adaptive mechanisms in alcoholism. *Science* **236**, 410–416 (1987).
61. Sutker, P. B., Archer, R. P. & Allain, A. N. Drug abuse patterns, personality characteristics, and relationships with sex, race, and sensation seeking. *J Consult Clin Psychol* **46**, 1374–1378 (1978).
62. Pattij, T. & De Vries, T. J. The role of impulsivity in relapse vulnerability. *Curr Opin Neurobiol* **23**, 700–705 (2013).
63. Adinoff, B. *et al.* Impulsivity, Neural Deficits, and the Addictions: The “Oops” Factor in Relapse. *J Addict Dis* **26**, 25 (2007).
64. De Wit, H. Impulsivity as a determinant and consequence of drug use: A review of underlying processes. *Addiction Biology* **14**, 22–31 (2009).
65. Jentsch, J. D. & Taylor, J. R. Impulsivity resulting from frontostriatal dysfunction in drug abuse: implications for the control of behavior by reward-related stimuli. *Psychopharmacology (Berl)* **146**, 373–390 (1999).
66. Conway, K. P., Swendsen, J. D., Rounsaville, B. J. & Merikangas, K. R. Personality, drug of choice, and comorbid psychopathology among substance abusers. *Drug Alcohol Depend* **65**, 225–234 (2002).
67. Carver, C. S., Sutton, S. K. & Scheier, M. F. Action, Emotion, and Personality: Emerging Conceptual Integration. <http://dx.doi.org/10.1177/0146167200268008> **26**, 741–751 (2000).
68. Castellanos-Ryan, N. & Conrod, P. Personality and Substance Misuse: Evidence for a Four-Factor Model of Vulnerability. in *Drug Abuse and Addiction in Medical Illness: Causes, Consequences and Treatment* (eds. Verster, J. C., Brady, K., Galatner, M. & Conrod, P.) 47–62 (2012).

69. Xu, P., Chen, A., Li, Y., Xing, X. & Lu, H. Medial prefrontal cortex in neurological diseases. *Physiol Genomics* **51**, 432–442 (2019).
70. Lapid, M. D. S. & Morilak, D. A. Noradrenergic modulation of cognitive function in rat medial prefrontal cortex as measured by attentional set shifting capability. *Neuroscience* **137**, 1039–1049 (2006).
71. Bondi, C. O., Jett, J. D. & Morilak, D. A. Beneficial effects of desipramine on cognitive function of chronically stressed rats are mediated by alpha1-adrenergic receptors in medial prefrontal cortex. *Prog Neuropsychopharmacol Biol Psychiatry* **34**, 913–923 (2010).
72. Arnsten, A. F. T. Catecholamine modulation of prefrontal cortical cognitive function. *Trends Cogn Sci* **2**, 436–447 (1998).
73. Arnsten, A. F. T. Stress signalling pathways that impair prefrontal cortex structure and function. *Nat Rev Neurosci* **10**, 410 (2009).
74. Datta, D. *et al.* Noradrenergic  $\alpha 1$ -Adrenoceptor Actions in the Primate Dorsolateral Prefrontal Cortex. *J Neurosci* **39**, 2722–2734 (2019).
75. Sutton, S. K. & Davidson, R. J. Prefrontal brain asymmetry: A Biological Substrate of the Behavioral Approach and Inhibition Systems. *Psychol Sci* **8**, 204–210 (1997).
76. Matthews, G. & Gilliland, K. The personality theories of H.J. Eysenck and J.A. Gray: a comparative review. *Pers Individ Dif* **26**, 583–626 (1999).
77. Wahlstrom, D., White, T. & Luciana, M. Neurobehavioral evidence for changes in dopamine system activity during adolescence. *Neurosci Biobehav Rev* **34**, 631–648 (2010).
78. Schreuders, E. *et al.* Contributions of Reward Sensitivity to Ventral Striatum Activity Across Adolescence and Early Adulthood. *Child Dev* **89**, 797 (2018).
79. Robinson, T. E. & Berridge, K. C. The neural basis of drug craving: An incentive-sensitization theory of addiction. *Brain Res Rev* **18**, 247–291 (1993).
80. Berridge, K. C. & Robinson, T. E. Liking, Wanting and the Incentive-Sensitization Theory of Addiction. *Am Psychol* **71**, 670 (2016).
81. Jones, J. A., Zuhlsdorff, K. & Dalley, J. W. Neurochemical substrates linked to impulsive and compulsive phenotypes in addiction: A preclinical perspective. *J Neurochem* **157**, 1525–1546 (2021).
82. Cools, R., Froböse, M., Aarts, E. & Hofmans, L. Dopamine and the motivation of cognitive control. *Handb Clin Neurol* **163**, 123–143 (2019).
83. Botvinick, M. & Braver, T. Motivation and Cognitive Control: From Behavior to Neural Mechanism. <https://doi.org/10.1146/annurev-psych-010814-015044> **66**, 83–113 (2015).

84. Kool, W., McGuire, J. T., Rosen, Z. B. & Botvinick, M. M. Decision making and the avoidance of cognitive demand. *J Exp Psychol Gen* **139**, 665–682 (2010).
85. Risko, E. F., Medimorec, S., Chisholm, J. & Kingstone, A. Rotating With Rotated Text: A Natural Behavior Approach to Investigating Cognitive Offloading. *Cogn Sci* **38**, 537–564 (2014).
86. Westbrook, A., Kester, D. & Braver, T. S. What Is the Subjective Cost of Cognitive Effort? Load, Trait, and Aging Effects Revealed by Economic Preference. *PLoS One* **8**, e68210 (2013).
87. McGuigan, S. *et al.* Dopamine restores cognitive motivation in Parkinson’s disease. *Brain* **142**, 719–732 (2019).
88. Froböse, M. I., Westbrook, A., Bloemendaal, M., Aarts, E. & Cools, R. Catecholaminergic modulation of the cost of cognitive control in healthy older adults. *PLoS One* **15**, e0229294 (2020).
89. Jongkees, B. J., Hommel, B., Kühn, S. & Colzato, L. S. Effect of tyrosine supplementation on clinical and healthy populations under stress or cognitive demands—A review. *J Psychiatr Res* **70**, 50–57 (2015).
90. Deijen, J. Tyrosine. in *Nutrition, brain and behavior* (eds. Lieberman, H., Kanarek, R. & Prasad, C.) 363–381 (2005).
91. Ren, J., Friedmann, D., Xiong, J., Huguenard, J. & Horowitz, M. A. Anatomically Defined and Functionally Distinct Dorsal Raphe Serotonin Sub-systems. *Cell* **175**, 472–487 (2018).
92. Zaborszky, L., Gaykema, R. P., Swanson, D. J. & Cullinan, W. E. Cortical input to the basal forebrain. *Neuroscience* **79**, 1051–1078 (1997).
93. Woolf, N. J. & Butcher, L. L. Cholinergic systems mediate action from movement to higher consciousness. *Behavioural Brain Research* **221**, 488–498 (2011).
94. Eckenstein, F. & Baughman, R. W. Two types of cholinergic innervation in cortex, one co-localized with vasoactive intestinal polypeptide. *Nature* **309**, 153–155 (1984).
95. Von Engelhardt, J., Eliava, M., Meyer, A. H., Rozov, A. & Monyer, H. Functional Characterization of Intrinsic Cholinergic Interneurons in the Cortex. *Journal of Neuroscience* **27**, 5633–5642 (2007).
96. MESULAM, M. -M. Cholinergic Pathways and the Ascending Reticular Activating System of the Human Brain. *Ann N Y Acad Sci* **757**, 169–179 (1995).
97. Bloem, B., Poorthuis, R. B. & Mansvelder, H. D. Cholinergic modulation of the medial prefrontal cortex: The role of nicotinic receptors in attention and regulation of neuronal activity. *Front Neural Circuits* **8**, 17 (2014).

98. Gotti, C., Zoli, M. & Clementi, F. Brain nicotinic acetylcholine receptors: native subtypes and their relevance. *Trends Pharmacol Sci* **27**, 482–491 (2006).
99. Albuquerque, E. X., Pereira, E. F. R., Alkondon, M. & Rogers, S. W. Mammalian nicotinic acetylcholine receptors: From structure to function. *Physiol Rev* **89**, 73–120 (2009).
100. Alkondon, M. & Albuquerque, E. X. The nicotinic acetylcholine receptor subtypes and their function in the hippocampus and cerebral cortex. *Prog Brain Res* **145**, 109–120 (2004).
101. Bubser, M., Byun, N., Wood, M. R. & Jones, C. K. Muscarinic receptor pharmacology and circuitry for the modulation of cognition. *Handb Exp Pharmacol* **208**, 121–166 (2012).
102. Brown, D. A. Muscarinic acetylcholine receptors (mAChRs) in the nervous system: Some functions and mechanisms. *Journal of Molecular Neuroscience* **41**, 340–346 (2010).
103. Levey, A. I., Kitt, C. A., Simonds, W. F., Price, D. L. & Brann, M. R. Identification and localization of muscarinic acetylcholine receptor proteins in brain with subtype-specific antibodies. *Journal of Neuroscience* **11**, 3218–3226 (1991).
104. Thiele, A. Muscarinic Signaling in the Brain. <https://doi.org/10.1146/annurev-neuro-062012-170433> **36**, 271–294 (2013).
105. Chédotal, A., Cozzani, C., Faure, M. P., Hartman, B. K. & Hamel, E. Distinct choline acetyltransferase (ChAT) and vasoactive intestinal polypeptide (VIP) bipolar neurons project to local blood vessels in the rat cerebral cortex. *Brain Res* **646**, 181–193 (1994).
106. Dudai, A. *et al.* Barrel cortex VIP/ChAT interneurons suppress sensory responses in vivo. *PLoS Biol* **18**, e3000613 (2020).
107. Granger, A. J. *et al.* Cortical ChAT+ neurons co-transmit acetylcholine and GABA in a target-and brain-region-specific manner. *Elife* **9**, 1–29 (2020).
108. Bayraktar, T. *et al.* Co-localization of vasoactive intestinal polypeptide, gamma-aminobutyric acid and choline acetyltransferase in neocortical interneurons of the adult rat. *Brain Res* **757**, 209–217 (1997).
109. Obermayer, J. *et al.* Prefrontal cortical ChAT-VIP interneurons provide local excitation by cholinergic synaptic transmission and control attention. *Nature Communications* 2019 10:1 **10**, 1–14 (2019).
110. Parikh, V., Kozak, R., Martinez, V. & Sarter, M. *Prefrontal acetylcholine release controls cue detection on multiple time scales.*

111. Gritton, H. J. *et al.* Cortical cholinergic signaling controls the detection of cues. *Proc Natl Acad Sci U S A* **113**, E1089–E1097 (2016).
112. Ballinger, E. C., Ananth, M., Talmage, D. A. & Role, L. W. Basal Forebrain Cholinergic Circuits and Signaling in Cognition and Cognitive Decline. *Neuron* vol. 91 1199–1218 Preprint at <https://doi.org/10.1016/j.neuron.2016.09.006> (2016).
113. Howe, W. M. *et al.* Prefrontal cholinergic mechanisms Instigating shifts from monitoring for cues to Cue-Guided performance: Converging electrochemical and fMRI evidence from rats and humans. *Journal of Neuroscience* **33**, 8742–8752 (2013).
114. Blondel, A., Sanger, D. J. & Moser, P. C. Characterisation of the effects of nicotine in the five-choice serial reaction time task in rats: antagonist studies. *Psychopharmacology* **149**, 293–305 (2000).
115. Tsutsui-Kimura, I. *et al.* The effects of serotonin and/or noradrenaline reuptake inhibitors on impulsive-like action assessed by the three-choice serial reaction time task: a simple and valid model of impulsive action using rats.
116. Tsutsui-Kimura, I. *et al.* Nicotine provokes impulsive-like action by stimulating  $\alpha 4\beta 2$  nicotinic acetylcholine receptors in the infralimbic, but not in the prelimbic cortex. *Psychopharmacology (Berl)* **209**, 351–359 (2010).
117. Ohmura, Y., Takahashi, T. & Kitamura, N. Discounting delayed and probabilistic monetary gains and losses by smokers of cigarettes. *Psychopharmacology (Berl)* **182**, 508–515 (2005).
118. Grottick, A. J. & Higgins, G. A. Effect of subtype selective nicotinic compounds on attention as assessed by the five-choice serial reaction time task. *Behavioural Brain Research* **117**, 197–208 (2000).
119. Dallery, J. & Locey, M. L. Effects of acute and chronic nicotine on impulsive choice in rats. *Behavioural Pharmacology* **16**, 15–23 (2005).
120. Tsutsui-Kimura, I. *et al.* Endogenous acetylcholine modulates impulsive action via  $\alpha 4\beta 2$  nicotinic acetylcholine receptors in rats. *Eur J Pharmacol* **641**, 148–153 (2010).
121. Maier, S. F., Amat, J., Baratta, M. V., Paul, E. & Watkins, L. R. Behavioral control, the medial prefrontal cortex, and resilience. *Dialogues Clin Neurosci* **8**, 397 (2006).
122. Perry, J. L. *et al.* Prefrontal Cortex and Drug Abuse Vulnerability: Translation to Prevention and Treatment Interventions. *Brain Res Rev* **65**, 124 (2011).
123. Gonçalves, L., Nogueira, M. I., Shammah-Lagnado, S. J. & Metzger, M. Prefrontal afferents to the dorsal raphe nucleus in the rat. *Brain Res Bull* **78**, 240–247 (2009).

124. Clarke, H. F., Dalley, J. W., Crofts, H. S., Robbins, T. W. & Roberts, A. C. Cognitive Inflexibility after Prefrontal Serotonin Depletion. *Science* (1979) **304**, 878–880 (2004).
125. Puig, M. V. & Gullledge, A. T. Serotonin and Prefrontal Cortex Function: Neurons, Networks, and Circuits. *Mol Neurobiol* **44**, 449 (2011).
126. Morales, M. & Bloom, F. E. The 5-HT<sub>3</sub> Receptor Is Present in Different Subpopulations of GABAergic Neurons in the Rat Telencephalon. *The Journal of Neuroscience* **17**, 3157 (1997).
127. Lüscher, C., Jan, L. Y., Stoffel, M., Malenka, R. C. & Nicoll, R. A. G protein-coupled inwardly rectifying K<sup>+</sup> channels (GIRKs) mediate postsynaptic but not presynaptic transmitter actions in hippocampal neurons. *Neuron* **19**, 687–695 (1997).
128. Groot, M. L., Normann, M. C., Nicklas, P. R., Jagielo-Miller, J. E. & McLaughlin, P. J. Biphasic effects of 5-HT<sub>1A</sub> agonism on impulsive responding are dissociable from effects on anxiety in the variable consecutive number task. *Naunyn Schmiedebergs Arch Pharmacol* **392**, 1455–1464 (2019).
129. Altieri, S. C., Garcia-Garcia, A. L., Leonardo, E. D. & Andrews, A. M. Rethinking 5-HT<sub>1A</sub> Receptors: Emerging Modes of Inhibitory Feedback of Relevance to Emotion-Related Behavior. *ACS Chem Neurosci* **4**, 72 (2013).
130. Pineyro, G. & Blier, P. Autoregulation of Serotonin Neurons: Role in Antidepressant Drug Action. *Pharmacol Rev* **51**, 533–591 (1999).
131. Jolas, T. *et al.* (-)Tertatolol is a potent antagonist at pre- and postsynaptic serotonin 5-HT<sub>1A</sub> receptors in the rat brain. *Naunyn Schmiedebergs Arch Pharmacol* **347**, 453–463 (1993).
132. Hjorth, S. & Sharp, T. Effect of the 5-HT<sub>1A</sub> receptor agonist 8-OH-DPAT on the release of 5-HT in dorsal and median raphe-innervated rat brain regions as measured by in vivo microdialysis. *Life Sci* **48**, 1779–1786 (1991).
133. Minzenberg, M. J. *et al.* Blunted Hormone Responses to Ipsapirone are Associated with Trait Impulsivity in Personality Disorder Patients. *Neuropsychopharmacology* 2006 31:1 **31**, 197–203 (2005).
134. Pitchot, W. *et al.* Hormonal and temperature responses to the 5-HT<sub>1A</sub> receptor agonist flesinoxan in normal volunteers. *Psychopharmacology (Berl)* **164**, 27–32 (2002).
135. Zuo, L. *et al.* Significant association between rare IPO11-HTR1A variants and attention deficit hyperactivity disorder in Caucasians. *Am J Med Genet B Neuropsychiatr Genet* **168**, 544 (2015).

136. Anastasio, N. C. *et al.* Serotonin (5-HT) 5-HT<sub>2A</sub> Receptor (5-HT<sub>2AR</sub>):5-HT<sub>2CR</sub> Imbalance in Medial Prefrontal Cortex Associates with Motor Impulsivity. *ACS Chem Neurosci* **6**, 1248–1258 (2015).
137. Fletcher, P. J., Tampakeras, M., Sinyard, J. & Higgins, G. A. Opposing effects of 5-HT<sub>2A</sub> and 5-HT<sub>2C</sub> receptor antagonists in the rat and mouse on premature responding in the five-choice serial reaction time test. *Psychopharmacology (Berl)* **195**, 223–234 (2007).
138. Winstanley, C. A. *et al.* Intra-prefrontal 8-OH-DPAT and M100907 improve visuospatial attention and decrease impulsivity on the five-choice serial reaction time task in rats. *Psychopharmacology (Berl)* **167**, 304–314 (2003).
139. Geyer, M. A. & Vollenweider, F. X. Serotonin research: Contributions to understanding psychoses. *Trends Pharmacol Sci* **29**, 445–453 (2008).
140. Diez-Alarcia, R. *et al.* Opposite alterations of 5HT<sub>2A</sub> receptor brain density in subjects with schizophrenia: relevance of radiotracers pharmacological profile. *Translational Psychiatry 2021 11:1* **11**, 1–10 (2021).
141. Vollenweider, F. X., Vollenweider-Scherpenhuyzen, M. F. I., Babler, A., Vogel, H. & Hell, D. Psilocybin induces schizophrenia-like psychosis in humans via a serotonin-2 agonist action. *Cogn Neurosci* **9**, (1998).
142. Jiang, K., Liu, X. & Su, R. Contrasting effects of DOI and lisuride on impulsive decision-making in delay discounting task. *Psychopharmacology 2022 239:11* **239**, 3551–3565 (2022).
143. Heerey, E. A., Robinson, B. M., McMahon, R. P. & Gold, J. M. Delay Discounting in Schizophrenia. *Cogn Neuropsychiatry* **12**, 213 (2007).
144. Land, M. A. *et al.* Serotonin 5-HT<sub>2C</sub> Receptor Cys23Ser Single Nucleotide Polymorphism Associates with Receptor Function and Localization In Vitro. *Sci Rep* **9**, (2019).
145. Anastasio, N. C. *et al.* Variation within the serotonin (5-HT) 5-HT<sub>2C</sub> receptor system aligns with vulnerability to cocaine cue reactivity. *Transl Psychiatry* **4**, e369 (2014).
146. Lerer, B. *et al.* Variability of 5-HT<sub>2C</sub> receptor cys23ser polymorphism among European populations and vulnerability to affective disorder. *Mol Psychiatry* **6**, 579–585 (2001).
147. Ni, X., Chan, D., Chan, K., McMMain, S. & Kennedy, J. L. Serotonin genes and gene-gene interactions in borderline personality disorder in a matched case-control study. *Prog Neuropsychopharmacol Biol Psychiatry* **33**, 128–133 (2009).
148. Evans, J. *et al.* Impulsiveness, serotonin genes and repetition of deliberate self-harm (DSH). *Psychol Med* **30**, 1327–1334 (2000).

149. Okada, M. *et al.* Modification of human 5-HT<sub>2C</sub> receptor function by Cys23Ser, an abundant, naturally occurring amino-acid substitution. *Molecular Psychiatry* 2004 9:1 **9**, 55–64 (2003).
150. Lappalainen, J. *et al.* Identification, Expression, and Pharmacology of a Cys23-Ser23 Substitution in the Human 5-HT<sub>2C</sub> Receptor Gene (HTR2C). *Genomics* **27**, 274–279 (1995).
151. Agster, K. L., Mejias-Aponte, C. A., Clark, B. D. & Waterhouse, B. D. Evidence for a regional specificity in the density and distribution of noradrenergic varicosities in rat cortex. *J Comp Neurol* **521**, 2195–2207 (2013).
152. Sestieri, C., Corbetta, M., Romani, G. L. & Shulman, G. L. Episodic memory retrieval, parietal cortex, and the default mode network: functional and topographic analyses. *J Neurosci* **31**, 4407–4420 (2011).
153. Tang, Y. Y., Rothbart, M. K. & Posner, M. I. Neural correlates of establishing, maintaining, and switching brain states. *Trends Cogn Sci* **16**, 330–337 (2012).
154. Buckner, R. L. The brain's default network: origins and implications for the study of psychosis. *Dialogues Clin Neurosci* **15**, 351 (2013).
155. Aston-Jones, G. & Cohen, J. D. Adaptive gain and the role of the locus coeruleus-norepinephrine system in optimal performance. *J Comp Neurol* **493**, 99–110 (2005).
156. Ross, J. A. & Van Bockstaele, E. J. The Locus Coeruleus- Norepinephrine System in Stress and Arousal: Unraveling Historical, Current, and Future Perspectives. *Front Psychiatry* **11**, 1581 (2021).
157. Hoffmann, C., Leitz, M. R., Oberdorf-Maass, S., Lohse, M. J. & Klotz, K. N. Comparative pharmacology of human beta-adrenergic receptor subtypes--characterization of stably transfected receptors in CHO cells. *Naunyn Schmiedebergs Arch Pharmacol* **369**, 151–159 (2004).
158. Ramos, B. P. *et al.* Dysregulation of protein kinase A signaling in the aged prefrontal cortex: New strategy for treating age-related cognitive decline. *Neuron* **40**, 835–845 (2003).
159. Taylor, J. R., Birnbaum, S., Ubriani, R. & Arnsten, A. F. Activation of cAMP-Dependent Protein Kinase A in Prefrontal Cortex Impairs Working Memory Performance. *The Journal of Neuroscience* **19**, RC23 (1999).
160. Hone, K., Obika, K., Foglar, R. & Tsujimoto, G. Selectivity of the imidazoline alpha-adrenoceptor agonists (oxymetazoline and cirazoline) for human cloned alpha 1-adrenoceptor subtypes. *Br J Pharmacol* **116**, 1611 (1995).
161. Jasper, J. R. *et al.* Ligand efficacy and potency at recombinant alpha<sub>2</sub> adrenergic receptors: agonist-mediated [<sup>35</sup>S]GTPgammaS binding. *Biochem Pharmacol* **55**, 1035–1043 (1998).

162. Ramos, B. P. & Arnsten, A. F. T. Adrenergic Pharmacology and Cognition: Focus on the Prefrontal Cortex. *Pharmacol Ther* **113**, 523 (2007).
163. Starke, K. Presynaptic autoreceptors in the third decade: focus on alpha2-adrenoceptors. *J Neurochem* **78**, 685–693 (2001).
164. Langer, S. Z. Presynaptic autoreceptors regulating transmitter release. *Neurochem Int* **52**, 26–30 (2008).
165. Gilsbach, R. & Hein, L. Presynaptic metabotropic receptors for acetylcholine and adrenaline/noradrenaline. *Handb Exp Pharmacol* **184**, 261–288 (2008).
166. Delaney, A. J., Crane, J. W. & Sah, P. Noradrenaline Modulates Transmission at a Central Synapse by a Presynaptic Mechanism. *Neuron* **56**, 880–892 (2007).
167. Misu, Y. & Kubo, T. Presynaptic  $\beta$ -adrenoceptors. *Med Res Rev* **6**, 197–225 (1986).
168. Rinne, A., Birk, A. & Búnemann, M. Voltage regulates adrenergic receptor function. *Proc Natl Acad Sci U S A* **110**, 1536–1541 (2013).
169. Okun, M. & Lampl, I. Instantaneous correlation of excitation and inhibition during ongoing and sensory-evoked activities. *Nature Neuroscience* 2008 11:5 **11**, 535–537 (2008).
170. Breton-Provencher, V. & Sur, M. Active control of arousal by a locus coeruleus GABAergic circuit. *Nature Neuroscience* 2019 22:2 **22**, 218–228 (2019).
171. Sigurdardottir, H. L. *et al.* Association of norepinephrine transporter methylation with in vivo NET expression and hyperactivity-impulsivity symptoms in ADHD measured with PET. *Mol Psychiatry* **26**, 1009–1018 (2021).
172. Kim, C. H., Waldman, I. D., Blakely, R. D. & Kim, K. S. Functional gene variation in the human norepinephrine transporter: association with attention deficit hyperactivity disorder. *Ann N Y Acad Sci* **1129**, 256–260 (2008).
173. Liao, C. *et al.* Transcriptome-wide association study of attention deficit hyperactivity disorder identifies associated genes and phenotypes. *Nature Communications* 2019 10:1 **10**, 1–7 (2019).
174. Bymaster, F. P. *et al.* Atomoxetine Increases Extracellular Levels of Norepinephrine and Dopamine in Prefrontal Cortex of Rat: A Potential Mechanism for Efficacy in Attention Deficit/Hyperactivity Disorder. *Neuropsychopharmacology* **27**, 699–711 (2002).
175. Chamberlain, S. R. *et al.* Atomoxetine Modulates Right Inferior Frontal Activation During Inhibitory Control: A Pharmacological Functional Magnetic Resonance Imaging Study. *Biol Psychiatry* **65**, 550–555 (2009).
176. Levy, F. Pharmacological and therapeutic directions in ADHD: Specificity in the PFC. *Behavioral and Brain Functions* **4**, 1–9 (2008).

177. Eagle, D. M., Bari, A. & Robbins, T. W. The neuropsychopharmacology of action inhibition: cross-species translation of the stop-signal and go/no-go tasks. *Psychopharmacology* 2008 199:3 **199**, 439–456 (2008).
178. Wang, M. *et al.* Alpha2A-adrenoceptors strengthen working memory networks by inhibiting cAMP-HCN channel signaling in prefrontal cortex. *Cell* **129**, 397–410 (2007).
179. Carr, D. B., Andrews, G. D., Glen, W. B. & Lavin, A. alpha2-Noradrenergic receptors activation enhances excitability and synaptic integration in rat prefrontal cortex pyramidal neurons via inhibition of HCN currents. *J Physiol* **584**, 437–450 (2007).
180. Franowicz, J. S. *et al.* Mutation of the alpha2A-adrenoceptor impairs working memory performance and annuls cognitive enhancement by guanfacine. *J Neurosci* **22**, 8771–8777 (2002).
181. Mao, Z. M., Arnsten, A. F. T. & Li, B. M. Local infusion of an alpha-1 adrenergic agonist into the prefrontal cortex impairs spatial working memory performance in monkeys. *Biol Psychiatry* **46**, 1259–1265 (1999).
182. Wang, M., Tang, Z. X. & Li, B. M. Enhanced visuomotor associative learning following stimulation of alpha 2A-adrenoceptors in the ventral prefrontal cortex in monkeys. *Brain Res* **1024**, 176–182 (2004).
183. Ramos, B. P. *et al.* The Beta-1 Adrenergic Antagonist, Betaxolol, Improves Working Memory Performance in Rats and Monkeys. *Biol Psychiatry* **58**, 894–900 (2005).
184. Ramos, B. P., Colgan, L. A., Nou, E. & Arnsten, A. F. T.  $\beta$ 2 adrenergic agonist, clenbuterol, enhances working memory performance in aging animals. *Neurobiol Aging* **29**, 1060 (2008).
185. Zhou, H. C. *et al.* Activation of  $\beta$ 2-adrenoceptor enhances synaptic potentiation and behavioral memory via cAMP-PKA signaling in the medial prefrontal cortex of rats. *Learn Mem* **20**, 274–284 (2013).
186. Torkaman-Boutorabi, A., Hashemi-Hezaveh, S. M., Sheidadoust, H. & Zarrindast, M. R. The possible role of medial prefrontal cortex beta-1-adrenoceptors in morphine-induced amnesia. *Pharmacology* **93**, 272–277 (2014).
187. Ji, X. H. *et al.* Pre- and postsynaptic beta-adrenergic activation enhances excitatory synaptic transmission in layer V/VI pyramidal neurons of the medial prefrontal cortex of rats. *Cereb Cortex* **18**, 1506–1520 (2008).
188. Aoki, C., Venkatesan, C. & Kurose, H. Noradrenergic modulation of the prefrontal cortex as revealed by electron microscopic immunocytochemistry. *Adv Pharmacol* **42**, 777–780 (1998).

189. Brocos-Mosquera, I. *et al.*  $\alpha$ 2A- and  $\alpha$ 2C-adrenoceptor expression and functionality in postmortem prefrontal cortex of schizophrenia subjects. *Eur Neuropsychopharmacol* **52**, 3–11 (2021).
190. Berridge, C. W. & Waterhouse, B. D. The locus coeruleus-noradrenergic system: Modulation of behavioral state and state-dependent cognitive processes. *Brain Res Rev* **42**, 33–84 (2003).
191. Bradshaw, S. E., Agster, K. L., Waterhouse, B. D. & Mcgaughy, J. A. Age-related changes in prefrontal norepinephrine transporter density: The basis for improved cognitive flexibility after low doses of atomoxetine in adolescent rats. *Brain Res* **1641**, 245–257 (2016).
192. Marijke Achterberg, E. J., Van Kerkhof, L. W. M., Damsteegt, R., Trezza, V. & Vanderschuren, L. J. M. J. Methylphenidate and atomoxetine inhibit social play behavior through prefrontal and subcortical limbic mechanisms in rats. *J Neurosci* **35**, 161–169 (2015).
193. Santana, N. & Artigas, F. Laminar and Cellular Distribution of Monoamine Receptors in Rat Medial Prefrontal Cortex. *Front Neuroanat* **11**, (2017).
194. Santana, N., Mengod, G. & Artigas, F. Expression of  $\alpha$ (1)-adrenergic receptors in rat prefrontal cortex: cellular co-localization with 5-HT(2A) receptors. *Int J Neuropsychopharmacol* **16**, 1139–1151 (2013).
195. Mitrano, D. A. *et al.*  $\alpha$ -1 Adrenergic receptors are localized on presynaptic elements in the nucleus accumbens and regulate mesolimbic dopamine transmission. *Neuropsychopharmacology* **37**, 2161–2172 (2012).
196. Berridge, C. W. & Waterhouse, B. D. The locus coeruleus-noradrenergic system: Modulation of behavioral state and state-dependent cognitive processes. *Brain Res Rev* **42**, 33–84 (2003).
197. Toussay, X., Basu, K., Lacoste, B. & Hamel, E. Locus Coeruleus Stimulation Recruits a Broad Cortical Neuronal Network and Increases Cortical Perfusion. *The Journal of Neuroscience* **33**, 3390 (2013).
198. Moorman, D. E. & Aston-Jones, G. Prefrontal neurons encode context-based response execution and inhibition in reward seeking and extinction. *Proceedings of the National Academy of Sciences* **112**, 9472–9477 (2015).
199. Fellows, L. K. Advances in understanding ventromedial prefrontal function: The accountant joins the executive. *Neurology* vol. 68 991–995 Preprint at <https://doi.org/10.1212/01.wnl.0000257835.46290.57> (2007).
200. Miller, E. K. & Cohen, J. D. AN INTEGRATIVE THEORY OF PREFRONTAL CORTEX FUNCTION. *Annu Rev Neurosci* **24**, 167–202 (2001).

201. Balodis, I. M. *et al.* Diminished frontostriatal activity during processing of monetary rewards and losses in pathological gambling. *Biol Psychiatry* (2012) doi:10.1016/j.biopsych.2012.01.006.
202. Balodis, I. M. *et al.* Monetary reward processing in obese individuals with and without binge eating disorder. *Biol Psychiatry* (2013) doi:10.1016/j.biopsych.2013.01.014.
203. London, E. D. Orbitofrontal Cortex and Human Drug Abuse: Functional Imaging. *Cerebral Cortex* (2000) doi:10.1093/cercor/10.3.334.
204. Pinna, F. *et al.* Behavioural addictions and the transition from DSM-IV-TR to DSM-5. *Journal of Psychopathology* **21**, 380–389 (2015).
205. Beck, A. *et al.* Ventral striatal activation during reward anticipation correlates with impulsivity in alcoholics. *Biol Psychiatry* (2009) doi:10.1016/j.biopsych.2009.04.035.
206. Wrase, J. *et al.* Dysfunction of reward processing correlates with alcohol craving in detoxified alcoholics. *Neuroimage* (2007) doi:10.1016/j.neuroimage.2006.11.043.
207. Kranzler, H. R. & McKay, J. R. Personalized treatment of alcohol dependence. *Current Psychiatry Reports* Preprint at <https://doi.org/10.1007/s11920-012-0296-5> (2012).
208. Loree, A. M., Lundahl, L. H. & Ledgerwood, D. M. Impulsivity as a predictor of treatment outcome in substance use disorders: Review and synthesis. *Drug and Alcohol Review* Preprint at <https://doi.org/10.1111/dar.12132> (2015).
209. Uher, R. & Treasure, J. Brain lesions and eating disorders. *Journal of Neurology, Neurosurgery and Psychiatry* Preprint at <https://doi.org/10.1136/jnnp.2004.048819> (2005).
210. Uher, R. *et al.* Medial prefrontal cortex activity associated with symptom provocation in eating disorders. *American Journal of Psychiatry* **161**, 1238–1246 (2004).
211. Striegel-Moore, R. H. *et al.* Gender difference in the prevalence of eating disorder symptoms. *International Journal of Eating Disorders* (2009) doi:10.1002/eat.20625.
212. Wall, N. R. *et al.* Brain-wide maps of synaptic input to cortical interneurons. *Journal of Neuroscience* **36**, 4000–4009 (2016).
213. Paxinos, G. & Franklin, K. B. J. *Paxinos and Franklin's the Mouse Brain in Stereotaxic Coordinates*. Academic Press (2001). doi:10.1364/OE.20.020998.

214. Sanchez-Roige, S., Peña-Oliver, Y. & Stephens, D. N. Measuring impulsivity in mice: the five-choice serial reaction time task. *Psychopharmacology* **219**:2 **219**, 253–270 (2011).
215. Warthen, D. M. *et al.* Activation of Pyramidal Neurons in Mouse Medial Prefrontal Cortex Enhances Food-Seeking Behavior While Reducing Impulsivity in the Absence of an Effect on Food Intake. *Front Behav Neurosci* **10**, 63 (2016).
216. Mena, J. D., Selleck, R. A. & Baldo, B. A. Mu-Opioid Stimulation in Rat Prefrontal Cortex Engages Hypothalamic Orexin/Hypocretin-Containing Neurons, and Reveals Dissociable Roles of Nucleus Accumbens and Hypothalamus in Cortically Driven Feeding. *Journal of Neuroscience* **33**, 18540–18552 (2013).
217. Mena, J. D., Sadeghian, K. & Baldo, B. A. Induction of Hyperphagia and Carbohydrate Intake by  $\mu$ -Opioid Receptor Stimulation in Circumscribed Regions of Frontal Cortex. *Journal of Neuroscience* **31**, 3249–3260 (2011).
218. Land, B. B. *et al.* Medial prefrontal D1 dopamine neurons control food intake. *Nature Neuroscience* **2014** *17*:2 **17**, 248–253 (2014).
219. Paul, A. *et al.* Transcriptional Architecture of Synaptic Communication Delineates GABAergic Neuron Identity. *Cell* **171**, 522–539.e20 (2017).
220. Aron, A. R., Robbins, T. W. & Poldrack, R. A. Inhibition and the right inferior frontal cortex. *Trends Cogn Sci* **8**, 170–177 (2004).
221. Aron, A. R. From reactive to proactive and selective control: developing a richer model for stopping inappropriate responses. *Biol Psychiatry* **69**, e55 (2011).
222. van den Oever, M. C., Spijker, S., Smit, A. B. & de Vries, T. J. Prefrontal cortex plasticity mechanisms in drug seeking and relapse. *Neurosci Biobehav Rev* **35**, 276–284 (2010).
223. Peters, J., Kalivas, P. W. & Quirk, G. J. Extinction circuits for fear and addiction overlap in prefrontal cortex. *Learn Mem* **16**, 279–288 (2009).
224. Gass, J. T. & Chandler, L. J. The Plasticity of Extinction: Contribution of the Prefrontal Cortex in Treating Addiction through Inhibitory Learning. *Front Psychiatry* **4**, (2013).
225. Yang, C. F. *et al.* Sexually Dimorphic Neurons in the Ventromedial Hypothalamus Govern Mating in Both Sexes and Aggression in Males. *Cell* **153**, 896–909 (2013).
226. Peirson, S. N., Brown, L. A., Pothecary, C. A., Benson, L. A. & Fisk, A. S. Light and the laboratory mouse. *J Neurosci Methods* **300**, 26–36 (2018).
227. Golden, S. A., Covington, H. E., Berton, O. & Russo, S. J. A standardized protocol for repeated social defeat stress in mice. *Nat Protoc* **6**, 1183–1191 (2011).

228. Gaykema, R. P. A. *et al.* Characterization of excitatory and inhibitory neuron activation in the mouse medial prefrontal cortex following palatable food ingestion and food driven exploratory behavior. *Front Neuroanat* **8**, 1–13 (2014).
229. Schwartz, M. W. & Porte, D. Diabetes, obesity, and the brain. *Science* **307**, 375–9 (2005).
230. MD, J. *et al.* 2013 AHA/ACC/TOS guideline for the management of overweight and obesity in adults: a report of the American College of Cardiology/American Heart Association Task Force on Practice Guidelines and The Obesity Society. *Circulation* **129**, (2014).
231. MacMahon, S. *et al.* Body-mass index and cause-specific mortality in 900 000 adults: collaborative analyses of 57 prospective studies. *Lancet* **373**, 1083–1096 (2009).
232. Flegal, K. M., Kruszon-Moran, D., Carroll, M. D., Fryar, C. D. & Ogden, C. L. Trends in Obesity Among Adults in the United States, 2005 to 2014. *JAMA* **315**, 2284 (2016).
233. Ogden, C. L. *et al.* Trends in Obesity Prevalence Among Children and Adolescents in the United States, 1988-1994 Through 2013-2014. *JAMA* **315**, 2292 (2016).
234. Abdelaal, M., le Roux, C. W. & Docherty, N. G. Morbidity and mortality associated with obesity. *Ann Transl Med* **5**, (2017).
235. Kim, D. D. & Basu, A. Estimating the Medical Care Costs of Obesity in the United States: Systematic Review, Meta-Analysis, and Empirical Analysis. *Value in Health* **19**, 602–613 (2016).
236. Swinburn, B. A. *et al.* The global obesity pandemic: Shaped by global drivers and local environments. *The Lancet* **378**, 804–814 (2011).
237. Ng, S. W. & Popkin, B. M. Time use and physical activity: a shift away from movement across the globe. *Obesity Reviews* **13**, 659–680 (2012).
238. Ladabaum, U., Mannalithara, A., Myer, P. A. & Singh, G. Obesity, Abdominal Obesity, Physical Activity, and Caloric Intake in US Adults: 1988 to 2010. *Am J Med* **127**, 717-727.e12 (2014).
239. Benton, D. & Young, H. A. Reducing Calorie Intake May Not Help You Lose Body Weight. *Perspectives on Psychological Science* **12**, 703 (2017).
240. Contreras, R. E., Schriever, S. C. & Pfluger, P. T. Physiological and Epigenetic Features of Yoyo Dieting and Weight Control. *Front Genet* **10**, (2019).
241. Drenowatz, C. Reciprocal Compensation to Changes in Dietary Intake and Energy Expenditure within the Concept of Energy Balance. *Advances in Nutrition* **6**, 592 (2015).

242. Foltin, R. W., Fischman, M. W., Emurian, C. S. & Rachlinski, J. J. Compensation for caloric dilution in humans given unrestricted access to food in a residential laboratory. *Appetite* **10**, 13–24 (1988).
243. Fothergill, E. *et al.* Persistent metabolic adaptation 6 years after ‘The Biggest Loser’ competition. *Obesity (Silver Spring)* **24**, 1612–1619 (2016).
244. Sumithran, P. & Proietto, J. The defence of body weight: a physiological basis for weight regain after weight loss. *Clin Sci* **124**, 231–241 (2013).
245. Jansson, J. O. *et al.* Body weight homeostat that regulates fat mass independently of leptin in rats and mice. *Proc Natl Acad Sci U S A* **115**, 427–432 (2017).
246. Chhabra, K. H. *et al.* Reprogramming the body weight set point by a reciprocal interaction of hypothalamic leptin sensitivity and Pomc gene expression reverts extreme obesity. *Mol Metab* **5**, 869 (2016).
247. Ravussin, Y. *et al.* Effects of chronic leptin infusion on subsequent body weight and composition in mice: Can body weight set point be reset? *Mol Metab* **3**, 432 (2014).
248. Halaas, J. L. *et al.* Physiological response to long-term peripheral and central leptin infusion in lean and obese mice. *Proc Natl Acad Sci U S A* **94**, 8878 (1997).
249. Krawczewski Carhuatanta, K. A. *et al.* Voluntary Exercise Improves High-Fat Diet-Induced Leptin Resistance Independent of Adiposity. *Endocrinology* **152**, 2655 (2011).
250. Lee, J. H., Nguyen, Q.-N. & Le, Q. A. Comparative effectiveness of 3 bariatric surgery procedures: Roux-en-Y gastric bypass, laparoscopic adjustable gastric band, and sleeve gastrectomy. doi:10.1016/j.soard.2016.01.020.
251. Manning, S., Pucci, A. & Batterham, R. L. Roux-en-Y gastric bypass: effects on feeding behavior and underlying mechanisms. *J Clin Invest* **125**, 939–948 (2015).
252. Hankir, M. K., Seyfried, F., Miras, A. D. & Cowley, M. A. Brain Feeding Circuits after Roux-en-Y Gastric Bypass. *Trends in Endocrinology & Metabolism* **29**, 218–237 (2018).
253. Ahn, C. H. *et al.* Vertical sleeve gastrectomy induces distinctive transcriptomic responses in liver, fat and muscle. *Sci Rep* **11**, (2021).
254. Tam, C. S. *et al.* Energy Metabolic Adaptation and Cardiometabolic Improvements One Year After Gastric Bypass, Sleeve Gastrectomy, and Gastric Band. *J Clin Endocrinol Metab* **101**, 3755–3764 (2016).
255. Halliday, T. M. *et al.* Comparison of surgical versus diet-induced weight loss on appetite regulation and metabolic health outcomes. *Physiol Rep* **7**, (2019).

256. González-González, J. G. *et al.* HOMA-IR as a predictor of Health Outcomes in Patients with Metabolic Risk Factors: A Systematic Review and Meta-analysis. *High Blood Press Cardiovasc Prev* **29**, 547–564 (2022).
257. Ravussin, E., Lillioja, S., Anderson, T. E., Christin, L. & Bogardus, C. Determinants of 24-hour energy expenditure in man. Methods and results using a respiratory chamber. *J Clin Invest* **78**, 1568–1578 (1986).
258. Lecoultre, V., Ravussin, E. & Redman, L. M. The Fall in Leptin Concentration Is a Major Determinant of the Metabolic Adaptation Induced by Caloric Restriction Independently of the Changes in Leptin Circadian Rhythms. *J Clin Endocrinol Metab* **96**, E1512–E1516 (2011).
259. Knuth, N. D. *et al.* Metabolic adaptation following massive weight loss is related to the degree of energy imbalance and changes in circulating leptin. *Obesity (Silver Spring)* **22**, 2563–2569 (2014).
260. Rosenbaum, M. *et al.* Low-dose leptin reverses skeletal muscle, autonomic, and neuroendocrine adaptations to maintenance of reduced weight. *J Clin Invest* **115**, 3579–3586 (2005).
261. Mullur, R., Liu, Y. Y. & Brent, G. A. Thyroid Hormone Regulation of Metabolism. *Physiol Rev* **94**, 355 (2014).
262. Lewandowski, K. Reference ranges for TSH and thyroid hormones. *Thyroid Res* **8**, A17 (2015).
263. Hall, K. D. & Kahan, S. Maintenance of Lost Weight and Long-Term Management of Obesity. doi:10.1016/j.mcna.2017.08.012.
264. Trexler, E. T., Smith-Ryan, A. E. & Norton, L. E. Metabolic adaptation to weight loss: Implications for the athlete. *J Int Soc Sports Nutr* **11**, 1–7 (2014).
265. Barrea, L. *et al.* Effects of very low-calorie ketogenic diet on hypothalamic–pituitary–adrenal axis and renin–angiotensin–aldosterone system. *Journal of Endocrinological Investigation* **2023** 1–12 (2023) doi:10.1007/S40618-023-02068-6.
266. Garthe, I., Raastad, T., Refsnes, P. E., Koivisto, A. & Sundgot-Borgen, J. Effect of two different weight-loss rates on body composition and strength and power-related performance in elite athletes. *Int J Sport Nutr Exerc Metab* **21**, 97–104 (2011).
267. Chaston, T. B., Dixon, J. B. & O’Brien, P. E. Changes in fat-free mass during significant weight loss: a systematic review. *International Journal of Obesity* **2007** *31*:5 **31**, 743–750 (2006).
268. Hao, Z. *et al.* Vagal Innervation of Intestine Contributes to Weight Loss After Roux-en-Y Gastric Bypass Surgery in Rats. *Obes Surg* **24**, 2145–2151 (2014).

269. Le Roux, C. W. *et al.* Gut hormones as mediators of appetite and weight loss after Roux-en-Y gastric bypass. *Ann Surg* **246**, 780–785 (2007).
270. Clemmensen, C. *et al.* Gut-Brain Cross-Talk in Metabolic Control. *Cell* **168**, 758–774 (2017).
271. Cheng, W. *et al.* Hindbrain circuits in the control of eating behaviour and energy balance. *Nature Metabolism* **2022** 4:7 **4**, 826–835 (2022).
272. Evrensel, A. & Ceylan, M. E. The Gut-Brain Axis: The Missing Link in Depression. *Clinical Psychopharmacology and Neuroscience* **13**, 239 (2015).
273. Mayer, E. A. Gut feelings: the emerging biology of gut-brain communication. *Nat Rev Neurosci* **12**, 453–466 (2011).
274. Forsythe, P., Sudo, N., Dinan, T., Taylor, V. H. & Bienenstock, J. Mood and gut feelings. *Brain Behav Immun* **24**, 9–16 (2010).
275. George, M. S. *et al.* A pilot study of vagus nerve stimulation (VNS) for treatment-resistant anxiety disorders. *Brain Stimul* **1**, 112–121 (2008).
276. Clark, K. B., Naritoku, D. K., Smith, D. C., Browning, R. A. & Jensen, R. A. Enhanced recognition memory following vagus nerve stimulation in human subjects. *Nat Neurosci* **2**, 94–98 (1999).
277. Clark, K. B. *et al.* Posttraining electrical stimulation of vagal afferents with concomitant vagal efferent inactivation enhances memory storage processes in the rat. *Neurobiol Learn Mem* **70**, 364–373 (1998).
278. Klarer, M. *et al.* Gut Vagal Afferents Differentially Modulate Innate Anxiety and Learned Fear. *Journal of Neuroscience* **34**, 7067–7076 (2014).
279. Breit, S., Kupferberg, A., Rogler, G. & Hasler, G. Vagus nerve as modulator of the brain-gut axis in psychiatric and inflammatory disorders. *Front Psychiatry* **9**, 44 (2018).
280. Wang, S. C., Chen, Y. C., Chen, S. J., Lee, C. H. & Cheng, C. M. Alcohol Addiction, Gut Microbiota, and Alcoholism Treatment: A Review. *International Journal of Molecular Sciences* **2020**, Vol. 21, Page 6413 **21**, 6413 (2020).
281. Ren, M. & Lotfipour, S. The role of the gut microbiome in opioid use. *Behavioural Pharmacology* **31**, 113–121 (2020).
282. Meckel, K. R. & Kiraly, D. D. A potential role for the gut microbiome in substance use disorders. *Psychopharmacology* **2019** 236:5 **236**, 1513–1530 (2019).
283. Perello, M., Stuart, R. C. & Nillni, E. A. Differential effects of fasting and leptin on proopiomelanocortin peptides in the arcuate nucleus and in the nucleus of the solitary tract. *Am J Physiol Endocrinol Metab* **292**, 1348–1357 (2007).

284. Schafer, M. K. H. *et al.* Gene expression of prohormone and proprotein convertases in the rat CNS: a comparative in situ hybridization analysis. *Journal of Neuroscience* **13**, 1258–1279 (1993).
285. Larsen, P. J., Tang-Christensen, M., Holst, J. J. & Ørskov, C. Distribution of glucagon-like peptide-1 and other proglucagon-derived peptides in the rat hypothalamus and brainstem. *Neuroscience* **77**, 257–270 (1997).
286. Bell, G. I., Sanchez-Pescador, R., Laybourn, P. J. & Najarian, R. C. Exon duplication and divergence in the human proglucagon gene. *Nature* **304**, 368–371 (1983).
287. Holt, M. K. *et al.* Proglucagon Neurons in the Nucleus of the Solitary Tract Are the Main Source of Brain GLP-1, Mediate Stress-Induced Hypophagia, and Limit Unusually Large Intakes of Food. *Diabetes* **68**, 21–33 (2019).
288. Shi, X. *et al.* Acute activation of GLP-1-expressing neurons promotes glucose homeostasis and insulin sensitivity. *Mol Metab* **6**, 1350–1359 (2017).
289. Williams, D. L. *et al.* GLP-1 action in the mouse bed nucleus of the stria terminalis. *Neuropharmacology* **131**, 83–95 (2018).
290. Brierley, D. I. *et al.* Central and peripheral GLP-1 systems independently suppress eating. *Nature Metabolism* **2021 3:2 3**, 258–273 (2021).
291. Baggio, L. L. & Drucker, D. J. Glucagon-like peptide-1 receptors in the brain: controlling food intake and body weight. *J Clin Invest* **124**, 4223 (2014).
292. Ciofi, P. *et al.* Brain-Endocrine Interactions: A Microvascular Route in the Mediobasal Hypothalamus. *Endocrinology* **150**, 5509 (2009).
293. Myers, M. G. How Is the Hungry Brain like a Sieve? *Cell Metab* **17**, 467 (2013).
294. Anini, Y. & Brubaker, P. L. Role of Leptin in the Regulation of Glucagon-Like Peptide-1 Secretion. *Diabetes* **52**, 252–259 (2003).
295. Zhao, X. *et al.* GLP-1 Receptor Agonists: Beyond Their Pancreatic Effects. *Front Endocrinol (Lausanne)* **12**, 1040 (2021).
296. SP, M. *et al.* Liraglutide and Cardiovascular Outcomes in Type 2 Diabetes. *N Engl J Med* **375**, 101 (2016).
297. Niswender, K. *et al.* Weight change with liraglutide and comparator therapies: an analysis of seven phase 3 trials from the liraglutide diabetes development programme. *Diabetes Obes Metab* **15**, 42–54 (2013).
298. Raun, K. *et al.* Liraglutide, a long-acting glucagon-like peptide-1 analog, reduces body weight and food intake in obese candy-fed rats, whereas a dipeptidyl peptidase-IV inhibitor, vildagliptin, does not. *Diabetes* **56**, 8–15 (2007).

299. Gabery, S. *et al.* Semaglutide lowers body weight in rodents via distributed neural pathways. *JCI Insight* **5**, (2020).
300. Tsai, V. W. W., Husaini, Y., Sainsbury, A., Brown, D. A. & Breit, S. N. The MIC-1/GDF15-GFRAL Pathway in Energy Homeostasis: Implications for Obesity, Cachexia, and Other Associated Diseases. *Cell Metab* **28**, 353–368 (2018).
301. Yang, L. *et al.* GFRAL is the receptor for GDF15 and is required for the anti-obesity effects of the ligand. *Nature Medicine* 2017 23:10 **23**, 1158–1166 (2017).
302. Sabatini, P. V. *et al.* GFRAL-expressing neurons suppress food intake via aversive pathways. *Proc Natl Acad Sci U S A* **118**, e2021357118 (2021).
303. Zhang, Y. *et al.* Activity-balanced GLP-1/GDF15 dual agonist reduces body weight and metabolic disorder in mice and non-human primates. *Cell Metab* **35**, 287-298.e4 (2023).
304. Frikke-Schmidt, H. *et al.* GDF15 acts synergistically with liraglutide but is not necessary for the weight loss induced by bariatric surgery in mice. *Mol Metab* **21**, 13 (2019).
305. Hartter, E. *et al.* Basal and stimulated plasma levels of pancreatic amylin indicate its co-secretion with insulin in humans. *Diabetologia* **34**, 52–54 (1991).
306. Riediger, T., Schmid, H. A., Lutz, T. & Simon, E. Amylin potently activates AP neurons possibly via formation of the excitatory second messenger cGMP. *Am J Physiol Regul Integr Comp Physiol* **281**, 1833–1843 (2001).
307. Lutz, T. A., Geary, N., Szabady, M. M., Del Prete, E. & Scharrer, E. Amylin decreases meal size in rats. *Physiol Behav* **58**, 1197–1202 (1995).
308. Osto, M., Wielinga, P. Y., Alder, B., Walser, N. & Lutz, T. A. Modulation of the satiating effect of amylin by central ghrelin, leptin and insulin. *Physiol Behav* **91**, 566–572 (2007).
309. Lutz, T. A. Amylinergic control of food intake. *Physiol Behav* **89**, 465–471 (2006).
310. Rushing, P. A. *et al.* Inhibition of central amylin signaling increases food intake and body adiposity in rats. *Endocrinology* **142**, 5035–5038 (2001).
311. Kong, M. F. *et al.* Infusion of pramlintide, a human amylin analogue, delays gastric emptying in men with IDDM. *Diabetologia* **40**, 82–88 (1997).
312. Young, A. A., Gedulin, B. R. & Rink, T. J. Dose-responses for the slowing of gastric emptying in a rodent model by glucagon-like peptide (7-36) NH<sub>2</sub>, amylin, cholecystokinin, and other possible regulators of nutrient uptake. *Metabolism* **45**, 1–3 (1996).

313. Hay, D. L., Chen, S., Lutz, T. A., Parkes, D. G. & Roth, J. D. Amylin: Pharmacology, Physiology, and Clinical Potential. *Pharmacol Rev* **67**, 564–600 (2015).
314. Bower, R. L. & Hay, D. L. Amylin structure-function relationships and receptor pharmacology: Implications for amylin mimetic drug development. *Br J Pharmacol* **173**, 1883–1898 (2016).
315. Christopoulos, G. *et al.* Multiple Amylin Receptors Arise from Receptor Activity-Modifying Protein Interaction with the Calcitonin Receptor Gene Product. *Mol Pharmacol* **56**, 235–242 (1999).
316. McLatchie, L. M. *et al.* RAMPs regulate the transport and ligand specificity of the calcitonin-receptor-like receptor. *Nature* 1998 393:6683 **393**, 333–339 (1998).
317. Liberini, C. G. *et al.* Amylin receptor components and the leptin receptor are co-expressed in single rat area postrema neurons. *European Journal of Neuroscience* **43**, 653–661 (2016).
318. Lutz, T. A. Gut hormones such as amylin and GLP-1 in the control of eating and energy expenditure. *International Journal of Obesity Supplements* 2016 6:1 **6**, S15–S21 (2016).
319. Lutz, T. A. Control of energy homeostasis by amylin. *Cellular and Molecular Life Sciences* 2011 69:12 **69**, 1947–1965 (2011).
320. Smith, S. R. *et al.* Sustained Weight Loss Following 12-Month Pramlintide Treatment as an Adjunct to Lifestyle Intervention in Obesity. *Diabetes Care* **31**, 1816–1823 (2008).
321. Hollander, P. *et al.* Effect of Pramlintide on Weight in Overweight and Obese Insulin-Treated Type 2 Diabetes Patients. *Obes Res* **12**, 661–668 (2004).
322. Liberini, C. G. *et al.* Combined Amylin/GLP-1 pharmacotherapy to promote and sustain long-lasting weight loss. *Scientific Reports* 2019 9:1 **9**, 1–11 (2019).
323. Bello, N. T., Kemm, M. H., Ofeldt, E. M. & Moran, T. H. Dose combinations of exendin-4 and salmon calcitonin produce additive and synergistic reductions in food intake in nonhuman primates. *Am J Physiol Regul Integr Comp Physiol* **299**, 945–952 (2010).
324. Trevaskis, J. L. *et al.* Improved Glucose Control and Reduced Body Weight in Rodents with Dual Mechanism of Action Peptide Hybrids. *PLoS One* **8**, e78154 (2013).
325. Pestel, J., Blangero, F., Watson, J., Pirola, L. & Eljaafari, A. Adipokines in obesity and metabolic-related-diseases. *Biochimie* **212**, 48–59 (2023).

326. Izaguirre, M. *et al.* GLP-1 Limits Adipocyte Inflammation and Its Low Circulating Pre-Operative Concentrations Predict Worse Type 2 Diabetes Remission after Bariatric Surgery in Obese Patients. *J Clin Med* **8**, 479 (2019).
327. Cowley, M. A. *et al.* Leptin activates anorexigenic POMC neurons through a neural network in the arcuate nucleus. *Nature* *2001* **411**:6836 **411**, 480–484 (2001).
328. Li, S. & Li, X. Leptin in normal physiology and leptin resistance. *Sci Bull (Beijing)* **61**, 1480–1488 (2016).
329. Obradovic, M. *et al.* Leptin and Obesity: Role and Clinical Implication. *Front Endocrinol (Lausanne)* **12**, 563 (2021).
330. Izquierdo, A. G., Crujeiras, A. B., Casanueva, F. F. & Carreira, M. C. Leptin, Obesity, and Leptin Resistance: Where Are We 25 Years Later? *Nutrients* **11**, (2019).
331. Westerterp-Plantenga, M. S., Saris, W. H. M., Hukshorn, C. J. & Campfield, L. A. Effects of weekly administration of pegylated recombinant human OB protein on appetite profile and energy metabolism in obese men. *Am J Clin Nutr* **74**, 426–434 (2001).
332. Hukshorn, C. J. *et al.* Weekly subcutaneous pegylated recombinant native human leptin (PEG-OB) administration in obese men. *J Clin Endocrinol Metab* **85**, 4003–4009 (2000).
333. Heymsfield, S. B. *et al.* Recombinant leptin for weight loss in obese and lean adults: a randomized, controlled, dose-escalation trial. *JAMA* **282**, 1568–1575 (1999).
334. Bojanowska, E. & Nowak, A. INTERACTIONS BETWEEN LEPTIN AND EXENDIN-4, A GLUCAGON-LIKE PEPTIDE-1 AGONIST, IN THE REGULATION OF FOOD INTAKE IN THE RAT.
335. Kanoski, S. E., Ong, Z. Y., Fortin, S. M., Schlessinger, E. S. & Grill, H. J. Liraglutide, leptin and their combined effects on feeding: additive intake reduction through common intracellular signalling mechanisms. *Diabetes Obes Metab* **17**, 285–293 (2015).
336. Goldstone, A. P. *et al.* Leptin interacts with glucagon-like peptide-1 neurons to reduce food intake and body weight in rodents. *FEBS Lett* **415**, 134–138 (1997).
337. Elias, C. F. *et al.* Chemical characterization of leptin-activated neurons in the rat brain. *Journal of Comparative Neurology* **423**, 261–281 (2000).
338. Goldstone, A. P. *et al.* Effect of Leptin on Hypothalamic GLP-1 Peptide and Brain-Stem Pre-proglucagon mRNA. *Biochem Biophys Res Commun* **269**, 331–335 (2000).

339. Nguyen, T. M. D. Adiponectin: Role in Physiology and Pathophysiology. *Int J Prev Med* **11**, 136 (2020).
340. Achari, A. E. & Jain, S. K. Adiponectin, a Therapeutic Target for Obesity, Diabetes, and Endothelial Dysfunction. *International Journal of Molecular Sciences* **2017**, Vol. 18, Page 1321 **18**, 1321 (2017).
341. Yang, W. S. *et al.* Plasma Adiponectin Levels in Overweight and Obese Asians. *Obes Res* **10**, 1104–1110 (2002).
342. Wang, A. *et al.* Exendin-4 Upregulates Adiponectin Level in Adipocytes via Sirt1/Foxo-1 Signaling Pathway. *PLoS One* **12**, e0169469 (2017).
343. Simental-Mendía, L. E. *et al.* Impact of glucagon-like peptide-1 receptor agonists on adiponectin concentrations: A meta-analysis of randomized controlled trials. *Br J Clin Pharmacol* **87**, 4140–4149 (2021).
344. Huber, J. *et al.* CC Chemokine and CC Chemokine Receptor Profiles in Visceral and Subcutaneous Adipose Tissue Are Altered in Human Obesity. *J Clin Endocrinol Metab* **93**, 3215–3221 (2008).
345. Zhang, W. *et al.* Adipocyte lipolysis-stimulated interleukin-6 production requires sphingosine kinase 1 activity. *Journal of Biological Chemistry* **289**, 32178–32185 (2014).
346. Absalon Gutierrez, A. D. *et al.* Anti-diabetic effects of GLP1 analogs are mediated by thermogenic interleukin-6 signaling in adipocytes II Anti-diabetic effects of GLP1 analogs are mediated by thermogenic interleukin-6 signaling in adipocytes. (2022) doi:10.1016/j.xcrm.2022.100813.
347. Nakazato, M. *et al.* A role for ghrelin in the central regulation of feeding. *Nature* **409**, 194–198 (2001).
348. Callahan, H. S. *et al.* Postprandial suppression of plasma ghrelin level is proportional to ingested caloric load but does not predict intermeal interval in humans. *J Clin Endocrinol Metab* **89**, 1319–1324 (2004).
349. Le Roux, C. W. *et al.* Postprandial Plasma Ghrelin Is Suppressed Proportional to Meal Calorie Content in Normal-Weight But Not Obese Subjects. *J Clin Endocrinol Metab* **90**, 1068–1071 (2005).
350. Toshinai, K. *et al.* Ghrelin-induced food intake is mediated via the orexin pathway. *Endocrinology* **144**, 1506–1512 (2003).
351. Cowley, M. A. Hypothalamic melanocortin neurons integrate signals of energy state. *Eur J Pharmacol* **480**, 3–11 (2003).
352. Decarie-spain, L. & Kanoski, S. E. Ghrelin and Glucagon-Like Peptide-1: A Gut-Brain Axis Battle for Food Reward. *Nutrients* **13**, 1–23 (2021).

353. Efendic, S. & Portwood, N. Overview of incretin hormones. *Hormone and Metabolic Research* **36**, 742–746 (2004).
354. Coskun, T. *et al.* LY3298176, a novel dual GIP and GLP-1 receptor agonist for the treatment of type 2 diabetes mellitus: From discovery to clinical proof of concept. *Mol Metab* **18**, 3 (2018).
355. Min, T. & Bain, S. C. The Role of Tirzepatide, Dual GIP and GLP-1 Receptor Agonist, in the Management of Type 2 Diabetes: The SURPASS Clinical Trials. *Diabetes Therapy* **12**, 143 (2021).
356. Finan, B. *et al.* Unimolecular dual incretins maximize metabolic benefits in rodents, monkeys, and humans. *Sci Transl Med* **5**, (2013).
357. Mentis, N. *et al.* GIP does not potentiate the antidiabetic effects of GLP-1 in hyperglycemic patients with type 2 diabetes. *Diabetes* **60**, 1270–1276 (2011).
358. Bergmann, N. C. *et al.* Effects of combined GIP and GLP-1 infusion on energy intake, appetite and energy expenditure in overweight/obese individuals: a randomised, crossover study. *Diabetologia* **62**, 665–675 (2019).
359. Mohammad, S. *et al.* A naturally occurring GIP receptor variant undergoes enhanced agonist-induced desensitization, which impairs GIP control of adipose insulin sensitivity. *Mol Cell Biol* **34**, 3618–3629 (2014).
360. Tang-Christensen, M., Larsen, P. J., Thulesen, J., Rømer, J. & Vrang, N. The proglucagon-derived peptide, glucagon-like peptide-2, is a neurotransmitter involved in the regulation of food intake. *Nature Medicine* **6**, 802–807 (2000).
361. Lovshin, J., Estall, J., Yusta, B., Brown, T. J. & Drucker, D. J. Glucagon-like Peptide (GLP)-2 Action in the Murine Central Nervous System is Enhanced by Elimination of GLP-1 Receptor Signaling. *Journal of Biological Chemistry* **276**, 21489–21499 (2001).
362. Kosinski, J. R. *et al.* The glucagon receptor is involved in mediating the body weight-lowering effects of oxyntomodulin. *Obesity (Silver Spring)* **20**, 1566–1571 (2012).
363. Baggio, L. L., Huang, Q., Brown, T. J. & Drucker, D. J. Oxyntomodulin and glucagon-like peptide-1 differentially regulate murine food intake and energy expenditure. *Gastroenterology* **127**, 546–558 (2004).
364. Patterson, M. *et al.* Hypothalamic Injection of Oxyntomodulin Suppresses Circulating Ghrelin-Like Immunoreactivity. *Endocrinology* **150**, 3513–3520 (2009).
365. Dakin, C. L. *et al.* Peripheral Oxyntomodulin Reduces Food Intake and Body Weight Gain in Rats. *Endocrinology* **145**, 2687–2695 (2004).

366. Evaluate the Safety, Tolerability, Pharmacokinetics, and Pharmacodynamics of IBI362 in Overweight or Obesity Subjects. <https://clinicaltrials.gov/ct2/show/NCT04440345>.
367. A Study of LY3305677 in Participants With Type 2 Diabetes. <https://clinicaltrials.gov/ct2/show/NCT03928379>.
368. A Study of LY3305677 in Participants With Obesity Or Overweight. <https://clinicaltrials.gov/ct2/show/NCT05623839>.
369. Valassi, E., Scacchi, M. & Cavagnini, F. Neuroendocrine control of food intake. *Metabolism & Cardiovascular Diseases* **18**, 158–168 (2008).
370. Talsania, T., Anini, Y., Siu, S., Drucker, D. J. & Brubaker, P. L. Peripheral Exendin-4 and Peptide YY3–36 Synergistically Reduce Food Intake through Different Mechanisms in Mice. *Endocrinology* **146**, 3748–3756 (2005).
371. Pittner, R. A. *et al.* Effects of PYY[3-36] in rodent models of diabetes and obesity. *Int J Obes Relat Metab Disord* **28**, 963–971 (2004).
372. Halatchev, I. G., Ellacott, K. L. J., Fan, W. & Cone, R. D. Peptide YY3-36 inhibits food intake in mice through a melanocortin-4 receptor-independent mechanism. *Endocrinology* **145**, 2585–2590 (2004).
373. Batterham, R. L. *et al.* Inhibition of food intake in obese subjects by peptide YY3-36. *N Engl J Med* **349**, 941–948 (2003).
374. Batterham, R. L. *et al.* Inhibition of food intake in obese subjects by peptide YY3-36. *N Engl J Med* **349**, 941–948 (2003).
375. Le Roux, C. W. *et al.* Attenuated peptide YY release in obese subjects is associated with reduced satiety. *Endocrinology* **147**, 3–8 (2006).
376. Cawthon, C. R. & de La Serre, C. B. The critical role of CCK in the regulation of food intake and diet-induced obesity. *Peptides (N.Y.)* **138**, (2021).
377. Irwin, N., Pathak, V. & Flatt, P. R. A Novel CCK-8/GLP-1 Hybrid Peptide Exhibiting Prominent Insulinotropic, Glucose-Lowering, and Satiety Actions With Significant Therapeutic Potential in High-Fat–Fed Mice. *Diabetes* **64**, 2996–3009 (2015).
378. Hornigold, D. C. *et al.* A GLP-1:CCK fusion peptide harnesses the synergistic effects on metabolism of CCK-1 and GLP-1 receptor agonism in mice. *Appetite* **127**, 334–340 (2018).
379. Baggio, L. L. & Drucker, D. J. Glucagon-like peptide-1 receptor co-agonists for treating metabolic disease. doi:10.1016/j.molmet.2020.101090.
380. Pories, W. J. Bariatric Surgery: Risks and Rewards. *J Clin Endocrinol Metab* **93**, S89 (2008).

381. Alruwaili, H., Dehestani, B. & Le Roux, C. W. Clinical impact of liraglutide as a treatment of obesity. *Clin Pharmacol* **13**, 53–60 (2021).
382. Astrup, A. *et al.* Effects of liraglutide in the treatment of obesity: a randomised, double-blind, placebo-controlled study. *The Lancet* **374**, 1606–1616 (2009).
383. Gaykema, R. P. *et al.* Activation of murine pre-proglucagon-producing neurons reduces food intake and body weight. *Journal of Clinical Investigation* **127**, 1031–1045 (2017).
384. Card, J. P. *et al.* GLP-1 neurons form a local synaptic circuit within the rodent nucleus of the solitary tract. *J Comp Neurol* **526**, 2149–2164 (2018).
385. Cani, P. D. *et al.* Metabolic endotoxemia initiates obesity and insulin resistance. *Diabetes* **56**, 1761–1772 (2007).
386. Sen, T. *et al.* Diet-driven microbiota dysbiosis is associated with vagal remodeling and obesity. *Physiol Behav* **173**, 305 (2017).
387. Peters, J. H., Gallaher, Z. R., Ryu, V. & Czaja, K. Withdrawal and Restoration of Central Vagal Afferents Within the Dorsal Vagal Complex Following Subdiaphragmatic Vagotomy. *J Comp Neurol* **521**, 3584 (2013).
388. Häring, M. *et al.* Neuronal atlas of the dorsal horn defines its architecture and links sensory input to transcriptional cell types. *Nat Neurosci* **21**, 869–880 (2018).
389. Saunders, A. *et al.* A Single-Cell Atlas of Cell Types, States, and Other Transcriptional Patterns from Nine Regions of the Adult Mouse Brain. *bioRxiv* 299081 (2018) doi:10.1101/299081.
390. Zeisel, A. *et al.* Molecular Architecture of the Mouse Nervous System. *Cell* **174**, 999–1014.e22 (2018).
391. Wu, Y. E., Pan, L., Zuo, Y., Li, X. & Hong, W. Detecting Activated Cell Populations Using Single-Cell RNA-Seq. *Neuron* **96**, 313–329.e6 (2017).
392. Attar, M. *et al.* A practical solution for preserving single cells for RNA sequencing. *Sci Rep* **8**, 1–10 (2018).
393. Alles, J. *et al.* Cell fixation and preservation for droplet-based single-cell transcriptomics. *BMC Biol* **15**, 44 (2017).
394. Bakken, T. E. *et al.* Single-nucleus and single-cell transcriptomes compared in matched cortical cell types. *PLoS One* **13**, e0209648 (2018).
395. Matson, K. J. E. *et al.* Isolation of Adult Spinal Cord Nuclei for Massively Parallel Single-nucleus RNA Sequencing. *Journal of Visualized Experiments* e58413 (2018) doi:10.3791/58413.

396. Forney, J. Isolation and Purification of Tetrahymena nuclei. [https://forney-lab.fandom.com/wiki/Isolation\\_and\\_Purification\\_of\\_Tetrahymena\\_nuclei](https://forney-lab.fandom.com/wiki/Isolation_and_Purification_of_Tetrahymena_nuclei).
397. Cummings, D. J. Methods for the Isolation of Nuclei from Ciliated Protozoans. in *Methods in Cell Biology* vol. XVI 97–112 (1977).
398. Christine Labno. Two Ways to Count Cells with ImageJ.
399. 10X Genomics. Nuclei Isolation from Cell Suspensions & Tissues for Single Cell RNA Sequencing. 1–8 (2021).
400. Hao, Y. *et al.* Dictionary learning for integrative, multimodal, and scalable single-cell analysis. *bioRxiv* 2022.02.24.481684 (2022) doi:10.1101/2022.02.24.481684.
401. Dowsett, G. K. C. *et al.* A survey of the mouse hindbrain in the fed and fasted states using single-nucleus RNA sequencing. *Mol Metab* **53**, (2021).
402. Varin, E. M. *et al.* Distinct Neural Sites of GLP-1R Expression Mediate Physiological versus Pharmacological Control of Incretin Action. *Cell Rep* **27**, 3371–3384.e3 (2019).
403. Sisley, S. *et al.* Neuronal GLP1R mediates liraglutide’s anorectic but not glucose-lowering effect. *Journal of Clinical Investigation* **124**, 2456–2463 (2014).
404. Ludwig, M. Q. *et al.* A genetic map of the mouse dorsal vagal complex and its role in obesity. *Nat Metab* **3**, 530–545 (2021).
405. Cawthon, C. R. & de La Serre, C. B. Gut bacteria interaction with vagal afferents. *Brain Res* **1693**, 134–139 (2018).
406. Kobayashi, K., Iwai, T., Sasaki-Hamada, S., Kamanaka, G. & Oka, J. I. Exendin (5-39), an antagonist of GLP-1 receptor, modulates synaptic transmission via glutamate uptake in the dentate gyrus. *Brain Res* **1505**, 1–10 (2013).
407. Liu, J. *et al.* Enhanced AMPA receptor trafficking mediates the anorexigenic effect of endogenous glucagon like peptide-1 in the paraventricular hypothalamus. *Neuron* **96**, 897 (2017).
408. Szulc, P. *et al.* High serum oxytocin is associated with metabolic syndrome in older men - The MINOS study. *Diabetes Res Clin Pract* **122**, 17–27 (2016).
409. Stock, S., Granström, L., Backman, L., Matthiesen, A. & Uvnäs-Moberg, K. Elevated plasma levels of oxytocin in obese subjects before and after gastric banding. *Int J Obes* (1989).
410. Schorr, M. *et al.* Oxytocin and Its Relationship to Body Composition, Bone Mineral Density, and Hip Geometry Across the Weight Spectrum. *J Clin Endocrinol Metab* **102**, 2814 (2017).

411. Hansotia, T. *et al.* Extrapancreatic incretin receptors modulate glucose homeostasis, body weight, and energy expenditure. *Journal of Clinical Investigation* **117**, 143 (2007).
412. Krieger, J. P., Langhans, W. & Lee, S. J. Novel role of GLP-1 receptor signaling in energy expenditure during chronic high fat diet feeding in rats. *Physiol Behav* **192**, 194–199 (2018).
413. Ayala, J. E. *et al.* Glucagon-Like Peptide-1 Receptor Knockout Mice Are Protected from High-Fat Diet-Induced Insulin Resistance. *Endocrinology* **151**, 4678 (2010).
414. Seurat - Guided Clustering Tutorial • Seurat. [https://satijalab.org/seurat/articles/pbmc3k\\_tutorial.html](https://satijalab.org/seurat/articles/pbmc3k_tutorial.html).
415. Single-cell RNA-seq: Clustering Analysis | Introduction to Single-cell RNA-seq - ARCHIVED. [https://hbctraining.github.io/scRNA-seq/lessons/08\\_SC\\_clustering\\_quality\\_control.html](https://hbctraining.github.io/scRNA-seq/lessons/08_SC_clustering_quality_control.html).
416. Graham, D. L. *et al.* A novel mouse model of glucagon-like peptide-1 receptor expression: A look at the brain. *J Comp Neurol* **528**, 2445–2470 (2020).
417. Alhadeff, A. L., Rupprecht, L. E. & Hayes, M. R. GLP-1 Neurons in the Nucleus of the Solitary Tract Project Directly to the Ventral Tegmental Area and Nucleus Accumbens to Control for Food Intake. *Endocrinology* **153**, 647 (2012).
418. Lammel, S. *et al.* Input-specific control of reward and aversion in the ventral tegmental area. *Nature* **491**, 212 (2012).
419. Lammel, S., Ion, D. I., Roeper, J. & Malenka, R. C. Projection-specific modulation of dopamine neuron synapses by aversive and rewarding stimuli. *Neuron* **70**, 855 (2011).
420. Graham, D. L., Erreger, K., Galli, A. & Stanwood, G. D. GLP-1 analog attenuates cocaine reward. *Mol Psychiatry* **18**, 961–962 (2013).
421. Sørensen, G. *et al.* The glucagon-like peptide 1 (GLP-1) receptor agonist exendin-4 reduces cocaine self-administration in mice. *Physiol Behav* **149**, 262–268 (2015).
422. Egecioglu, E., Engel, J. A. & Jerlhag, E. The glucagon-like peptide 1 analogue, exendin-4, attenuates the rewarding properties of psychostimulant drugs in mice. *PLoS One* **8**, (2013).
423. Schmidt, H. D., Anderson, S. M., Famous, K. R., Kumaresan, V. & Pierce, R. C. Anatomy and pharmacology of cocaine priming-induced reinstatement of drug seeking. *Eur J Pharmacol* **526**, 65–76 (2005).
424. Schmidt, H. D. *et al.* Glucagon-Like Peptide-1 Receptor Activation in the Ventral Tegmental Area Decreases the Reinforcing Efficacy of Cocaine. *Neuropsychopharmacology* **41**, 1917–1928 (2016).

425. Hernandez, N. S., O'Donovan, B., Ortinski, P. I. & Schmidt, H. D. Activation of glucagon-like peptide-1 receptors in the nucleus accumbens attenuates cocaine seeking in rats. *Addiction biology* **24**, 170 (2019).
426. Hernandez, N. S. *et al.* Glucagon-like peptide-1 receptor activation in the ventral tegmental area attenuates cocaine seeking in rats. *Neuropsychopharmacology* **43**, 2000–2008 (2018).
427. Schmidt, H. D. & Pierce, R. C. Cocaine-induced neuroadaptations in glutamate transmission: potential therapeutic targets for craving and addiction. *Ann N Y Acad Sci* **1187**, 35–75 (2010).
428. Schmidt, H. D. *et al.* ADAR2-dependent GluA2 editing regulates cocaine seeking. *Mol Psychiatry* **20**, 1460–1466 (2015).
429. Park, K., Clare, K., Volkow, N. D., Pan, Y. & Du, C. Cocaine's effects on the reactivity of the medial prefrontal cortex to ventral tegmental area stimulation: optical imaging study in mice. *Addiction* **117**, 2242–2253 (2022).
430. Erreger, K. *et al.* Exendin-4 decreases amphetamine-induced locomotor activity. *Physiol Behav* **106**, 574–578 (2012).
431. Sirohi, S., Schurdak, J. D., Seeley, R. J., Benoit, S. C. & Davis, J. F. Central & peripheral glucagon-like peptide-1 receptor signaling differentially regulate addictive behaviors. *Physiol Behav* **161**, 140–144 (2016).
432. Lautar, S. L. *et al.* DPP IV inhibitor blocks mescaline-induced scratching and amphetamine-induced hyperactivity in mice. *Brain Res* **1048**, 177–184 (2005).
433. Colussi-Mas, J., Geisler, S., Zimmer, L., Zahm, D. S. & Béro, A. Activation of afferents to the ventral tegmental area in response to acute amphetamine: a double-labelling study. *Eur J Neurosci* **26**, 1011–1025 (2007).
434. Vallöf, D., Vestlund, J. & Jerlhag, E. Glucagon-like peptide-1 receptors within the nucleus of the solitary tract regulate alcohol-mediated behaviors in rodents. *Neuropharmacology* **149**, 124–132 (2019).
435. Davis, J. F. *et al.* Gastric bypass surgery attenuates ethanol consumption in ethanol-preferring rats. *Biol Psychiatry* **72**, 354–360 (2012).
436. Shirazi, R. H., Dickson, S. L. & Skibicka, K. P. Gut peptide GLP-1 and its analogue, Exendin-4, decrease alcohol intake and reward. *PLoS One* **8**, (2013).
437. Marty, V. N. *et al.* Long-Acting Glucagon-Like Peptide-1 Receptor Agonists Suppress Voluntary Alcohol Intake in Male Wistar Rats. *Front Neurosci* **14**, (2020).
438. Vallöf, D., Vestlund, J. & Jerlhag, E. Glucagon-like peptide-1 receptors within the nucleus of the solitary tract regulate alcohol-mediated behaviors in rodents. *Neuropharmacology* **149**, 124–132 (2019).

439. Klausen, M. K. *et al.* Exenatide once weekly for alcohol use disorder investigated in a randomized, placebo-controlled clinical trial. *JCI Insight* **7**, (2022).
440. Schier, C. J., Dilly, G. A. & Gonzales, R. A. Intravenous Ethanol Increases Extracellular Dopamine in the Medial Prefrontal Cortex of the Long-Evans Rat. *Alcohol Clin Exp Res* **37**, 740 (2013).
441. Robinson, D. L., Howard, E. C., McConnell, S., Gonzales, R. A. & Wightman, R. M. Disparity between tonic and phasic ethanol-induced dopamine increases in the nucleus accumbens of rats. *Alcohol Clin Exp Res* **33**, 1187 (2009).
442. Koob, G. F. & Volkow, N. D. Neurocircuitry of Addiction. *Neuropsychopharmacology* **35**, 217 (2010).
443. Trevisan, L. A., Boutros, N., Petrakis, I. L. & Krystal, J. H. Complications of Alcohol Withdrawal: Pathophysiological Insights. *Alcohol Health Res World* **22**, 61 (1998).
444. Tremlett, H., Bauer, K. C., Appel-Cresswell, S., Finlay, B. B. & Waubant, E. The gut microbiome in human neurological disease: A review. *Ann Neurol* **81**, 369–382 (2017).
445. Dinan, T. G. & Cryan, J. F. The Microbiome-Gut-Brain Axis in Health and Disease. *Gastroenterol Clin North Am* **46**, 77–89 (2017).
446. Foster, J. A. & McVey Neufeld, K. A. Gut-brain axis: how the microbiome influences anxiety and depression. *Trends Neurosci* **36**, 305–312 (2013).
447. Han, W. *et al.* A Neural Circuit for Gut-Induced Reward. *Cell* **175**, 665-678.e23 (2018).
448. Suarez, A. N. *et al.* Gut vagal sensory signaling regulates hippocampus function through multi-order pathways. *Nature Communications* 2018 9:1 **9**, 1–15 (2018).
449. Maniscalco, J. W. & Rinaman, L. Vagal interoceptive modulation of motivated behavior. *Physiology* **33**, 151–167 (2018).
450. Raybould, H. E. & Zumpano, D. L. Microbial metabolites and the vagal afferent pathway in the control of food intake. *Physiol Behav* **240**, (2021).
451. De Vadder, F. *et al.* Microbiota-generated metabolites promote metabolic benefits via gut-brain neural circuits. *Cell* **156**, 84–96 (2014).
452. Li, Z. *et al.* Butyrate reduces appetite and activates brown adipose tissue via the gut-brain neural circuit. *Gut* **67**, 1269–1279 (2018).
453. de La Serre, C. B., de Lartigue, G. & Raybould, H. E. Chronic exposure to Low dose bacterial lipopolysaccharide inhibits leptin signaling in vagal afferent neurons. *Physiol Behav* **139**, 188 (2015).

454. Bravo, J. A. *et al.* Ingestion of Lactobacillus strain regulates emotional behavior and central GABA receptor expression in a mouse via the vagus nerve. *Proc Natl Acad Sci U S A* **108**, 16050–16055 (2011).
455. Lyte, M., Li, W., Opitz, N., Gaykema, R. P. A. & Goehler, L. E. Induction of anxiety-like behavior in mice during the initial stages of infection with the agent of murine colonic hyperplasia *Citrobacter rodentium*. *Physiol Behav* **89**, 350–357 (2006).
456. Bercik, P. *et al.* Chronic Gastrointestinal Inflammation Induces Anxiety-Like Behavior and Alters Central Nervous System Biochemistry in Mice. *Gastroenterology* **139**, 2102-2112.e1 (2010).
457. Bercik, P. *et al.* The intestinal microbiota affect central levels of brain-derived neurotropic factor and behavior in mice. *Gastroenterology* **141**, (2011).
458. Singh, R. K. *et al.* Influence of diet on the gut microbiome and implications for human health. *J Transl Med* **15**, (2017).
459. Wilson, A. S. *et al.* Diet and the Human Gut Microbiome: An International Review. *Dig Dis Sci* **65**, 723–740 (2020).
460. Ezra-Nevo, G., Henriques, S. F. & Ribeiro, C. The diet-microbiome tango: how nutrients lead the gut brain axis. *Curr Opin Neurobiol* **62**, 122–132 (2020).
461. González-Arancibia, C. *et al.* Do your gut microbes affect your brain dopamine? *Psychopharmacology 2019 236:5* **236**, 1611–1622 (2019).
462. Frankot, M. A. *et al.* Acute gut microbiome changes after traumatic brain injury are associated with chronic deficits in decision-making and impulsivity in male rats. *Behavioral neuroscience* **137**, (2023).
463. Lyte, M., Li, W., Opitz, N., Gaykema, R. P. A. & Goehler, L. E. Induction of anxiety-like behavior in mice during the initial stages of infection with the agent of murine colonic hyperplasia *Citrobacter rodentium*. *Physiol Behav* **89**, 350–357 (2006).
464. Wang, N., Gao, X., Zhang, Z. & Yang, L. Composition of the Gut Microbiota in Attention Deficit Hyperactivity Disorder: A Systematic Review and Meta-Analysis. *Front Endocrinol (Lausanne)* **13**, (2022).
465. Langmajerová, M., Roubalová, R., Šebela, A. & Vevera, J. The effect of microbiome composition on impulsive and violent behavior: A systematic review. *Behavioural brain research* **440**, (2023).
466. Yussof, A. *et al.* A meta-analysis of the effect of binge drinking on the oral microbiome and its relation to Alzheimer's disease. *Scientific Reports 2020 10:1* **10**, 1–11 (2020).

467. Leclercq, S. *et al.* Intestinal permeability, gut-bacterial dysbiosis, and behavioral markers of alcohol-dependence severity. *Proc Natl Acad Sci U S A* **111**, E4485–E4493 (2014).
468. Bull-Ottersson, L. *et al.* Metagenomic Analyses of Alcohol Induced Pathogenic Alterations in the Intestinal Microbiome and the Effect of Lactobacillus rhamnosus GG Treatment. *PLoS One* **8**, e53028 (2013).
469. Engen, P. A., Green, S. J., Voigt, R. M., Forsyth, C. B. & Keshavarzian, A. The Gastrointestinal Microbiome: Alcohol Effects on the Composition of Intestinal Microbiota. *Alcohol Res* **37**, 223 (2015).
470. Hartmann, P. *et al.* Deficiency of intestinal mucin-2 ameliorates experimental alcoholic liver disease in mice. *Hepatology* **58**, 108–119 (2013).
471. Yan, A. W. *et al.* Enteric dysbiosis associated with a mouse model of alcoholic liver disease. *Hepatology* **53**, 96–105 (2011).
472. Casafont Morencos, F. *et al.* Small bowel bacterial overgrowth in patients with alcoholic cirrhosis. *Dig Dis Sci* **41**, 552–556 (1996).
473. Bode, J. C., Bode, C., Heidelbach, R., Dürr, H. K. & Martini, G. A. Jejunal microflora in patients with chronic alcohol abuse. *Hepatogastroenterology* **31**, 30–34 (1984).
474. Ezquer, F. *et al.* Innate gut microbiota predisposes to high alcohol consumption. *Addiction biology* **26**, (2021).
475. Bergeson, S. E., Nipper, M. A., Jensen, J., Helms, M. L. & Finn, D. A. Tigecycline Reduces Ethanol Intake in Dependent and Nondependent Male and Female C57BL/6J Mice. *Alcohol Clin Exp Res* **40**, 2491–2498 (2016).
476. Xiao, H. wen *et al.* Gut microbiota modulates alcohol withdrawal-induced anxiety in mice. *Toxicol Lett* **287**, 23–30 (2018).
477. Jadhav, K. S. *et al.* Gut microbiome correlates with altered striatal dopamine receptor expression in a model of compulsive alcohol seeking. *Neuropharmacology* **141**, 249–259 (2018).
478. Kiraly, D. D. *et al.* Alterations of the Host Microbiome Affect Behavioral Responses to Cocaine. *Scientific Reports 2016 6:1* **6**, 1–12 (2016).
479. Lee, K. *et al.* The gut microbiota mediates reward and sensory responses associated with regimen-selective morphine dependence. *Neuropsychopharmacology 2018 43:13* **43**, 2606–2614 (2018).
480. Chi, L. *et al.* Nicotine Alters the Gut Microbiome and Metabolites of Gut-Brain Interactions in a Sex-Specific Manner. *Chem Res Toxicol* **30**, 2110–2119 (2017).

481. Valori, I., Della Longa, L., Angeli, A., Marfia, G. & Farroni, T. Reduced motor planning underlying inhibition of prepotent responses in children with ADHD. *Scientific Reports* 2022 12:1 **12**, 1–11 (2022).
482. Marx, I., Hacker, T., Yu, X., Cortese, S. & Sonuga-Barke, E. ADHD and the Choice of Small Immediate Over Larger Delayed Rewards: A Comparative Meta-Analysis of Performance on Simple Choice-Delay and Temporal Discounting Paradigms. <https://doi.org/10.1177/1087054718772138> **25**, 171–187 (2018).
483. Weafer, J. & de Wit, H. Sex differences in impulsive action and impulsive choice. *Addictive behaviors* **39**, 1573 (2014).
484. Nishizono, H., Hayano, Y., Nakahata, Y., Ishigaki, Y. & Yasuda, R. Rapid generation of conditional knockout mice using the CRISPR-Cas9 system and electroporation for neuroscience research. *Mol Brain* **14**, 1–5 (2021).
485. Sciolino, N. R. *et al.* Recombinase-Dependent Mouse Lines for Chemogenetic Activation of Genetically Defined Cell Types. *Cell Rep* **15**, 2563–2573 (2016).
486. Zhang, C. *et al.* Area Postrema Cell Types that Mediate Nausea-Associated Behaviors. *Neuron* **109**, 461-472.e5 (2021).
487. Kupari, J., Häring, M., Agirre, E., Castelo-Branco, G. & Ernfors, P. An Atlas of Vagal Sensory Neurons and Their Molecular Specialization. *Cell Rep* **27**, 2508-2523.e4 (2019).
488. Bai, L. *et al.* Genetic Identification of Vagal Sensory Neurons That Control Feeding. *Cell* **179**, 1129-1143.e23 (2019).
489. Warfvinge, K., Krause, D. & Edvinsson, L. The distribution of oxytocin and the oxytocin receptor in rat brain: Relation to regions active in migraine. *Journal of Headache and Pain* **21**, 1–13 (2020).
490. Li, Y., Hassett, A. L. & Seng, J. S. Exploring the mutual regulation between oxytocin and cortisol as a marker of resilience. *Arch Psychiatr Nurs* **33**, 164 (2019).
491. van Rossum, E. F. C. Obesity and cortisol: New perspectives on an old theme. *Obesity* **25**, 500–501 (2017).